A LONG ARC APPROACH TO GPS SATELLITE ORBIT IMPROVEMENT

DING-SHENG CHEN

May 1991

A LONG ARC APPROACH TO GPS SATELLITE ORBIT IMPROVEMENT

Ding-Sheng Chen

Department of Geodesy and Geomatics Engineering
University of New Brunswick
P.O. Box 4400
Fredericton, N.B.
Canada
E3B 5A3

PREFACE

In order to make our extensive series of technical reports more readily available, we have scanned the old master copies and produced electronic versions in Portable Document Format. The quality of the images varies depending on the quality of the originals. The images have not been converted to searchable text.

PREFACE

This technical report is a reproduction of a thesis submitted in partial fulfillment of the requirements for the degree of Master of Science in Engineering in the Department of Surveying Engineering, April 1991. The research was supervised by Dr. Richard B. Langley and funding was provided partially by the Natural Sciences and Engineering Research Council of Canada and by the Canadian International Development Agency.

As with any copyrighted material, permission to reprint or quote extensively from this report must be received from the author. The citation to this work should appear as follows:

Chen, Ding-Sheng (1991). *A Long Arc Approach to GPS Satellite Orbit Improvement.* M.Sc.E. thesis, Department of Surveying Engineering Technical Report No. 154, University of New Brunswick, Fredericton, New Brunswick, Canada, 216 pp.

ABSTRACT

The object of this thesis was to design a model, implement software, and test the model and the software for improving the accuracy of the orbits of the satellites of the Navstar Global Positioning System (GPS) using double difference GPS phase observations. A dynamical long arc approach is used and satellite orbits are integrated continuously over multiple days.

The model includes: the coordinate system transformation between the geocentric inertial coordinate system and the Earth-fixed coordinate system; the modelling of the forces acting on the GPS satellites; the integration methods for the solution of the equations of motion for the GPS satellites, and the partial derivatives of the satellite position vectors with respect to initial state vectors and dynamical parameters; the designation of unknown parameters which are solved for in data processing; the handling of biases in GPS observations; and the adjustment and computational algorithms.

A software package associated with the above model has been developed for the Macintosh computer family. The software development is partially based on the GPS DIfferential POsitioning Program (DIPOP) package of the Department of Surveying Engineering of the University of New Brunswick, and the new software package is called DIPOP-E (Enhanced version of DIPOP). The main-processor of DIPOP-E differs significantly from the main-processor of DIPOP due to a much more sophisticated model in the new version, although DIPOP-E inherits most of the features of the main-processor in DIPOP; the pre-processor has been modified only to accommodate new features in the main-processor, and to improve operational efficiency for processing large data sets. A

new special utility tool has been developed for cycle slip detection and correction. The tool uses window, menu, button, mouse, and graphic display features of the Macintosh computer, which greatly enhances the operational efficiency of the package. Other auxiliary programs have been developed to facilitate the use of the main-processor.

The model and software development have been tested thoroughly with the Standard GPS Data Set of the International Association of Geodesy Special Study Group 1.104. All tests show that the most accurate results were for the latitude components, followed by the baseline lengths, the longitude components, and finally height components. This phenomenon is due to the sky distribution of the GPS satellites. The optimistic results of formal uncertainties show that there are some remaining systematic biases in the model. The daily repeatabilities show that the latitude component and baseline length determination were mostly better than 0.1 ppm. For the regional and continental stations, 0.05 ppm level repeatabilities were achieved for the lengths of baselines. The worse results for the short baselines (in terms of ppm) and for the height components may be due to the residual tropospheric effects as no observed meteorological data have been used in the data processing.

TABLE OF CONTENTS

vi

LIST OF TABLES

LIST OF FIGURES

LIST OF SYMBOLS USED

Notice: some of the symbols have completely different meaning in different locations

A	is the effective cross-section surface area of a satellite experiencing solar radiation pressure
a, e, Ω, i, M, and ω	are Keplerian orbital elements
a_0, e_0, Ω_0, i_0, M_0, and ω_0	are Keplerian orbital elements at the initial epoch
a_0, a_1, and a_2	are the coefficients of the satellite clock offset (from GPS time) obtained from the broadcast navigation messages
a_E	is the equation of the equinoxes
a_e	is the mean equatorial radius of the Earth
a_i	are the $v+1$ unknown coefficient vectors of the base functions
$A^p_{v,k}$	are the integration coefficients for the predictor for the first order differential equations
$A^c_{v,k}$	are the integration coefficients for the corrector for the first order differential equations
a_s	is the mean radius of the Earth's orbit around the Sun
A_{zx}	represents the matrix of the linear mapping function from x to z, while x and z are vectors of variances
$B^p_{v,k}$	are the integration coefficients for the predictor for the second order differential equations
$B^c_{v,k}$	are the integration coefficients for the corrector for the second order differential equations
c	is the velocity of the light
C_{nm}, S_{nm}	are the denormalized geopotential coefficients

$\overline{C}_{nm}, \overline{S}_{nm}$	are the normalized geopotential coefficients
C_r	is the reflection constant in the effect of solar radiation on a GPS satellite
$d_{ion}(t)$	is the bias of the ionospheric delay
δ_m	is the Kronecker delta function; $\delta_m = 1$ for $m = 0$, and $\delta_m = 0$ for $m \neq 0$
d_{trop}°	is the approximate tropospheric delay from the surface weather data and the tropospheric model
$dT(t)$	is the bias of the receiver clock
$dt(t)$	is the bias of the satellite clock
$d_{trop}(t)$	is the bias of the tropospheric delay
e_0	is the unit vector pointing from the satellite to the Sun
e_y	is the unit vector in the y-direction
ε	is the random measurement noise in a carrier phase measurement
ε'	is the observation noise in the ionospheric free combination
ε	is the true obliquity angle of the ecliptic
$\overline{\varepsilon}$	is the mean obliquity angle of the elliptic
$\delta\varepsilon$	is the nutation in the obliquity
f	represents the value of the function which maps the position into its second order differential
f_x, f_y, f_z	are the specific force components in the direction of x, y, and z on a GPS satellite
$F_r, F_\lambda,$ and F_ϕ	are the force components in the directions of r, λ, and ϕ respectively
F	$= (\dot{x}, \dot{y}, \dot{z}, f_x, f_y, f_z)$
ϕ	is the geocentric spherical latitude
$\phi(t)$	is the carrier beat phase measurement in cycles
f1, f2	represent the frequencies corresponding to L1 and L2 carriers

$\phi 1, \phi 2$	represent the phase observations corresponding to L1 and L2 carriers
$\mathbf{g}$	is a vector function relating the parameters to the observation
g	is the gravity at the Earth's surface
GM	is the gravitational constant of the Earth
GM_d	is the gravitational constant of a third body
GAST	represents Greenwich Apparent Sidereal Time, is the hour angle of the mean equinox of date
GMST	represents Greenwich Mean Sidereal Time, is the hour angle of the mean equinox of date
h	is the first Love number for the second order tidal effect
$\mathbf{i}$	is the unit vector completing a right-handed coordinate system together with $\mathbf{j}$ and $\mathbf{k}$
$\mathbf{j}$	is defined as the normalized cross product of $\mathbf{k}$ with the unit vector pointing from the satellite to the Sun
$\mathbf{k}$	is the unit vector from the mass center of a satellite to the geocenter
k_2	is the second Love's number of second order harmonic
κ	is the initial state vector of the GPS satellites
κ'	is the partitioned vector formed by the initial state vector and the dynamical parameters of a satellite
κ°	is the approximate initial state vector of the GPS satellites
ℓ	is a double difference observation
ℓ	is an observation vector
λ	is the geocentric east longitude of the satellite
$\lambda 1, \lambda 2$	represent the carrier wavelength corresponding to the L1 and L2 carriers
$\lambda\phi|_{t_{GPS}=T_R}$	is the converted phase observation at the GPS time of the value T_R
$\lambda\phi_{|T_R}$	is the recorded phase observation at the receiver clock time T_R

m	is the order of the geopotential coefficient
m	is the mass of the satellite
N	is the integer carrier beat phase ambiguity
N1, N2	represent the phase ambiguities corresponding to L1 and L2 carriers
$\mathbf{N}$	is the nutation matrix
v	is the eclipse factor (0 or 1, depending on whether the satellite is in the shadow of the Earth or not)
n	is the mean motion and is calculated as $n = (u / a^3)^{1/2}$
n	is the degree of the geopotential coefficient
n_0	is the mean motion of a satellite at an initial epoch
N1, N2	represent the phase ambiguities corresponding to L1 and L2 carriers
$\mathbf{N_o}, \mathbf{P_o}$	are the nutation and precession matrices to transform from J2000.0 to the initial epoch of the equations of motion
N_T	is the total electron content along the propagation path in electrons/m^2
$\mathbf{P}$	is the precession matrix
$\mathbf{P}$	represents the sum of the perturbing forces on the satellite
P	is the pseudorange measurement
$\mathbf{p}$	is the vector of parameters other than κ, $\mathbf{R}$, $\mathbf{p_d}$ in observation equations
$\mathbf{p_d}$	is the vector of dynamical parameters
$\mathbf{p_d}^\circ$	is the vector of approximate values of the dynamical parameters
$P_n^m(\sin\phi)$	is the associated Legendre function
$\mathbf{P_{ra}}$	is the direct radiation pressure
p_s	is the solar radiation pressure in Newton/m^2
p_y	is the unknown parameter for y-bias radiation pressure
$\mathbf{P_{y\text{-}bias}}$	is the solar radiation acceleration in the y-direction
$\mathbf{p}^\circ$	is the vector of approximate values of other parameters

q and **q**	are the position and velocity vectors respectively (with components specified in the orbital coordinate system)
Q_{11}	is the covariance of the coordinates of one station forming the baseline
Q_{12}, Q_{21}	is the covariance between coordinates of the two stations
Q_{22}	is the covariance of the coordinates of the other station forming the baseline
Q_{bb}	is the covariance of the baseline components
Q_{xx}	represents the covariance matrix of a vector of variables
Q_{zz}	represents the covariance matrix of a vector of functional variables
q^z_{ij}	represents an element of Q_{zz}
R	is the position vector of the receiver
R	is the geocentric distance of the station
r	is the geocentric distance of the satellite
r	is the geocentric position vector of the satellite
r	is the position vector of the satellite, or the satellite state vector (position and velocity)
$\ddot{\mathbf{r}}$	is the second derivative of **r** with respect to time (acceleration)
ρ	is the geometric distance from a receiver at the time of signal reception to the satellite at the time of signal transmission
$\dot{\rho}$	is the derivative of the distance ρ with respect to GPS time
R_1	is the matrix for a rotation around the x-axis
R_2	is the matrix for a rotation around the y-axis
R_3	is the matrix for a rotation around the z-axis
r^{CT}	is the state vector in the Earth-fixed coordinate system
r_d	is the geocentric position vector of a third body
r_d	is the geocentric distance of a third body

r^I	is a vector in the mean equatorial coordinate system of the standard reference epoch
ρ^o	is the signal propagation distance computed from the broadcast ephemeris or an *a priori* orbit. $\rho\vert_{t_{GPS}=T_R}^o$ is ρ^o corresponding to the GPS time of the value T_R; $\rho\vert_{t_{GPS}=T_R-\Delta t}^o$ is ρ^o corresponding to the GPS time of the value $T_R - \Delta t$
r_S	is the geocentric position vector of the Sun
r^{true}	is a vector in the true equatorial coordinate system of date
$r^{true}\vert_{t_0}$	is a vector in the true equatorial coordinate system of epoch t_0
R°	is the approximate value of station position vector
r°	is the approximate value of satellite state vector
s_{trop}	is the tropospheric scale parameter
t	is the time
t_0	is the ephemeris reference epoch
t_0	is the time of the initial epoch for the equations of motion
T_{GPS}	is the GPS time
T_R	is the receiver clock time
t_w	is the time at the beginning of the GPS week corresponding to initial epoch of integration
u	is the gravitational constant GM
v	is the order of approximation
v	is the order of the integrator
v	is the residual vector of the observations
V_b	is the solid Earth tidal potential
ω	is the rate of the Earth rotation
W_d	is the generating potential from the gravitational attraction of a third body (the Sun or the Moon)

$\mathbf{X}$	$= (x_1, x_2, x_3, x_4, x_5, x_6) = (x, y, z, \dot{x}, \dot{y}, \dot{z})$
x, y, z	represent the coordinates of the satellite
$\dot{x}, \dot{y}, \dot{z}$	represent the velocity components of the satellite
Z	is the angle between the geocentric vectors of the satellite and that of the third body
z	is the zenith distance (angle) of the third body at the station
Z_{p0}	is the vector of partials of a satellite position vector with respect to the direct solar radiation parameter
Z_{py}	is the vector of partials of a satellite position vector with respect to the y-bias solar radiation parameter
Δ	represents the difference of GPS observations between two stations
ΔH_{phase}	is the height of the antenna phase center about the geodetic marker
Δt	is the clock offset of the receiver with respect to GPS time
Δt	is the step of the integration
∇	represents the difference of GPS observations between two satellites
$\zeta_A, z_A,$ and θ_A	are angles specifying the positions of the mean equinox and equator of date with respect to the mean equinox and the equator of the standard reference epoch
$\delta\psi$	is the nutation in the longitude

ACKNOWLEDGEMENTS

First of all, I would like to express my particular appreciation to my supervisor, Prof. Richard B. Langley. His support, knowledge, suggestions, and critical discussions were valuable to my thesis. I would also like to thank him for permission to use department facilities, mostly, the extensive use of a Macintosh computer. I am deeply impressed by his patience with my English at the early stage of my study and I am grateful to him for the many days he spent reading my thesis and papers. He was always there, and said: "It (English) is going to improve."

I wish to express my thanks to Rock Santerre for useful discussions on modelling GPS observables and to Mike Craymer for sharing his knowledge of the workings of the Macintosh computer. I would also like to acknowledge the assistance provided by Ken Doucet, Phil Rapatz, Nick Christou, Yola Georgiadou, Alfred Kleusberg, David E. Wells, Petr Vanicek and many other members of the Department of Surveying Engineering, all of whom have shared their knowledge and expertise in the related area.

Thanks also to Yehuda Bock and the U.S. National Geodetic Survey for access to the SSG 1.104 standard data set. I would also like to thank Gerhard Beutler and his team at

the University of Bern for providing me with a set of station coordinates from their analyses of the SSG 1.104 data set.

Special thanks to my colleague, John Streicker, for offering to read the first draft of this thesis (the first five chapters). Proof reading by Karen Braun is also appreciated. I should also thank Prof. Alfred Kleusberg and Prof. Ronald Lees, in their capacity as examiners of this thesis. They spent their precious time in reading the manuscript and made valuable suggestions.

I should also like to thank to Dr. Yong-Qi Chen and Prof. Ben-Cao Tao who recommended that I study at UNB. Support and help from many of my friends is also appreciated.

Finally, I emphasize my thanks to Liu-Qing Wang for her patience and support for my ever-lasting graduate study. As a wife of a student (me), she has made many sacrifices.

CHAPTER 1

INTRODUCTION

The accuracy limitation of the broadcast ephemerides of the Global Positioning System (GPS) satellites leads to the effort to improve the determination of the satellite orbits using the post-processing approach. This thesis is a contribution to this effort, and reports on the investigation and design of a model for the improvement of the orbit determination of GPS satellite orbits and its testing. Beginning with a brief introduction to GPS in Section 1, the basic concept connecting the whole model of the improvement of the accuracy of GPS satellite orbits is described in Section 2. The scope of the thesis is also given in Section 2, followed by the contributions and the limitations of the thesis in the last section.

1.1 The Global Positioning System

This section gives only a very brief description of the Global Positioning System (GPS). The readers can get more details from the "Guide to GPS Positioning" by Wells et al. [1987].

The Navstar Global Positioning System is being developed primarily for the military forces of the North Atlantic Treaty Organization (NATO) allies for world-wide, real time positioning and continuous navigation. It is being provided by the U.S. Department of Defense whose goal is to develop a space-based radio positioning system that will operate continuously using one-way ranging (to avoid giving away one's position) to provide

1

accurate three dimensional position, velocity, and time information for users located any where on or near the surface of the Earth.

GPS has three components: the satellite system, the control system, and the users.

The satellite system is still in its developing stages. The fully operational satellite system will consist of 21 primary satellites with three active spares orbiting in six planes at an approximate inclination of 55°, and at an altitude of approximately 20 200 km. The orbits are designed to be near-circular and have 12 hour sidereal periods. The intention of the three spares is to ensure at least 21 satellites are always available and that adequate coverage is maintained. Although the satellite system is still in its developing stages, it is forecasted that the primary satellite constellation will be implemented by 1994. Once implemented, at least four satellites will be visible from any one point to permit three dimensional positioning and continuous navigation all over the world at any time.

Two L-band carrier signals are emitted from each satellite, namely, L1 at 1575.42 MHz, and L2 at 1227.60 MHz. The two carriers are modulated by two kinds of pseudo random noise (PRN) codes: one is the coarse/acquisition-code (C/A-code), and the other is the precision code (P-code). The L1 carrier is modulated by the both codes, and L2 is modulated only by the P-code. Both carriers also carry the broadcast message.

The control system is operated by the U.S. Air Force for the Joint Program Office of the Department of Defense. This system consists of five monitoring stations distributed almost evenly in longitude around the world. The tracking stations receive signals from the satellites, and monitor the health of the satellites. The collected data are transmitted to the master control station where new broadcast ephemerides are computed and the navigation messages are prepared for injection into the satellites.

The third component of GPS consists of the users. The user population is composed of military and civilian personnel who wish to determine their positions by receiving signals from GPS satellites. Measurements on these signals yield the observations. Possible observables in satellite positioning are angle, phase, time delay, etc. The following observables have been implemented in GPS receivers presently available:

- pseudorange using the C/A-code,

- pseudorange using the P-code,

- the rate of phase change of a carrier,

- carrier beat phase.

A pseudorange is the measure of the distance from a satellite to a receiver using the time shift required to align (correlate) a replica of the GPS PRN code generated in the receiver, with the code transmitted from the GPS satellite. The phase of a carrier signal can also be used for positioning by differencing (beating) the received Doppler-shifted satellite carrier with a signal of constant frequency generated in the receiver. The measurement of the rate of phase change is a Doppler measurement.

A carrier beat phase measurement is more precise than a code pseudorange measurement, since the wavelength of a GPS carrier is much shorter than that of the C/A- or P-code. Among the different measurements, the carrier phase measurement is potentially the most powerful measurement for precise static applications.

As high accuracy GPS receivers are becoming very affordable, GPS surveying can provide a general coordinate system which may form the basis for efficient land information systems. The results of these benefits will produce extensive use of GPS within the surveying community, and GPS will provide many services to the public at large. Precise positioning using GPS will find use in precise geodetic surveying,

deformation surveys, surveys for detecting and monitoring tectonic movements, etc. [Wells et al., 1987].

For highly accurate positioning, there is a high demand in the compensation of biases. The bias sources limiting the accuracy of current relative GPS positioning (positioning with respect to a reference station) can be grouped into three categories: station dependent biases, observation dependent biases, and satellite dependent biases [Wells et al., 1987]. The station dependent biases are comprised of coordinate offsets of a reference station and receiver clock offsets. The observation dependent biases include the signal propagation delays in the ionosphere and troposphere, and carrier phase ambiguities. The satellite dependent biases include the satellite orbit biases and the satellite clock biases. Ephemeris errors are the result of uncertainties in the predicted orbits of broadcast ephemerides. The satellite orbits transmitted in the navigation message in the past have been in error by as much as 4 ppm, but theses errors are currently much smaller — approaching 0.1 ppm [Langley, 1986b; Georgiadou, 1987; Kleusberg and Georgiadou, 1988; Remondi, 1989].

The effect of the orbital error in relative positioning accuracy is approximately proportional to the length of the baseline. Thus, a long baseline is affected more significantly. For most precise geodetic and geodynamic applications, improved orbits are required.

1.2 The Principle of Orbit Improvement

To improve the accuracy of satellite orbits, some researchers have used a short arc approach; for example, Buffett [1985], Wanless [1985], and Parrot [1989]. Here, the short arc approach means the continuous integration of the orbital arc within one revolution

of the satellite. The advantage of the short arc approach is that we can use a simplified force model and coordinate system. However, the problem with the short arc approach is lower separability of the orbital elements and other parameters and the uncertainties in the observation model and observations will be easily mapped into the final orbits and other parameters.

To overcome the disadvantage of the short arc approach, a long orbital arc is used in this research. Here in this thesis, the term long orbital arc implies an orbital arc of more than one revolution of a satellite around the Earth. It is continuous and smooth over the whole observation period. The advantage of the long arc approach is a higher separability of the orbital elements and other parameters. There is a smaller number of the unknown parameters for the solution and the geometry is stronger.

In contrast to the short arc approach, the problem with the long arc approach is its more stringent requirements on the force model, the coordinate system transformation, the precision of the integration of the equations of motion, and the software implementation.

Before discussing the orbit improvement model in detail, a very basic concept of the orbit improvement is presented in this subsection, which will link Chapters 2 through 5, especially for the reader unfamiliar with orbital mechanics.

To solve an orbit improvement problem, the measurement related to the positions of the satellites is required. The results of the measurement are called observations. Since the carrier phase observable is the most precise, this signal is used for orbit improvement in this research and is discussed in detail in Chapter 5. The mathematical equation which expresses an observation as a function of various physical parameters is called an observation equation.

The improvement of the accuracy of the orbits is a process to adjust the orbits of satellites, together with other parameters, so that these parameters are consistent with the observations such as carrier phase. These observations are nonlinear functions of the satellite positions, $r(t)$, (and possibly of the velocities, $\dot{r}(t)$). The positions and the velocities at observation time epoch are in turn nonlinear functions of the state vectors (including both position and velocity vectors) of the satellites at some arbitrary initial time (these initial state vectors are also called initial conditions in the solution of the equations of motion of the satellites) and the dynamical parameters which describe the forces acting on the satellites, such as solar radiation parameters (they are discused in Chapters 3 and 4).

Mathematically speaking, the orbital parameters and other parameters can usually be determined uniquely, if (i) there are no observation errors; (ii) one observation cannot be derived from other observations; (iii) the number of observations is equal to that of the unknown parameters; (iv) there is no singularity. In practice, such is not the case. Furthermore, an observation equation has more or less unmodelled distortions in describing the physical relationship between an observation and physical parameters. Therefore, it is necessary to have more observations than unknown parameters. This practice takes into account observation errors and allows the reduction of the effects of random errors. When the problem is over-determined, there is usually no set of values for the parameter group which can satisfy all observation equations perfectly. Therefore, a compromise solution is chosen to satisfy all observations as closely as possible according to certain criteria, usually associated with the least squares parameter adjustment procedure. That is the procedure we have adopted.

The direct handling of the nonlinear functions describing the observations is intractable, so the observation model is linearized prior to the adjustment. The linearization in the orbit improvement model is made in three steps:

6

First, observations are related to the satellite positions, station positions, and other parameters at the epochs of the observations. The nonlinear model of observation is

$$\ell = g(R, r, p) + v \; , \tag{1.1}$$

and it is linearized as follows (neglecting higher order terms):

$$\ell = g(R°, r°, p°) + \frac{\partial g}{\partial R}(R - R°) + \frac{\partial g}{\partial r}(r - r°) + \frac{\partial g}{\partial p}(p - p°) + v \; , \tag{1.2}$$

where

ℓ	is an observation vector,
R	is the station position vector,
r	is the satellite state vector (position and velocity),
p	is the vector of other parameters,
$R°$	is the approximate station position vector,
$r°$	is the approximate satellite state vector,
$p°$	is the vector of approximate values of other parameters,
g	is a vector function relating R, r, and p to the observation,
v	is the residual vector of the observations.

The observation model is discussed in more detail in Chapter 5.

In the second step, the state vector r is related to the initial state vector κ, and dynamical parameters p_d:

$$r = r(\kappa, p_d) \; , \tag{1.3}$$

with the corresponding linearized model as

$$r = r(\kappa°, p_d°) + \frac{\partial r}{\partial \kappa}(\kappa - \kappa°) + \frac{\partial r}{\partial p_d}(p_d - p_d°) \; , \tag{1.4}$$

where

κ	is the initial state vector of the GPS satellites,

7

$\mathbf{p_d}$ is the vector of dynamical parameters,

κ° is the approximate initial state vector of the GPS satellites,

$\mathbf{p_d}^\circ$ is the vector of approximate values of the dynamical parameters.

As seen from the above, the approximate satellite positions and velocities, and the associated partial derivatives are required to establish an observation equation which can be expressed as functions of the approximate initial state vector and the dynamical parameters of a satellite. In principle, they are the solutions of the systems of the differential equations describing the motion of the satellites. The complication here is that there are no rigorous analytical expressions for the satellite state vectors, and their partial derivatives as functions of the initial conditions. This problem is discussed in Chapter 4, before the discussion of the observation equations, since it is required to understand the formation of the observation equations.

Finally, using the chain rule, we can get a complete linearized observation model as follows:

$$\ell = g(\mathbf{R}^\circ, \mathbf{r}^\circ, \mathbf{p}^\circ) + \frac{\partial g}{\partial \mathbf{R}}(\mathbf{R} - \mathbf{R}^\circ) + \frac{\partial g}{\partial \mathbf{r}}\frac{\partial \mathbf{r}}{\partial \kappa}(\kappa - \kappa^\circ) + \frac{\partial g}{\partial \mathbf{r}}\frac{\partial \mathbf{r}}{\partial \mathbf{p_d}}(\mathbf{p_d} - \mathbf{p_d}^\circ) +$$
$$\frac{\partial g}{\partial \mathbf{p}}(\mathbf{p} - \mathbf{p}^\circ) + \mathbf{v} \ . \tag{1.5}$$

In this derivation, we use the relationship

$$\mathbf{r}^\circ = \mathbf{r}(\kappa^\circ, \mathbf{p_d}^\circ) \ ; \tag{1.6}$$

that is, the approximate position vector of a satellite should be the rigorous solution of the equations of motion, corresponding to its approximate initial conditions (the initial state vector) and the approximate values of the dynamical parameters.

Before we can establish the observation equations and the equations of motion of the satellites, a certain coordinate system has to be selected. The observation equations are

established in an Earth-fixed coordinate system. On the other hand, the equations of motion are usually expressed in a geocentric inertial (space-fixed) coordinate system. Thus, a coordinate system transformation is required and this is discussed in Chapter 2.

To form the equations of motion, the various forces acting on the GPS satellites have to be investigated. The coordinate system transformations are also involved in the force modelling. Therefore, the GPS satellite force modelling is described in Chapter 3, following the discussion on the coordinate system transformation.

In summary, the requirements for the improvement in the accuracy of the orbits are as follows: to identify the forces acting on a GPS satellite (Chapter 3); to obtain the positions and their partial derivatives with respect to the approximate initial state vectors and dynamical parameters of a satellite by integrating the equations of motion of the satellites (Chapter 4); to establish and linearize the observation equations (Chapter 5), and to find a solution using the least squares adjustment method. Both the force modelling and formation of the observation equations involve coordinate system transformation (Chapter 2).

In Chapter 6, the state of the software implementation using the model described in the preceding chapters is described. In addition, other software development related to the implementation of the orbital improvement model is also discussed, for example, data pre-analysis, and auxiliary software development. Some of the computational algorithms and processing strategies designed to speed up the processing are also discussed.

The new version of the software has been used to process the so-called "Standard Data Set" of Special Study Group 1.104 of the International Association of Geodesy (Chapter 7). This data set consists of carrier phase and pseudorange observations from Texas Instruments TI 4100 receivers operated at 18 sites in the U.S.A. and Canada between 3 and 7 January 1987. The lengths of intersite baselines used range from 37 km

to 2 240 km spanning local, regional, and continental scales. The testing of our software and the analysis of this data set are presented in Chapter 7.

In Chapter 8, a summary is drawn and recommendations for further research are made. The recommendations include both model and software development aspects.

1.3 Contributions of the Thesis

The main contribution of this thesis is the development of an orbit improvement model for GPS satellites, specifically, a long arc orbital algorithm which includes the short orbital arc as a special case; the software implementation of this orbit improvement model; the testing of the model and the software development. The model includes the rotation of the Earth in space and associated coordinate system transformations, force modelling, integration technique, parameter design and observation equations, bias handling, computation and adjustment algorithms. The software corresponding to the described model has been implemented. The orbit improvement model and its associated software was tested with a standard data set.

There is a limitation of the thesis. The problem of GPS satellite orbit improvement covers a wide range of background knowledge. It includes celestial mechanics, numerical analysis, astronomy, geodesy, physics, and mathematics. No attempt is made to give a complete background introduction to all of these aspects. Only those models and equations directly used are described. Almost all derivations of the formulae are omitted and only hints or references for the derivations are given. Some of the general knowledge in the area of surveying and geodesy is also omitted, such as details on the adjustment algorithm and polynomial fitting and interpolation, assuming readers would already be familiar with them. Some of the simple formulae are also omitted from the text.

It should be pointed out that, although the basic model and algorithm appear to be correct, more work should be done towards an even more accurate and robust model and the associated software implementation.

CHAPTER 2
COORDINATE SYSTEM TRANSFORMATIONS

As introduced in Chapter 1, coordinate systems are involved in both observation equations and equations of motion of GPS satellites. On the one hand, the equations of motion of a satellite are expressed in a geocentric inertial coordinate system and the positions of the satellite are integrated directly from the equations of motion. On the other hand, observations are carried out on the surface of the Earth and observation equations are established in an earth-fixed coordinate system. Thus, it is necessary to transform the coordinates of the positions (or other vectors) from the inertial coordinate system to the Earth-fixed system, and vice versa. Here, the "geocentric inertial coordinate system" is space-fixed, and has a constant rotational relationship with the mean equatorial coordinate system of the standard reference epoch (the standard reference epoch used in our model is J2000.0*). The Earth-fixed geocentric coordinate system is the conventional terrestrial coordinate system (CT) [Vanicek and Krakiwsky, 1986].

All forces acting on a GPS satellite should also be transformed to the coordinate system in which the equations of motion are formed. The coordinate system transformations are also involved in the computation of the partials with respect to satellite related parameters (Chapter 4). The coordinate system transformations are discussed in the first section of this chapter.

---

* Beginning in 1984, the standard epoch of the fundamental astronomical coordinate system is year 2000 January 1, 12^h (JD 2451545.0), denoted as J2000.0 [Nautical Almanac Office, 1987].

It should be pointed out that all coordinate systems discussed in this thesis are geocentric. That is, the mass center of the Earth is the origin of the coordinate systems.

The phase centers of the antennas of both satellites and receivers are required in forming observation equations, since the measurement of the corresponding GPS signals is referred to these phase centers. Thus, the offsets of the mass centers of satellites and the station geodetic markers from their respective antenna phase centers must be taken into account. The transformation to the antenna phase center of a satellite is discussed in Section 2, while the transformation to the antenna phase center of a receiver is discussed in Section 3. The temporal variation of the coordinates of the receiver caused by the solid Earth tide has to be modelled before the transformation, and the discussion of this variation is included in Section 3.

2.1 Coordinate System Transformations

The transformation from the inertial to the Earth-fixed coordinate system is separated into three steps: i) transformation from the mean equatorial coordinate system of the standard reference epoch (J2000.0) to the true equatorial coordinate system of date (Section 2.1.1); ii) transformation from the true to the instantaneous terrestrial coordinate system (Section 2.1.2); iii) transformation from the instantaneous terrestrial to the conventional terrestrial coordinate system (Section 2.1.3).

2.1.1 Precession and Nutation

The first step in the transformation from the inertial to the Earth-fixed coordinate system is from the mean equatorial coordinate system of the standard reference epoch

13

(J2000.0) to the true equatorial coordinate system of date. This transformation is described by precession and nutation.

Precession and nutation are caused by torque from external gravitational forces. Under the torque from external gravitational forces, such as from the Moon, the Sun, and other planets, the rotation pole of the Earth is oscillating in space. The oscillation is divided into two components: one includes a long period harmonic motion called precession; the other includes the remaining short-period oscillations called nutation.

Taking into account both motions, the transformation from the mean equatorial coordinate system of the standard reference epoch to the true of date is expressed as

$$r^{true} = N\ P\ r^I\ ,$$ (2.1)

where

r^I is a position vector in the mean equatorial coordinate system of the standard reference epoch,

r^{true} is a position vector in the true equatorial coordinate system of date,

P is the precession matrix,

N is the nutation matrix.

The angles in both nutation and precession matrices are referenced by Julian date 2451545.0 (J2000.0). They are computed from polynomial and trigonometric series as functions of Barycentric Dynamical Time (TDB) (see Sections 2.1.1.1 and 2.1.1.2). The time scale, TDB (also used to reference the planetary ephemerides), is related to Terrestrial Dynamical Time (TDT) by equations:

$$TDB = TDT + 0^s.001\ 658\ \sin g + 0^s.000\ 014\ \sin 2g\ ,$$ (2.2)

$$g\ \ = 357°.53 + 0°.985\ 600\ 28\ (JD - 2\ 451\ 545.0)\ ,$$ (2.3)

where higher-order terms are neglected, and g is the mean anomaly of the orbit of the Earth around the Sun [Nautical Almanac Office, 1987].

14

In practice, the time scale used in GPS is GPS time. GPS time is a time scale based on the atomic second and its starting epoch is defined at January 6, 1980, UTC 0^h exactly.

The difference between the UTC time and the GPS time is the accumulated number of integer leap seconds inserted into the UTC time scale since the initial GPS epoch (January 6, 1980, UTC 0^h). The GPS time has a constant offset with respect to TDT, i.e.,

$$\text{TDT} = \text{T}_{\text{GPS}} + 51^{\text{s}}.184 \quad , \tag{2.4}$$

where

$\quad \text{T}_{\text{GPS}}$ is the GPS time of a particular epoch.

Another notation accompanying GPS time is GPS week which is defined as the week number reckoned from January 6, 1980. The first GPS week is week 0 (note: it is not 1).

All time arguments used in the computation of precession and nutation are measured in centuries of TDB from J2000.0, i.e.,

$$T = \frac{\text{Julian Day of TDB} - 2451545.0}{36525} \quad . \tag{2.5}$$

So far in this subsection, the acquisition of the time scale used in the computation of nutation and precession has been discussed. The computation of the precession and nutation matrices is discussed separately in the following two sub-subsections.

2.1.1.1 *Precession Matrix*

As described in equation (2.1), one transformation from the mean equatorial coordinate system of the standard reference epoch (i.e., J2000.0) to the true of date is due to precession, where **P** is the associated transformation matrix. The word "mean" as used

in this sub-subsection implies that the effect of the short period (less than 18.6 years) terms of nutation has been removed.

The precession matrix is,

$P =$

$$
\begin{pmatrix}
\cos \zeta_A \cos \theta_A \cos z_A - \sin \zeta_A \sin z_A & -\sin \zeta_A \cos \theta_A \cos z_A - \cos \zeta_A \sin z_A & -\sin \theta_A \cos z_A \\
\cos \zeta_A \cos \theta_A \sin z_A + \sin \zeta_A \cos z_A & -\sin \zeta_A \cos \theta_A \sin z_A + \cos \zeta_A \cos z_A & -\sin \theta_A \sin z_A \\
\cos \zeta_A \sin \theta_A & -\sin \zeta_A \sin \theta_A & \cos \theta_A
\end{pmatrix} ,
$$

$$(2.6)$$

where ζ_A, z_A, and θ_A are angles specifying the positions of the mean equinox and equator of date with respect to the mean equinox and the equator of the standard reference epoch.

With the angular units in degrees, the arguments in equation (2.6) are as follows [Nautical Almanac Office, 1987]:

$$\zeta_A = 0°.640\ 6161\ T + 0°.000\ 0839\ T^2 + 0°.000\ 0050\ T^3 \ ,$$

$$z_A = 0°.640\ 6161\ T + 0°.000\ 3041\ T^2 + 0°.000\ 0051\ T^3 \ ,$$

$$\theta_A = 0°.556\ 7530\ T - 0°.000\ 1185\ T^2 - 0°.000\ 0116\ T^3 \ , \qquad (2.7)$$

where T is defined by equation (2.5).

2.1.1.2 Nutation Matrix

The other transformation from the mean equatorial to the true equatorial coordinate system is due to nutation. In the true equatorial coordinate system, the z-axis coincides with the instantaneous spin-axis of the Earth, while the true vernal equinox defines the direction of the x-axis. The effect of nutation N is usually spelled out in terms of the

16

nutation in longitude $\delta\psi$ and the nutation in obliquity $\delta\varepsilon$. The nutation matrix is written as [Vanicek and Krakiwsky, 1986]

$$N = R_1(-\varepsilon)\, R_3(-\delta\psi)\, R_1(\bar{\varepsilon}) \quad , \tag{2.8}$$

where

$\bar{\varepsilon}$ is the mean obliquity angle of the elliptic,

ε is the true obliquity angle of the ecliptic,

$\delta\psi$ is the nutation in longitude,

R_1 is the matrix for a rotation around the x-axis,

R_3 is the matrix for a rotation around the z-axis.

The relationship between ε and $\bar{\varepsilon}$ is

$$\varepsilon = \bar{\varepsilon} + \delta\varepsilon \quad . \tag{2.9}$$

where

$\delta\varepsilon$ is the nutation in the obliquity.

Equation (2.8) can be expanded as

$$N = \begin{pmatrix} \cos\delta\psi & -\cos\bar{\varepsilon}\,\sin\delta\psi & -\sin\bar{\varepsilon}\,\sin\delta\psi \\ \cos\varepsilon\,\sin\delta\psi & \cos\bar{\varepsilon}\,\cos\varepsilon\,\cos\delta\psi + \sin\bar{\varepsilon}\,\sin\varepsilon & \sin\bar{\varepsilon}\,\cos\varepsilon\,\cos\delta\psi - \cos\bar{\varepsilon}\,\sin\varepsilon \\ \sin\varepsilon\,\sin\delta\psi & \cos\bar{\varepsilon}\,\sin\varepsilon\,\cos\delta\psi - \sin\bar{\varepsilon}\,\cos\varepsilon & \sin\bar{\varepsilon}\,\sin\varepsilon\,\cos\delta\psi + \cos\bar{\varepsilon}\,\cos\varepsilon \end{pmatrix} . \tag{2.10}$$

The 1980 IAU (International Astronomical Union) nutation model [Kaplan, 1981] is used to obtain the angles in the above formula. The mean obliquity is

$$\bar{\varepsilon} = 23°21'26''.448 - 46''.8150\, T - 5''.9 \times 10^{-4}\, T^2 + 1''.813 \times 10^{-3}\, T^3 \quad . \tag{2.11}$$

The nutation in the longitude $\delta\psi$ and in the obliquity $\delta\varepsilon$, are expressed by a series expansion of sines and cosines of linear combinations of five fundamental arguments. These arguments are as follows [Kaplan, 1981]:

1. The mean anomaly of the Moon is

$$\alpha_1 = \ell = 485866''.733 + (1325^r + 715922''.633)\, T + 31''.310\, T^2 + 0''.064\, T^3 ; \tag{2.12}$$

2. The mean anomaly of the Sun is

$$\alpha_2 = \ell' = 1287099''.804 + (99^r + 1292581''.224)\, T - 0''.577\, T^2 - 0''.012\, T^3 \; ; \quad (2.13)$$

3. The mean argument of latitude of the Moon is

$$\alpha_3 = F = 335778''.877 + (1342^r + 295263''.137)\, T - 13''.257\, T^2 + 0''.011\, T^3 \; ; \; (2.14)$$

4. The mean elongation of the Moon from the Sun is

$$\alpha_4 = D = 1072261''.307 + (1236^r + 1105601''.328)\, T - 6''.891\, T^2 + 0''.019\, T^3 \; ; (2.15)$$

5. The mean longitude of the ascending lunar node is

$$\alpha_5 = \Omega = 450160''.280 - (5^r + 482890''.539)\, T + 7''.455\, T^2 + 0''.008\, T^3 \; ; \quad (2.16)$$

The superscript 'r' stands for:

$$1^r = 360^\circ = 1296000''.$$

In terms of these fundamental arguments, the nutation quantities are represented by

$$\delta\psi = \sum_{j=1}^{N} \left[(A_{0j} + A_{1j}\,T)\sin\left[\sum_{i}^{5} k_{ji}\,\alpha_i(T) \right] \right] , \qquad (2.17)$$

and

$$\delta\varepsilon = \sum_{j=1}^{N} \left[(B_{0j} + B_{1j}\,T)\cos\left[\sum_{i}^{5} k_{ji}\,\alpha_i(T) \right] \right] , \qquad (2.18)$$

where the various α_i, k_{ij}, A_{0j}, A_{1j}, B_{0j}, and B_{1j} are listed in Table 2.1, and N is the number of the components included.

Table 2.1 1980 IAU Theory of Nutation.

Index j	Period (days)	Argument coefficient $k_{j1}\ k_{j2}\ k_{j3}\ k_{j4}\ k_{j5}$					Sin coefficient $A_{0j}\qquad A_{1j}$ (0''.0001)		Cos coefficient $B_{0j}\qquad B_{1j}$ (0''.0001)	
1	6798.4	0	0	0	0	1	-171996	-174.2	92025	8.9
2	3399.2	0	0	0	0	2	2061	.2	-894	.5
3	1305.5	-2	0	2	0	1	45	.0	-24	.0
4	1095.2	2	0	-2	0	0	11	.0	0	.0
5	1615.7	-2	0	2	0	2	-3	.0	1	.0
6	3232.9	1	-1	0	-1	0	-3	.0	0	.0

18

Table 2.1 Continued

Index j	Period (days)	Argument coefficient k_{j1} k_{j2} k_{j3} k_{j4} k_{j5}					Sin coefficient A_{0j} A_{1j} (0".0001)		Cos coefficient B_{0j} B_{1j} (0".0001)	
7	6786.3	0	-2	2	-2	1	-2	.0	1	.0
8	943.2	2	0	-2	0	1	1	.0	0	.0
9	182.6	0	0	2	-2	2	-13186	-1.6	5735	-3.1
10	365.3	0	1	0	0	0	1426	-3.4	54	-.1
11	121.7	0	1	2	-2	2	-517	1.2	223	-.6
12	365.2	0	-1	2	-2	2	217	-.5	-94	.3
13	177.8	0	0	2	-2	1	129	.1	-70	.0
14	205.9	2	0	0	-2	0	48	.0	1	.0
15	173.3	0	0	2	-2	0	-22	.0	0	.0
16	182.6	0	2	0	0	0	17	-.1	0	.0
17	386.0	0	1	0	0	1	-15	.0	8	.0
18	91.3	0	2	2	-2	2	-16	.1	6	.0
19	346.6	0	-1	0	0	1	-12	.0	6	.0
20	199.8	-2	0	0	2	1	-6	.0	3	.0
21	346.6	0	-1	2	-2	1	-5	.0	3	.0
22	212.3	2	0	0	-2	1	4	.0	-2	.0
23	119.6	0	1	2	-2	1	4	.0	-2	.0
24	411.8	1	0	0	-1	0	-4	.0	0	.0
25	131.7	2	1	0	-2	0	1	.0	0	.0
26	169.0	0	0	-2	2	1	1	.0	0	.0
27	329.8	0	1	-2	2	0	-1	.0	0	.0
28	409.2	0	1	0	0	2	1	.0	0	.0
29	388.3	-1	0	0	1	1	1	.0	0	.0
30	117.5	0	1	2	-2	0	-1	.0	0	.0
31	13.7	0	0	2	0	2	-2273	-.2	977	-.5
32	27.6	1	0	0	0	0	711	.1	-6	.0
33	13.6	0	0	2	0	1	-386	-.4	200	.0
34	9.1	1	0	2	0	2	-301	.0	129	-.1
35	31.8	1	0	0	-2	0	-158	.0	-1	.0
36	27.1	-1	0	2	0	2	123	.0	-53	.0
37	14.8	0	0	0	2	0	63	.0	-2	.0
38	27.7	1	0	0	0	1	63	.1	-32	.0
39	27.4	-1	0	0	0	1	-58	-.1	32	.0
40	9.6	-1	0	2	2	2	-58	.0	25	.0
41	9.1	1	0	2	0	1	-51	.0	27	.0
42	7.1	0	0	2	2	2	-37	.0	16	.0
43	13.8	2	0	0	0	0	29	.0	-1	.0
44	23.9	1	0	2	-2	2	29	.0	-12	.0
45	6.9	2	0	2	0	2	-31	.0	12	.0
46	13.6	0	0	2	0	0	25	.0	-1	.0
47	27.0	-1	0	2	0	1	21	.0	-10	.0
48	32.0	-1	0	0	2	1	16	.0	-8	.0
49	31.7	1	0	0	-2	1	-12	.0	6	.0
50	9.5	-1	0	2	2	1	-10	.0	5	.0
51	34.8	1	1	0	-2	0	-6	.0	0	.0

Table 2.1 Continued

Index j	Period (days)	k_{j1}	k_{j2}	k_{j3}	k_{j4}	k_{j5}	A_{0j}	A_{1j}	B_{0j}	B_{1j}
		Argument coefficient					Sin coefficient (0".0001)		Cos coefficient (0".0001)	
52	13.2	0	1	2	0	2	6	.0	-3	.0
53	14.2	0	-1	2	0	2	-6	.0	3	.0
54	5.6	1	0	2	2	2	-8	.0	3	.0
55	9.6	1	0	0	2	0	6	.0	0	.0
56	12.8	2	0	2	-2	2	6	.0	-3	.0
57	14.8	0	0	0	2	1	-6	.0	3	.0
58	7.1	0	0	2	2	1	-6	.0	3	.0
59	23.9	1	0	2	-2	1	6	.0	-3	.0
60	14.7	0	0	0	-2	1	-5	.0	3	.0
61	29.8	1	-1	0	0	0	5	.0	0	.0
62	6.9	2	0	2	0	1	-5	.0	3	.0
63	15.4	0	1	0	-2	0	-4	.0	0	.0
64	26.9	1	0	-2	0	0	4	.0	0	.0
65	29.5	0	0	0	1	0	-4	.0	0	.0
66	25.6	1	1	0	0	0	-3	.0	0	.0
67	9.1	1	0	2	0	0	3	.0	0	.0
68	9.4	1	-1	2	0	2	-3	.0	1	.0
69	9.8	-1	-1	2	2	2	-3	.0	1	.0
70	13.7	-2	0	0	0	1	-2	.0	1	.0
71	5.5	3	0	2	0	2	-3	.0	1	.0
72	7.2	0	-1	2	2	2	-3	.0	1	.0
73	8.9	1	1	2	0	2	2	.0	-1	.0
74	32.6	-1	0	2	-2	1	-2	.0	1	.0
75	13.8	2	0	0	0	1	2	.0	-1	.0
76	27.8	1	0	0	0	2	-2	.0	1	.0
77	9.2	3	0	0	0	0	2	.0	0	.0
78	9.3	0	0	2	1	2	2	.0	-1	.0
79	27.3	-1	0	0	0	2	1	.0	-1	.0
80	10.1	1	0	0	-4	0	-1	.0	0	.0
81	14.6	-2	0	2	2	2	1	.0	-1	.0
82	5.8	-1	0	2	4	2	-2	.0	1	.0
83	15.9	2	0	0	-4	0	-1	.0	0	.0
84	22.5	1	1	2	-2	2	1	.0	-1	.0
85	5.6	1	0	2	2	1	-1	.0	1	.0
86	7.3	-2	0	2	4	2	-1	.0	1	.0
87	9.1	-1	0	4	0	2	1	.0	0	.0
88	29.3	1	-1	0	-2	0	1	.0	0	.0
89	12.8	2	0	2	-2	1	1	.0	-1	.0
90	4.7	2	0	2	2	2	-1	.0	0	.0
91	9.6	1	0	0	2	1	-1	.0	0	.0
92	12.7	0	0	4	-2	2	1	.0	0	.0
93	8.7	3	0	2	-2	2	1	.0	0	.0
94	23.8	1	0	2	-2	0	-1	.0	0	.0
95	13.1	0	1	2	0	1	1	.0	0	.0
96	35.0	-1	-1	0	2	1	1	.0	0	.0

Table 2.1 Continued

Index j	Period (days)	Argument coefficient k_{j1} k_{j2} k_{j3} k_{j4} k_{j5}					Sin coefficient A_{0j} A_{1j} (0".0001)		Cos coefficient B_{0j} B_{1j} (0".0001)	
97	13.6	0	0	-2	0	1	-1	.0	0	.0
98	25.4	0	0	2	-1	2	-1	.0	0	.0
99	14.2	0	1	0	2	0	-1	.0	0	.0
100	9.5	1	0	-2	-2	0	-1	.0	0	.0
101	14.2	0	-1	2	0	1	-1	.0	0	.0
102	34.7	1	1	0	-2	1	-1	.0	0	.0
103	32.8	1	0	-2	2	0	-1	.0	0	.0
104	7.1	2	0	0	2	0	1	.0	0	.0
105	4.8	0	0	2	4	2	-1	.0	0	.0
106	27.3	0	1	0	1	0	1	.0	0	.0

2.1.2 Rotation Matrix of Sidereal Time

As stated in the beginning of this section, the next step in the transformation from the inertial to the Earth-fixed coordinate system is from the true equatorial coordinate system of date to the instantaneous terrestrial (IT) coordinate system. IT system differs from the true equatorial system by a rotation around the z^{IT}-axis which coincides with the instantaneous spin-axis. The true equatorial and IT coordinate systems are related by true sidereal time. The true sidereal time is defined as the angle between the true equinox and the mean Greenwich meridian, denoted as GAST (Greenwich Apparent Sidereal Time), reckoned about the z-axis.

The equation of the transformation is

$$r^{IT} = R_3(GAST) \, r^{true} \, .$$ (2.19)

The transformation matrix in equation (2.19) is

$$R_3(GAST) = \begin{pmatrix} \cos(GAST) & \sin(GAST) & 0 \\ -\sin(GAST) & \cos(GAST) & 0 \\ 0 & 0 & 1 \end{pmatrix} \, ,$$ (2.20)

21

and the angle, GAST, is composed of two components, i.e.,

$$GAST = GMST + a_E \; ,$$

(2.21)

where

GMST   Greenwich Mean Sidereal Time, is the hour angle of the mean equinox of

date,

a_E is called the equation of the equinoxes.

a_E is equal to the total nutation in longitude multiplied by the cosine of the true obliquity of

the elliptic:

$$a_E = \cos \varepsilon \; \delta\psi \; .$$

(2.22)

GMST is related to UT1 by

$$GMST = UT1 + 24\ 110^s.548\ 41 + 8640\ 184^s.812\ 866\ T_u + 0^s.093\ 104\ T_u^2$$
$$- 6^s.2 \times 10^{-6}\ T_u^3 \; ,$$

(2.23)

where

$$T_u = (UT1 \text{ Julian date} - 2\ 451\ 545.0)/36\ 525 \; .$$

(2.24)

If the IRIS (International Radio Interferometric Surveying) [IAG, 1987] UT1-UTC

value (at intervals of five days) is used, UT1 - UTC value between tabulated epochs should

be interpolated. For interpolation, three points should be mentioned:

1. The base functions for the interpolation are polynomials.

2. Since UTC has leap seconds, UT1 - T_{GPS} values are actually used for

interpolation. T_{GPS} is calculated from UTC = T_{GPS} + leap seconds since Jan. 5, 1980.

3. The tidal variation $\Delta UT1_{tide}$ in UT1 has to be removed before the interpolation

since the short period tidal variation cannot be represented by the polynomials.

Therefore, UT1 at any time is the interpolated value plus the tidal variation term. The tidal variation term, $\Delta UT1_{tide}$, is represented as

$$\Delta UT1_{tide} = \sum_{i=1}^{N} \left[A_i \sin\left[\sum_{j=1}^{5} k_{ij} \, \alpha_j \right] \right] \, ,$$

(2.25)

where N is chosen to include all contributions with periods less than 35 days. There are no other contributions until a period of 90 days is reached. These omitted long period contributions in equation (2.25) can be well interpolated by polynomials. The values for k_{ij} and A_i, along with the periods involved, are given in Table 2.2. The α_j for $j = 1, 5$, are the angles defined already for the nutation series: ℓ, ℓ', F, D, and Ω.

2.1.3   Rotation Matrix of Polar Wobble

The last step in the transformation from the inertial to the Earth-fixed coordinate system is from the instantaneous terrestrial to the conventional terrestrial coordinate system. This transformation is necessitated by polar motion, since the instantaneous spin-axis of the Earth is not fixed in the Earth (instead, it wobbles around the z^{CT}-axis). The polar wobble is described by two parameters, x_p, and y_p (the angular displacements of the instantaneous spin-axis from the conventional terrestrial pole).

The transformation to the Earth-fixed system is accomplished through the following expression [Vanicek and Krakiwsky, 1986]:

$$r^{CT} = R_2(-x_p) \, R_1(-y_p) \, r^{IT} \, .$$

(2.26)

23

Table 2.2 Periodic tidally induced variations in UT1 with
periods less than 35 days.

Index i	Period (days)	Argument coefficient					A_i (0".0001)
		k_{i1}	k_{i2}	k_{i3}	k_{i4}	k_{i5}	
1	5.64	1	0	2	2	2	-.02
2	6.85	2	0	2	0	1	-.04
3	6.86	2	0	2	0	2	-.10
4	7.09	0	0	2	2	1	-.05
5	7.10	0	0	2	2	2	-.12
6	9.11	1	0	2	0	0	-.04
7	9.12	1	0	2	0	1	-.41
8	9.13	1	0	2	0	2	-.99
9	9.18	3	0	0	0	0	-.02
10	9.54	-1	0	2	2	1	-.08
11	9.56	-1	0	2	2	2	-.20
12	9.61	1	0	0	2	0	-.08
13	12.81	2	0	2	-2	2	.02
14	13.17	0	1	2	0	2	.03
15	13.61	0	0	2	0	0	-.30
16	13.63	0	0	2	0	1	-3.21
17	13.66	0	0	2	0	2	-7.76
18	13.75	2	0	0	0	-1	.02
19	13.78	2	0	0	0	0	-.34
20	13.81	2	0	0	0	1	.02
21	14.19	0	-1	2	0	2	-.02
22	14.73	0	0	0	2	-1	.05
23	14.77	0	0	0	2	0	-.73
24	14.80	0	0	0	2	1	-.05
25	15.39	0	-1	0	2	0	-.05
26	23.86	1	0	2	-2	1	.05
27	23.94	1	0	2	-2	2	.10
28	25.62	1	1	0	0	0	.04
29	26.88	-1	0	2	0	0	.05
30	26.98	-1	0	2	0	1	.18
31	27.09	-1	0	2	0	2	.44
32	27.44	1	0	0	0	-1	.53
33	27.56	1	0	0	0	0	-8.26
34	27.67	1	0	0	0	1	.54
35	29.53	0	0	0	1	0	.05
36	29.80	1	-1	0	0	0	-.06
37	31.66	-1	0	0	2	-1	.12
38	31.81	-1	0	0	2	0	-1.82
39	31.96	-1	0	0	2	1	.13
40	32.61	1	0	-2	2	-1	.02
41	34.85	-1	-1	0	2	0	-.09

Developing the trigonometrical functions in the above equation into power series, and neglecting second and higher order terms, the above equation becomes

$$\mathbf{r}^{CT} = \begin{pmatrix} 1 & 0 & x_p \\ 0 & 1 & -y_p \\ -x_p & y_p & 1 \end{pmatrix} \mathbf{r}^{\Pi} \quad . \tag{2.27}$$

Since polar motion values, x_p, y_p, are published only at certain epochs, just as UT1 - UTC, polar motion values for other epochs have to be interpolated using polynomials.

2.1.4 Coordinate System for the Equations of Motion

The coordinate system used to establish the equations of motion in our orbit improvement model is chosen to have a constant orientation with respect to the mean equatorial coordinate system at J2000.0 for the entire observation period. This coordinate system is defined by the following equation:

$$\mathbf{r}_0 = \mathbf{R}_3(-\omega \, (t_0 - t_w)) \, \mathbf{r}^{true}|_{t_0} \quad , \tag{2.28}$$

where

t_0 is the time of the initial epoch for the equations of motion (see Chapter 4) and selected to be the beginning epoch of the related data set to be processed,

t_w is the time at the beginning of the GPS week corresponding to t_0,

$\mathbf{r}^{true}|_{t_0}$ is a vector in the true equatorial coordinate system of epoch t_0,

$\mathbf{r}_0$ is the vector after the transformation,

ω is the rate of the Earth rotation as defined in the World Geodetic System 1984 (WGS 84) [Decker, 1986].

Throughout the rest of the thesis, the coordinate system defined by equation (2.28) is called the inertial coordinate system of initial condition (or simply, the initial condition system). The rationale for using this system is that the approximate initial state vector of a GPS satellite is more readily available in this system. The coordinate system transformation between the Earth-fixed and the inertial coordinate system of initial condition is derived as follows:

$$ r^{CT} = R_2(-x_p)\, R_1(-y_p)\, R_3(GAST)\, N\, P\, (N_o\, P_o)^T\, R_3(\omega\, (t_0 - t_w))\, r_0 \; , \qquad (2.29) $$

where

N_o, P_o are the nutation and precession matrices to transform from J2000.0 to the initial epoch of the equations of motion,

r^{CT} is the state vector in the Earth-fixed coordinate system,

and the remaining parameters have been defined earlier.

2.2 Conversion to the Antenna Phase Center of a GPS Satellite

There is an offset between the mass center of a GPS satellite and the electrical phase center of its antenna. The solution of the equations of motion of the satellite gives the coordinates of the mass center, whereas a GPS signal is measured from the antenna phase center. Therefore, the position of the satellite should be transformed to its antenna phase center before it is used in the observation equation.

The relationship between the mass and the antenna phase centers is [Sovers and Border, 1988]:

$$ r_{phase} = r_{mass} + (0.211\, i + 0.886\, k)\ \text{meters} \; , \qquad (2.30) $$

where

26

k   is the unit vector from the mass center of the satellite to the geocenter,

i   is the unit vector completing a right-handed coordinate system together with **j** and **k**. Here, **j** is defined as the normalized cross product of **k** with the unit vector pointing from the satellite to the Sun.

2.3 Conversion to the Antenna Phase Center of a Receiver

It is necessary to relate the station coordinates to the phase center of the receiver's antenna to form the observation equations. A GPS signal is measured with respect to the antenna phase center of a receiver, but the antenna phase center has an offset from the station position (usually, a geodetic marker imbedded in the ground). Furthermore, the position of the station is subject to variations. Therefore, the transformation to the phase center of the antenna is divided into two parts: the first is to transfer the mean coordinates of the station to instantaneous coordinates of the station; the second is to transfer the instantaneous position of the station to the position of the antenna phase center. The first part is discussed in Section 2.3.1, and the second part is discussed in Section 2.3.2.

2.3.1 Tidal Variation of a Station

Only the solid Earth tidal displacement is considered for the instantaneous variation, since it is the most prominent effect. The solid Earth tidal displacement is caused by the deformation under the luni-solar gravitational attractions. In our model, only the vertical displacement of the solid Earth tide (the most significant effect) is considered.

The vertical tidal displacement, dH, is expressed as [Vanicek and Krakiwsky, 1986]

$$dH = \frac{h\, W_d}{g} \,,$$

(2.31)

$$W_d = \frac{3GM_d R^2}{2r_d^3} (\cos^2 Z - \frac{1}{3}) \ , \tag{2.32}$$

where

W_d is the perturbing potential from the gravitational attraction of a third body (the

Sun or the Moon),

R is geocentric distance of the station,

g is the gravity at the Earth's surface,

GM_d is the gravitational constant of the third body,

R is the geocentric distance of the station,

r_d is the geocentric distance of the third body,

h is the first Love number for the second order tidal effect,

Z is the zenith distance (angle) of the third body at the station.

The effect of this term in the instantaneous station position is

$$\delta R = \frac{R}{R} \ dH \ , \tag{2.33}$$

where $\mathbf{R}$ is the station position vector.

The permanent tide should also be taken into account, if the mean station coordinates include this term. The permanent tide is the permanent displacement in the tidal variation as expressed in equations (2.31) and (2.32). If the position of the station includes the permanent tidal displacement, this term has to be subtracted from dH in equation (2.31).

The total permanent tidal effect for both the Sun and the Moon [Boucher, 1988] is

$$\Delta H_{perm} = -0.121 \ (3/2 \sin^2 \phi - 1/2) \quad (m) \ , \tag{2.34}$$

where

ϕ is the geocentric spherical latitude.

28

2.3.2 Conversion to the Antenna Phase Center

To form an observation equation, the instantaneous position of a station has to be converted to the position of the antenna phase center of its receiver. The offset between the station mark and the antenna phase center is usually just in the height. Therefore, the conversion from the station mark to the antenna phase center, $\delta \mathbf{R}$, is

$$\Delta \mathbf{R} = \frac{\mathbf{R}}{R} \Delta H_{phase} \quad , \tag{2.35}$$

where

ΔH_{phase} is the height of the antenna phase center above the geodetic marker.

To end this chapter, it should be pointed out that the CT coordinate system is often realized by the coordinate system defined by the fiducial points (points held fixed in the adjustment process). More details on the fiducial point approach used in our data processing will be discussed in Chapter 7.

CHAPTER 3
FORCE MODELLING FOR GPS SATELLITES

The forces acting on GPS satellites must be modelled to establish their equations of motion. The force modelling for a GPS satellite is one of the major factors affecting the precision of the orbit improvement. A major difference between a long arc approach and a short arc approach is that the long arc approach requires a more precise force model.

In addition to the well-known geocentric components of gravitation, various other forces acting on a GPS satellite cause the perturbation of the elliptical orbit of the satellite. In the presence of the perturbing forces, the equations of motion of the satellite in a geocentric inertial coordinate system can be written as,

$$\ddot{\mathbf{r}} = -\frac{GM\,\mathbf{r}}{r^3} + \mathbf{P} , \qquad\qquad (3.1)$$

where

  $\mathbf{r}$ is the geocentric position vector of the satellite,

  r is the geocentric distance of the satellite,

  $\ddot{\mathbf{r}}$ is the second derivative of the position with respect to time (acceleration),

  GM is the gravitational constant of the Earth,

  $\mathbf{P}$ represents the sum of the perturbing forces on the satellite,

and the first term on the right side in the above equation is the central component of the Earth's gravitational force per unit mass.

The perturbing forces investigated in this research are:

  1) The non-spherical gravitational component of the Earth;

2) The gravitational attraction of the Moon and the Sun;

3) The solar radiation pressure;

4) The solid Earth tidal gravity.

The modeling of the above forces is discussed in Sections 1, 2, 3, and 4. The final section discusses the forces not included in our model.

3.1 Perturbation due to the Earth's Gravitation

The most significant perturbation of the elliptical motion of a GPS satellite is caused by the non-spherical components of gravitation of the Earth. The gravitational potential of the Earth, U, can be represented by a spherical harmonic expansion [Vanicek and Krakiwsky, 1986],

$$U = \frac{GM}{r} \left\{ 1 + \sum_{n=2}^{\infty} \sum_{m=0}^{n} \left(\frac{a_e}{r}\right)^n P_n^m(\sin\phi) \left[C_{nm} \cos m\lambda + S_{nm} \sin m\lambda \right] \right\}, \qquad (3.2)$$

where

ϕ is the geocentric latitude of the satellite in the Earth-fixed coordinate system,

λ is the geocentric east longitude of the satellite,

a_e is the mean equatorial radius of the Earth,

n is the degree of the geopotential coefficient,

m is the order of the geopotential coefficient,

$P_n^m(\sin\phi)$ is the associated Legendre function (see Vanicek and Krakiwsky [1986]),

C_{nm}, S_{nm} are the denormalized geopotential coefficients.

31

The first term in equation (3.2) is the geocentric potential responsible for the elliptical motion of the satellite; the remaining terms are regarded as the gravitational perturbing potential.

The geopotential coefficients are often given in the normalized format [Vanicek and Krakiwsky, 1986]. The relationship between the normalized and denormalized coefficients is

$$\begin{pmatrix} \overline{C}_{nm} \\ \overline{S}_{nm} \end{pmatrix} = \left[\frac{(n+m)!}{(n-m)!\,(2n+1)\,(2-\delta_m)} \right]^{1/2} \begin{pmatrix} C_{nm} \\ S_{nm} \end{pmatrix} , \tag{3.3}$$

where

$\overline{C}_{nm}, \overline{S}_{nm}$ are the normalized geopotential coefficients,

δ_m is the Kronecker delta function; $\delta_m = 1$ for $m = 0$, and $\delta_m = 0$ for $m \neq 0$.

Equation (3.3) is derived from the relationship between denormalized and normalized harmonic Legendre functions [Vanicek and Krakiwsky, 1986].

By taking partial derivatives of equation (3.2) with respect to the radial, longitude, and latitude directions of the satellite, the components of the gravitational perturbing force per unit mass as functions of spherical coordinates can be derived as follows:

$$F_r = -\frac{GM}{r^2} \left\{ \sum_{n=2}^{\infty} \sum_{m=0}^{n} \left(\frac{a_e}{r}\right)^n (n+1)\, P_n^m(\sin\phi) \left[C_{nm}\cos m\lambda + S_{nm} \sin m\lambda \right] \right\} ,$$

$$F_\lambda = \frac{GM}{r^2 \cos f} \left\{ \sum_{n=2}^{\infty} \sum_{m=0}^{n} \left(\frac{a_e}{r}\right)^n m\, P_n^m(\sin\phi) \left[S_{nm}\cos m\lambda - C_{nm} \sin m\lambda \right] \right\} ,$$

$$F_\phi = \frac{GM}{r^2} \left\{ \sum_{n=2}^{\infty} \sum_{m=0}^{n} \left(\frac{a_e}{r}\right)^n \frac{\partial}{\partial\phi} \left[P_n^m(\sin\phi) \right] \left[C_{nm}\cos m\lambda + S_{nm} \sin m\lambda \right] \right\} ,$$

$$\tag{3.4}$$

where

F_r, F_λ, and F_ϕ are the force components in the directions of r, λ, and ϕ respectively, and

$$\frac{\partial}{\partial \phi}\left[P_n^m(\sin \phi)\right] = P_n^{m+1}(\sin \phi) - m(\tan \phi) P_n^m(\sin \phi) \quad . \tag{3.5}$$

The above components should be transformed to the same coordinate system as the equations of motion of the satellite. They are first transformed to the Earth-fixed geocentric coordinate system, and then are transformed to an inertial coordinate system of initial condition (see Chapter 2). The latter transformation is the reverse of equation (2.29).

The coefficient, C_2^0 (represents the flattening of the geopotential), causes the most significant perturbation of the satellite orbit and this perturbation is at least one thousand times larger than the other gravitational perturbations. It is responsible for the slow precession of the nodal line of the satellite orbit (see Chapter 4) around the equator of the Earth. Because a GPS satellite is in a high stable orbit of approximately 20 000 km altitude, higher order gravitational terms have much less effect on its orbit. Therefore, the geopotential coefficients up to degree and order 8 are sufficient for the computation of a GPS satellite orbit. Tests were made during the software development, and the effect of the higher order gravitation was below 10 cm for an orbital arc of one week.

3.2 Gravitational Effects of the Sun and the Moon

The gravitational effect of a third body (also called the external body) is expressed as:

$$\mathbf{P_d} = GM_d\left[\frac{\mathbf{r_d} - \mathbf{r}}{|\mathbf{r_d} - \mathbf{r}|^3} - \frac{\mathbf{r_d}}{|\mathbf{r_d}|^3}\right] \quad , \tag{3.6}$$

where

GM_d is the gravitational constant of the third body,

$\mathbf{r_d}$ is the geocentric position vector of the third body.

The perturbation due to the Sun and the Moon is the second most significant, next to the gravitational perturbation. In our present orbit improvement model, the third bodies include only the Sun and the Moon.

To be used in the equations of motion, the expression in equation (3.6) should be transformed to a coordinate system of initial condition (Section 2.1.4). The coordinate system transformation should also be applied to the effect of the solar radiation pressure and the solid Earth tidal deformation (described in Sections 3 and 4 of this chapter).

3.3 Effect of Solar Radiation Pressure

The solar radiation pressure is caused by the absorption and reflection of the solar radiation incident on a GPS satellite. Two components of the solar radiation pressure are considered in this research. One is the direct component, and the other is the y-direction component. They are discussed separately in the following two subsections.

3.3.1 Direct Radiation Pressure

Direct solar radiation pressure is the solar radiation pressure in the direction from the Sun to a GPS satellite, and it is the primary radiation pressure on the satellite. The effect is usually approximated by the following expression [Rizos and Stolz, 1985]:

$$\mathbf{P}_{ra} = \nu \; p_s \, C_r \frac{A}{m} \frac{a_s^2 (\mathbf{r} - \mathbf{r}_s)}{|\mathbf{r} - \mathbf{r}_s|^3} \; , \tag{3.7}$$

where

$\mathbf{P}_{ra}$ is the direct radiation pressure,

v	is the eclipse factor (0 or 1, depending on whether the satellite is in the shadow of the Earth or not),
a_s	is the mean radius of the Earth's orbit around the Sun,
p_s	is the solar radiation pressure in Newton/m^2,
C_r	is the reflection constant,
A	is the effective cross-section surface area of the satellite experiencing solar radiation pressure,
m	is the mass of the satellite,
r_s	is the geocentric position vector of the Sun.

The difficulty encountered in analyzing the solar radiation pressure is that not all parameters are available to the general scientific community. Therefore, in this research, the unknown constants p_s, C_r, and $\frac{A}{m}$ are grouped together into one parameter, called the direct solar radiation pressure parameter, p_0. The effect of the solar radiation pressure is then described as

$$\mathbf{P}_{ra} = -\ v\ p_0 \frac{a_s^2}{|\mathbf{r} - \mathbf{r}_s|^2}\ \mathbf{e}_0 \quad ,$$ (3.8)

where

$\mathbf{e}_0$ is the unit vector pointing from the satellite to the Sun.

The direct solar radiation pressure parameter, p_0, is designated as an unknown for each satellite in our orbit improvement model. In our present software implementation, the single value is used for the whole orbital arc.

In equation (3.8), the intensity variation due to the motion of the satellite can be neglected. The simplified description used in our model is,

$$\mathbf{P}_{ra} = -\ v\ p_0 \mathbf{e}_0 \quad ,$$ (3.9)

The *a priori* value used for p_0 is 0.90D-7 m/sec^2.

35

Note that the estimated parameter, p_0, can partially absorb other effects such as thermal radiation of the satellite in the direction from the satellite to the Sun. Also, ν changes gradually as a satellite moves into (or moves out of) the Earth's shadow. This gradual change of ν is not taken into account in our present model, and a test of this gradual change is discussed in Chapter 7.

3.3.2 y-Direction Radiation Pressure

To describe the y-direction solar radiation pressure, it is necessary to describe the orientation of the satellite surfaces with respect to the Sun. The satellite z-axis is positive along its antenna and therefore, is nominally toward the center of the Earth. The y-axis is along the solar panel beam normal to the plane containing the Sun, the Earth, and the satellite. A step motor rotates the solar panel about the y-axis so that it presents a maximum possible area toward the Sun.

The effect of the y-bias is due to structural misalignments and thermal radiation of the satellite. The causes are explained as follows [Fliegel et al., 1985]:

1) Structural misalignments: By design, the solar array center beam should be perfectly straight and normal to the line between the satellite and the Sun. These conditions may be violated for three reasons. First, the axes of the two "wings" containing the solar panels do not lie on a perfect straight line; secondly, the active solar sensor for steering the panels may not be perfectly normal to the solar panel axis; thirdly, it is expected there are some biases in the direction control of the panels.

2) Thermal radiation: Excess heat from the satellite is vented through louvers, preferentially in the y-direction. Furthermore, because a satellite is not in a thermal steady

state, thermal transients may cause the deformation of the solar panel center beam, and this contributes to the y-direction radiation pressure.

In the model for direct radiation pressure, a parameter for the y-bias radiation pressure is incorporated and treated as an unknown since the various parameters governing the y-bias radiation pressure are usually not precisely known. Thus, the effect of the y-direction radiation pressure can be expressed as

$$\mathbf{P}_{y\text{-bias}} = v\, p_y\, \mathbf{e}_y \quad , \tag{3.10}$$

where

$\mathbf{P}_{y\text{-bias}}$ is the solar radiation acceleration in the y-direction,

p_y is the unknown parameter for y-bias radiation pressure,

$\mathbf{e}_y$ is the unit vector in the y-direction.

The parameter p_y is designated and solved for in the data processing.

3.4 The Solid Earth Tidal Effect

The gravitational attraction of a third body on the Earth causes a deformation of the solid Earth body, and this deformation, in turn, causes a variation in the geopotential. This geopotential adds a perturbation to the motion of a GPS satellite. According to Melchior [1983], the generating tidal potential (the potential caused by the gravity of the third body) in a first-order approximation at a point on the Earth's surface is given as

$$W_d = \frac{GM_d}{r_d^3}\, a_e^2\, P_2(\cos Z) \quad , \tag{3.11}$$

where

W_d is the generating tidal potential,

GM_d is the gravitational constant of the third body,

37

r_d is the geocentric distance of the third body,

Z   is the angle between the geocentric vectors of the satellite and that of the

        third body.

The solid Earth tidal potential caused by this deformation is described as [Melchior, 1983]

$$V_b = \left(\frac{a_e}{r}\right)^3 k_2 W_d \quad , \tag{3.12}$$

where

V_b is the solid Earth tidal potential,

r   is the geocentric distance of the satellite,

k_2 is the second Love's number of order 2. It describes the response of the

        Earth to the generating potential as in equation (3.11). The value we have

        used is 0.29 [Vanicek and Krakiwsky, 1986].

The perturbing force is obtained by taking the partial derivative of equation (3.12) with respect to the satellite position vector. The result of the derivation is

$$P_b = \frac{3}{2} \frac{GM_d \, a_e^5}{r_d^3 \, r^4} k_2 \left[\left(1 - 3\cos^2 Z\right) \frac{\mathbf{r}}{r} - 2 \sin Z \cos Z \, \mathbf{e}_Z \right] \quad , \tag{3.13}$$

where

$\mathbf{P}_b$ is the acceleration caused by the solid Earth tide,

$\mathbf{e}_Z$ is the unit vector in the plane of the angle Z, and is perpendicular to $\mathbf{r}$ (the

        geocentric position of the satellite).

The above equation is equivalent to [Rizos and Stolz, 1985]

$$P_b = \frac{3}{2} \frac{GM_d \, a_e^5}{r_d^3 \, r^4} k_2 \left[\left(1 - 5\cos^2 Z\right) \frac{\mathbf{r}}{r} + 2 \cos Z \, \frac{r_d}{r_d} \right] \quad . \tag{3.14}$$

It is sufficient to take into account the solid Earth tide corresponding to only the Moon and the Sun. The effect of the solid Earth tide on the GPS satellite orbits is at about the one or two meter level for an orbital arc of one week.

3.5 Other Perturbations

Perturbations not included in our orbit improvement model are the effects of ocean tides, the gravitational fields of planets, air drag, albedo, relativity, higher order (higher than 8) gravitational components of the Earth, and maneuvering of satellites. However, for completeness, they are described briefly as follows:

1) The effect of ocean tides: The gravitation of a third body causes the redistribution of the ocean water (called ocean tides), and in turn, the ocean tides change the gravitation of the Earth. The effect of the ocean tides on a GPS satellite orbit is in the order of ten centimeters for an orbital arc of one week [Landau and Hagmaier, 1986].

2) The effect of planets: The gravitational effect of the planets also causes the perturbation of a satellite orbit. The total gravitational effect of the other planets is about 30 centimeters for an orbital arc of one week [Landau and Hagmaier, 1986].

3) The effect of albedo: This effect is caused by the reflection of solar radiation by the Earth. The Earth also radiates its own energy. The effect of this radiation on satellite orbits is the most difficult perturbation to model. The difficulty comes from various factors. The reflection and radiation of the Earth at different locations are irregular and they vary from 20% to 80% from a nominal value; they are also weather dependent [Rizos and Stolz, 1985]. The effect is absorbed partially in the uncertainty of the gravitational constant of the Earth.

4) The effect of relativity: The dynamical motion in our model is described by Newtonian physics, and the relativistic effect has been neglected. The effect of relativity effect is well below 1 m for a GPS satellite [Laurence, 1985].

5) The effect of thermal radiation: A GPS satellite emits its own thermal radiation and so there is a corresponding force acting on the satellite. The constant components in the direction to the Sun and the y-direction are absorbed in the corresponding solar radiation parameters, and the component in the direction to the Earth center is absorbed in the uncertainty of the GM value.

6) The effect of the higher order gravitational components of the Earth: This refers to the gravitational effect of degree and order higher than 8. These terms are negligible due to the high altitude of a GPS satellite. As stated in Section 3.1, the effect is much below one meter for an orbital arc of one week.

7) The effect of satellite maneuvering: The orbit of a satellite is sometimes required to be adjusted and it is realized by the releasing of the energy stored in the satellite. This effect is difficult to model. It happens rarely, but is significant if it does happen. A possible approach is that a new set of the initial conditions is used after each maneuver.

8) The effect of air drag: The effect of air drag is negligible due to the high altitude of a GPS satellite.

Most of the above effects should be taken into account for a more precise orbit improvement model. The effect of maneuvering should be taken into account in the planning of a GPS project, and in the design of the data processing approach.

CHAPTER 4
ORBIT INTEGRATION METHODS

An integration technique is required to solve the differential equations of motion of GPS satellites. Whereas the force model dictates the accuracy of the equations of motion, the integration technique dictates the precision of the solution of the equations of motion. The force modelling has been discussed in Chapter 3, and the integration technique is discussed in this chapter. The orbit of a satellite under the action of a central gravitational field is discussed in Section 1, and various integration methods for a satellite trajectory are discussed in Section 2.

When the improvement of the initial condition and the force model of the satellite is involved (e.g., to estimate the two radiation parameters for each satellite), we must know the partial derivatives with respect to initial conditions and certain dynamical parameters. To obtain these partial derivatives, the integration technique is also required. The integration technique for the partial derivatives is discussed in Section 3.

4.1 Elliptical Orbit under the Geocentric Gravitation

If a GPS satellite is subject to only the central component of the Earth's gravitational field, its trajectory is an ellipse with the mass centre of the Earth as one of two foci of the ellipse (the general relativistic effect is not considered here). A satellite's elliptical motion can be described by the Keplerian orbital elements which describe the size, shape, and the orientation of the ellipse, and the relative location of the satellite on the ellipse.

41

The size and the shape of the ellipse are determined by its semi-major axis, a, and the eccentricity, e (see Figure 4.1). The orientation of the ellipse is defined by the argument of perigee, ω, the inclination of the orbital plane with respect to the equator, i, and the right ascension of the ascending node (the intersection of the orbital plane with the equator), Ω (see Figure 4.2). The position of the satellite in the orbital plane is specified by the true anomaly, f, defined as the angle formed by the perigee, the focus, and the satellite, or equivalently, by the eccentric anomaly, E, (see Figure 4.1). The relationship between f and E is given as [Laurence, 1985]

$$\tan\frac{f}{2} = \left[\frac{1+e}{1-e}\right]^{1/2}\tan\frac{E}{2} \quad . \tag{4.1}$$
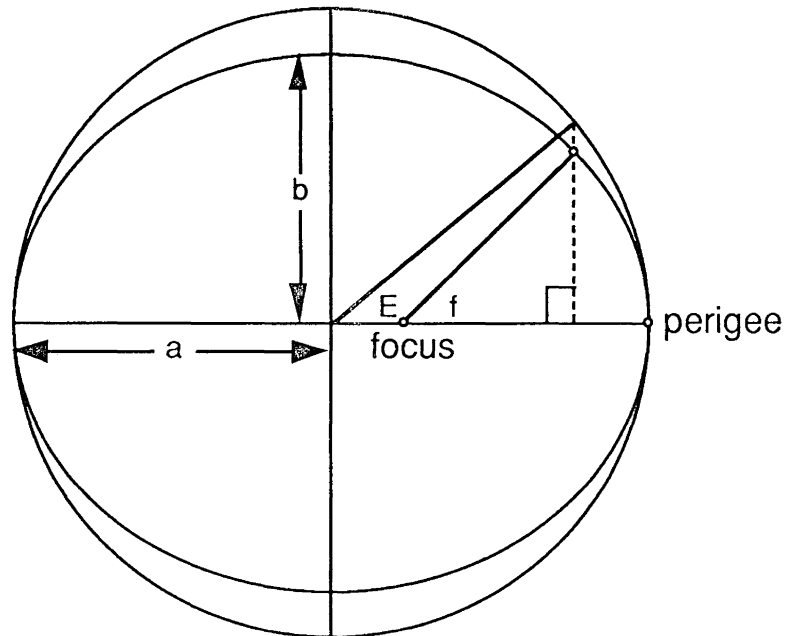
Figure 4.1 Elliptical orbit of a satellite

42
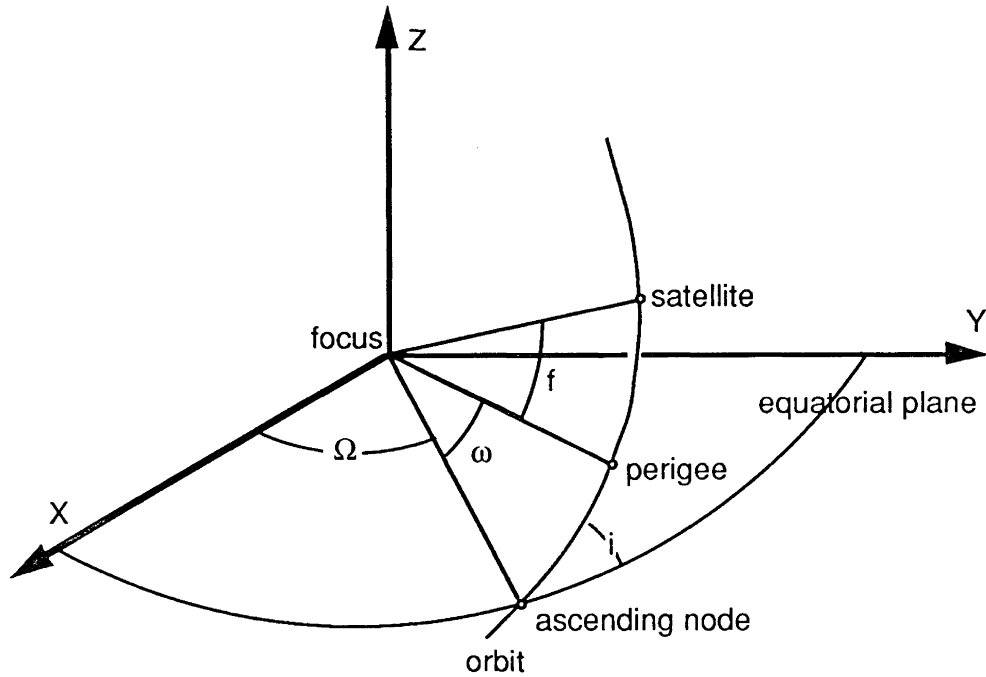
Figure 4.2 Orientation of the orbit of a satellite

Thus, the elliptical motion of a satellite is described by the set, $\{a, e, i, \omega, \Omega, \tau\}$, where τ is the time of perigee passage. The eccentric anomaly is calculated from the mean anomaly. The mean anomaly M is defined as the angle between the line from the focus to the perigee and the line from the focus to an imaginary satellite moving in a circular orbit with a speed equal to the mean motion (defined below) of the actual satellite. The imaginary satellite in this motion passes through the perigee at the same time as the actual satellite. The mean anomaly M can be calculated using

$$M = n\,(t - \tau) \quad, \tag{4.2}$$

where

t   is the time,

n   is the mean motion and is calculated as

$$n = (u\,/\,a^3)^{1/2} \quad, \tag{4.3}$$

u   is the gravitational constant GM.

43

The eccentric anomaly is related to the mean anomaly implicitly through Kepler's equation as follows:

$$M = E - e \sin E \ .$$

<div align="right">(4.4)</div>

Under perturbations acting on a satellite, the motion of the satellite is not precisely elliptical, but Keplerian orbital elements are still used to describe the perturbed orbits. This is done through the use of osculating Keplerian orbital elements. The osculating Keplerian orbital elements at a specific epoch are defined as the Keplerian orbital elements of the orbit in which a satellite will move around if all perturbing forces on the satellite disappear completely at that epoch [Langley, 1988a].

The position and velocity of a satellite can be represented by the osculating Keplerian orbital elements. Since the state vector of a satellite corresponds uniquely to a set of the osculating elements at any given instant, the state vector of the satellite can be described as functions of the varying osculating Keplerian elements. The relationship of the position and velocity vector of a satellite with the six osculating Keplerian elements in the orbital system is [Wells et al., 1987]

$$\mathbf{q} = \frac{a\,(1 - e^2)}{(1 + e \cos f)} \begin{bmatrix} \cos f \\ \sin f \\ 0 \end{bmatrix} = \begin{bmatrix} a \cos E - a\,e \\ a\,\sqrt{1 - e^2}\,\sin E \\ 0 \end{bmatrix} \ ,$$

<div align="right">(4.5)</div>

$$\dot{\mathbf{q}} = \frac{n\,a}{(1 - e \cos E)} \begin{bmatrix} -\sin E \\ \sqrt{1 - e^2}\,\cos E \\ 0 \end{bmatrix} \ ,$$

<div align="right">(4.6)</div>

where

<div align="center">44</div>

q and $\dot{q}$ are the position and velocity vectors respectively (with components specified in the orbital coordinate system).

The position and velocity in the inertial coordinate system of the initial conditions are

$$r_0 = R_{xq}\, q \qquad \text{and}$$

$$\dot{r}_0 = R_{xq}\, \dot{q} \quad , \tag{4.7}$$

where

$$R_{xq} = R_3(-\Omega)\, R_1(-i)\, R_3(-\omega) \quad . \tag{4.8}$$

There are two methods to solve for the position vector of a satellite from the equations of motion under perturbing forces: one is called the analytical method and the other is the numerical method. Emphasis in this thesis is on the numerical method since it was used in our research.

4.2 Integration of the Initial Value Problem

The integration of the initial value problem is discussed in this section. An analytical method is introduced briefly in subsection 1 and numerical methods are discussed in subsection 2.

4.2.1 Analytical Method

The difficulty as posed in equation (3.1) is that the direct analytical solution in a Cartesian coordinate system is intractable. To tackle this problem, the equations of motion are expressed as the Lagrangian equations and are solved using the method of variations. The Lagrangian equations for Keplerian orbital elements can be developed as [Laurence, 1985],

$$\frac{da}{dt} = 2\sqrt{\frac{a}{u}}\, \frac{\partial R}{\partial M} \quad ,$$

$$\frac{de}{dt} = \frac{1}{\sqrt{ua}} \left[\frac{(1-e^2)}{e}\, \frac{\partial R}{\partial M} - \frac{(1-e^2)^{1/2}}{e}\, \frac{\partial R}{\partial \omega} \right] \quad ,$$

$$\frac{d\omega}{dt} = \frac{1}{\sqrt{ua}} \left[\frac{(1-e^2)^{1/2}}{e}\, \frac{\partial R}{\partial e} - \frac{\cot i}{(1-e^2)^{1/2}}\, \frac{\partial R}{\partial i} \right] \quad ,$$

$$\frac{di}{dt} = \frac{1}{\sqrt{ua}} \left[\frac{\cot i}{(1-e^2)^{1/2}}\, \frac{\partial R}{\partial \omega} - \frac{1}{(1-e^2)^{1/2}\sin i}\, \frac{\partial R}{\partial \Omega} \right] \quad ,$$

$$\frac{d\Omega}{dt} = \frac{1}{\sqrt{ua}} \left[\frac{1}{(1-e^2)^{1/2}\sin i}\, \frac{\partial R}{\partial i} \right] \quad ,$$

$$\frac{dM}{dt} = \sqrt{\frac{a}{u}} \left[\frac{u}{a^2} - \frac{(1-e^2)}{a\,e}\, \frac{\partial R}{\partial e} - 2\frac{\partial R}{\partial a} \right] \quad , \tag{4.9}$$

where the function R represents the perturbing potentials.

To demonstrate the analytical approach of the orbital integration, only the gravitational perturbation of the Earth is considered. Since C_{20} is at least one thousand times as large as any of the other non-central gravitational terms, the following secularly-varying Keplerian elements can be obtained by simplifying the right side of equation (4.9). In this first attempt of the solution, all perturbing terms except the C_{20} are disregarded, and all Keplerian elements on the right side of equation (4.9) are replaced with those of some initial epoch. The simplified equations of motion can be shown to be [Kaula, 1966]

$$\dot{\omega} = \frac{3}{4}\, \frac{n_0}{(1-e_0^2)^2}\, C_{20} \left[\frac{a_e}{a_0} \right]^2 (1-5\cos^2 i_0) \quad ,$$

$$\dot{\Omega} = \frac{3}{2}\, \frac{n_0}{(1-e_0^2)^2}\, C_{20} \left[\frac{a_e}{a_0} \right]^2 \cos i_0 \quad ,$$

$$\dot{M} = n_0 - \frac{3}{4} \frac{n_0}{(1-e_0^2)^{3/2}} C_{20} \left[\frac{a_e}{a_0}\right]^2 (3\cos^2 i_0 - 1) \; , \tag{4.10}$$

$$\dot{i} = 0 \; ,$$

$$\dot{a} = 0 \; ,$$

$$\dot{e} = 0 \; ,$$

where

a_0, e_0, Ω_0, i_0, M_0, and ω_0 are Keplerian orbital elements at the initial epoch,

a_e is the equatorial radius of the Earth,

n_0 is described by equation (4.3). It corresponds to the initial epoch.

The secular solution derived from the above equations is,

$$\omega = \omega_0 + \dot{\omega} \, (t - t_0) \; ,$$

$$\Omega = \Omega_0 + \dot{\Omega} \, (t - t_0) \; ,$$

$$M = M_0 + \dot{M} \, (t - t_0) \; ,$$

$$a = a_0 \; ,$$

$$e = e_0 \; ,$$

$$i = i_0 \; , \tag{4.11}$$

where t_0 is the time of the initial epoch.

The solution given by equations (4.11) is called the secular solution. Using the above equations to replace all Keplerian elements on the right side of equation (4.9), a first order approximation solution can be derived. However, for a GPS satellite, the first order solution is not accurate enough and a higher order solution is required.

The higher order solution can be derived using a method similar to the first order solution. For example, the second order solution can be obtained by replacing the Keplerian orbital elements on the right side of equations (4.9) with the first order solution described above, the solution is then derived from integrating the right side of the equations.

There are some other methods for the analytical solution of the orbit, for instance, the Lie-Hori perturbation method which is based on finding quantities which are constant in the perturbing problem. The approach is based on the canonical transformation for the equations of motion in which some of variables become constants, and the resulting equations can be integrated easily [Gaposchkin, 1973].

The main disadvantage of the analytical approach is heavy mathematical derivation and high computational demand. Another disadvantage of the analytical approach is the difficulty in incorporating various kinds of force models. For GPS applications, it is more practical to use a numerical method. Various numerical techniques are discussed in the next subsection.

4.2.2 Numerical Integration Methods

There are many numerical integration methods for solving the problem of orbital motion. The underlying principle of a numerical integration technique is to approximate a rigorous solution with a truncated Taylor series. In the following subsections, several numerical integration methods are examined.

4.2.2.1 *Runge-Kutta Method*

In using the Runge-Kutta Method, the system of the equations of motion of a satellite is written as

$$\dot{X} = F \quad , \tag{4.12}$$

where

$$X = (x_1, x_2, x_3, x_4, x_5, x_6) = (x, y, z, \dot{x}, \dot{y}, \dot{z}) \quad ,$$

$$F = (x_4, x_5, x_6, f_x, f_y, f_z) \quad , \tag{4.13}$$

x, y, z represent the coordinates of the satellite,

$\dot{x}, \dot{y}, \dot{z}$ represent the velocity components of the satellite,

f_x, f_y, f_z represent the specific force components acting on the satellite.

The initial condition of equation (4.12) is,

$$x_0 = (x_0, y_0, z_0, \dot{x}_0, \dot{y}_0, \dot{z}_0) \quad . \tag{4.14}$$

where $x_0, y_0, z_0, \dot{x}_0, \dot{y}_0, \dot{z}_0$ are the position and velocity components at the initial epoch.

The integration of equation (4.12) can be carried out using the fourth order Runge-Kutta method [Kaula, 1966] as follows:

$$k^1 = F(X_{i-1}, t_{i-1}) \Delta t \quad ,$$

$$k^2 = F(X_{i-1} + k^1 / 2, t_{i-1} + \Delta t / 2) \Delta t \quad ,$$

$$k^3 = F(X_{i-1} + k^2 / 2, t_{i-1} + \Delta t / 2) \Delta t \quad ,$$

$$k^4 = F(X_{i-1} + k^3, t_{i-1} + \Delta t) \Delta t \quad ,$$

$$X_i = X_{i-1} + k^1 / 6 + k^2 / 3 + k^3 / 3 + k^4 / 6 \quad , \tag{4.15}$$

where

k^1, k^2, k^3, k^4, are the intermediate results to compute the final X_i,

i   denotes the epoch ($\Delta t = t_i - t_{i-1}$).

Higher order Runge-Kutta methods are given by Lambert [1973]. However, as the order of the integrator increases, the computation burden increases greatly. Therefore, the precision of the integration is usually increased by reducing integration steps (the time interval Δt) instead of increasing the order of the integration in the Runge-Kutta method.

4.2.2.2   Predictor-Corrector Method

There are two methods in which the predictor-corrector method may be applied. The first one is exploited for the system of the first order differential equation (4.12). In this method, the entire time period for the integration is divided into equal intervals (called steps) and two formulae are involved: one is called the predictor, and the other is called the corrector. In the predictor, F_{i-k} corresponding to epoch i-k (k and i are integer numbers; i represents the current epoch) are employed (the value F_i of the current epoch is not included), i.e.,

$$X_i = X_{i-1} + \Delta t \sum_{k=1}^{v+1} A^p_{v,k} F_{i-k} \ , \tag{4.16}$$

and the corrector uses both the value F_i of the current epoch and the value F_{i-k} of the previous epochs, i.e.,

$$X_i = X_{i-1} + \Delta t \sum_{k=0}^{v} A^c_{v,k} F_{i-k} \ , \tag{4.17}$$

where

v   is the order of the integrator,

Δt is the step of the integration,

50

$A^p_{v,k}$, $A^c_{v,k}$ are the integration coefficients obtained using the solutions of Taylor expansion [Velez and Maury, 1970]. Superscripts, p, and c, represent the predictor and corrector respectively.

Value F_i on the right side of the corrector formula is calculated from the predicted value X_i. The procedure in using this integration method is

1) Get the predicted value using equation (4.16).

2) Get the corrected value using equation (4.17) with X_i from step 1.

3) Repeat the steps until convergence.

4) Repeat steps 1 through 3 for the subsequent epochs, until the end of the orbital arc.

The second type of the predictor-corrector method is designed for the direct integration of the second order differential equations of motion of a GPS satellite.

The equation of motion can be written as $\ddot{r} = f(r)$. Since the force model of the GPS satellite does not contain a velocity term, positions of the satellite can be obtained by the direct integration of the system of the second order differential equations of motion. Here, predictor and corrector formulae similar to those used for the first order equation can be applied directly.

The predictor for the solution of the above equation is

$$r_i = 2\, r_{i-1} - r_{i-2} + \Delta t^2 \sum_{k=1}^{v} B^p_{v,k}\, f_{i-k} \quad ,$$

and the corrector is

$$r_i = 2\, r_{i-1} - r_{i-2} + \Delta t^2 \sum_{k=0}^{v-1} B^c_{v,k}\, f_{i-k} \quad , \tag{4.18}$$

where

    r represents the position of the satellite,

f   represents the value of the function which maps the position into its second

order derivative,

$B^c_{v,k}$ and $B^p_{v,k}$ are integration coefficients which can be obtained from Velez and

Maury, [1970].

The procedure of using the above equations is the same as that used in solving the

first order differential equations except that the velocity terms cannot be obtained directly.

The advantage of this method over the former one is that it requires less computer memory

and computation time.

4.2.2.3 *Approximation Function Method*

In this method, the true solution is approximated by a finite series, $r^*(t)$ (a linear

combination of some known base functions, $g_i(t)$) [Beutler et al., 1984], i.e.:

$$r^*(t) = \sum_{i=0}^{v} a_i \, g_i(t) \quad , \tag{4.19}$$

where

v   is the order of approximation,

a_i are the v+1 unknown coefficient vectors of the base functions. The base

functions $g_i(t)$ are usually algebraic polynomials, i.e.,

$$g_i = (t_0 - t_i)^i \quad , \qquad i = 0, 1, 2, 3 \ldots v, \tag{4.20}$$

where, t_0 is the time of the epoch chosen for the reference.

The purpose of this numerical integration procedure is to determine coefficients, a_i.

The procedure is usually carried out in the following steps:

1) The approximating function $r^*(t)$ should satisfy the initial conditions

corresponding to the differential equation.

2) The approximating function $r^*(t)$ should satisfy the differential equations describing the motion of the satellite at v-1 different epochs, t_i, i = 0, 1, ...v-2.

3) Together with the initial conditions, the system of equations formed in steps 1 and 2 is solved.

4.2.2.4 *Comparisons*

In contrast to the predictor-corrector method, the advantages of the Runge-Kutta method are

• Easy to program, no requirement for a starting algorithm.

• Easy to change step size, easy to deal with a sudden change in the force model.

The disadvantage of the Runge-Kutta method is that it requires more computational effort.

The advantages of the predictor-corrector method are:

• More efficient computation.

• Easy to evaluate local truncation errors.

The disadvantages of the predictor-corrector method are:

• Requires starting algorithm to carry on the forward calculation. This can be done either using the Runge-Kutta method or polynomial approximation function method for the computation of the starting points. The requirement of the starting algorithm complicates programming.

• Difficult to change the step size and to take into account a sudden change of the force model.

In contrast to the predictor-corrector method, the approximation function method has the advantage of not requiring a starting algorithm, and simpler programming. The disadvantage is less computational efficiency.

53

4.2.2.5 *Integration Technique Used in our Model*

The integration technique used in this research is the predictor-corrector method applied to the second order differential equations directly. Since the predictor-corrector method requires known position vectors at some beginning epochs for starting its computation, the polynomial method is employed for this purpose.

4.3 Integration Problem in Partial Derivatives

As discussed in Chapter 1, the orbit improvement process requires observations related to the position vectors of satellites. The positions are then related to the initial conditions. The initial state vector and the uncertainties in the force modelling are solved for as unknown parameters. The partial derivatives with respect to the initial conditions and the dynamical parameters, are required to solve for the unknowns.

In principle, the partials can be obtained by solving the differential equations and this problem is stated as follows:

The equations of motion of a satellite can be written in the form of,

$$\ddot{r} = f(r, \dot{r}, p_d) \quad . \tag{4.21}$$

By taking total differentials with respect to the initial state vector and dynamical parameters, the following differential equations can be obtained for the partials of the position vector with respect to the initial state vector, and the dynamical parameters:

for the initial state vector,

$$\ddot{Z}_K = \frac{\partial f}{\partial r} Z_K \quad , \tag{4.22}$$

54

where

$$Z_\kappa = \frac{\partial r}{\partial \kappa} \quad ,$$

κ Keplerian orbital elements;

for the dynamical parameters,

$$\ddot{Z}_{p_d} = \frac{\partial f}{\partial r} Z_{p_d} + \frac{\partial f}{\partial p_d} \quad , \tag{4.23}$$

where

$$Z_{p_d} = \frac{\partial r}{\partial p_d} \quad ,$$

and p_d represents the dynamical parameters.

It should be noticed that the above two equations are usually formed in a geocentric inertial coordinate system. The partials from the above equations have to be transformed to the Earth-fixed coordinate system in which the observation equations are established.

Because it involves a large system of equations, the numerical solution for the precise model consumes a great deal of computational time. To tackle this problem, some simplification is made for the force model in equations (4.22) and (4.23). In this research, the force model for the partial derivatives includes only the central component of the Earth's gravitational field. While that affects the speed of the convergence a bit, it has no significant effect on the final results.

The partials with respect to the initial state vector can be simplified further by using the elliptical characteristics of the satellite orbit under solely geocentric gravitation. That is, the partial derivatives with respect to the initial Keplerian elements can be simplified as taking partial derivatives of the analytical equations (4.3), (4.5), and (4.7). These results are as follows [Langley et al., 1984]:

55

Let

$$\tilde{r} = \begin{bmatrix} a\cos E - ae \\ a\sqrt{1-e^2}\,\sin E \\ 0 \end{bmatrix} , \qquad (4.24)$$

$$\underline{M}_0 = \begin{bmatrix} \cos\Omega\cos\omega - \sin\Omega\cos i\sin\omega, & -\cos\Omega\sin\omega - \sin\Omega\cos i\cos\omega \\ \sin\Omega\cos\omega + \cos\Omega\cos i\sin\omega, & -\sin\Omega\sin\omega + \cos\Omega\cos i\cos\omega \\ \sin i\sin\omega, & \sin i\cos\omega \end{bmatrix} , \qquad (4.25)$$

$$\underline{M}_i = \begin{bmatrix} \sin\Omega\sin i\sin\omega, & \sin\Omega\sin i\cos\omega \\ -\cos\Omega\sin i\sin\omega, & -\cos\Omega\sin i\cos\omega \\ \cos i\sin\omega, & \cos i\cos\omega \end{bmatrix} , \qquad (4.26)$$

$$\underline{M}_\Omega = \begin{bmatrix} -\sin\Omega\cos\omega - \cos\Omega\cos i\sin\omega, & \sin\Omega\sin\omega - \cos\Omega\cos i\cos\omega \\ \cos\Omega\cos\omega - \sin\Omega\cos i\sin\omega, & -\cos\Omega\sin\omega - \sin\Omega\cos i\cos\omega \\ 0, & 0 \end{bmatrix} , \qquad (4.27)$$

$$\underline{M}_\omega = \begin{bmatrix} -\cos\Omega\sin\omega - \sin\Omega\cos i\cos\omega, & -\cos\Omega\cos\omega + \sin\Omega\cos i\sin\omega \\ -\sin\Omega\sin\omega + \cos\Omega\cos i\cos\omega, & -\sin\Omega\cos\omega - \cos\Omega\cos i\sin\omega \\ \sin i\cos\omega, & -\sin i\sin\omega \end{bmatrix} , \qquad (4.28)$$

$$E_a = \frac{dE}{da} = -\frac{3}{2}\left(\frac{GM}{a^3}\right)^{1/2}\frac{1}{r}(t-\tau) , \qquad (4.29)$$

$$E_e = \frac{dE}{de} = \frac{a}{r}\sin E , \qquad (4.30)$$

$$E_\tau = \frac{dE}{d\tau} = -\left(\frac{GM}{a^3}\right)^{1/2} \frac{a}{r} \quad , \tag{4.31}$$

$$\frac{\partial \mathbf{r}}{\partial a} = \underline{M}_0 \left\{ \frac{1}{a} \tilde{\mathbf{r}} + \left[\begin{array}{c} -a \sin E \ E_a \\ a(1-e^2)^{1/2} \cos E \ E_a \end{array} \right] \right\} \quad , \tag{4.32}$$

$$\frac{\partial \mathbf{r}}{\partial e} = \underline{M}_0 \left[\begin{array}{c} -a(1 + \sin E \ E_e) \\ -a(e/(1-e^2)^{1/2} \sin E + (1-e^2)^{1/2} \cos E \ E_e) \end{array} \right] \quad , \tag{4.33}$$

$$\frac{\partial \mathbf{r}}{\partial i} = \underline{M}_i \tilde{\mathbf{r}} \quad , \tag{4.34}$$

$$\frac{\partial \mathbf{r}}{\partial \Omega} = \underline{M}_\Omega \tilde{\mathbf{r}} \quad , \tag{4.35}$$

$$\frac{\partial \mathbf{r}}{\partial \omega} = \underline{M}_\omega \tilde{\mathbf{r}} \quad , \tag{4.36}$$

$$\frac{\partial \mathbf{r}}{\partial \tau} = \underline{M}_0 \left[\begin{array}{c} -a \sin E \ E_\tau \\ a \cos E \ (1-e^2)^{1/2} E_\tau \end{array} \right] \quad . \tag{4.37}$$

To obtain the partials of satellite positions with respect to solar radiation parameters, all perturbation forces except the solar radiation effect can be ignored in applying equation (4.22). By taking the partial derivative of geocentric gravitation ($-GM \, \mathbf{r}/r^3$) with respect to a satellite position vector, and partial derivatives of equations (3.9) and (3.10) with respect to the solar radiation parameters, the differential equations for the partials of positions with respect to the two solar radiation parameters are derived using equation (4.23) as follows:

$$\ddot{\mathbf{Z}}_{p0} = -\frac{GM}{r^3} \mathbf{Z}_{p0} + 3 \frac{GM}{r^5} (\mathbf{r} \cdot \mathbf{Z}_{p0}) \mathbf{r} \ -v \ \mathbf{e}_0 \, ,$$

$$\ddot{\mathbf{Z}}_{py} = -\frac{GM}{r^3} \mathbf{Z}_{py} + 3 \frac{GM}{r^5} (\mathbf{r} \cdot \mathbf{Z}_{py}) \mathbf{r} \ +v \ \mathbf{e}_y \, , \tag{4.38}$$

where

57

Z_{p_0} is the vector of partials with respect to the direct solar radiation parameter,

Z_{p_y} is the vector of partials with respect to the y-bias solar radiation parameter.

To summarize this chapter: The predictor-corrector method is used for the integration of the positions of GPS satellites. To obtain the partials of satellite positions with respect to the initial conditions, a satellite orbit is simplified as a Keplerian orbit and the partials are directly obtained from a set of analytic expressions. To obtain the partials with respect to the solar radiation parameters, second order differential equations are established and the partials are then obtained from the solution of the equations using the same predictor-corrector integration technique.

CHAPTER 5
GPS PHASE OBSERVABLES

As stated in Chapter 1, we should accurately measure signals and relate these signals to the unknown parameters (that is, the forming of the observation equations) rigorously to derive the desired information. When there are signals at hand, the problem is to establish observation equations and to derive the desired information from them. To form observation equations, we have to deal with coordinate system transformations, force modelling, and integration of the equations of motion, all of which have been discussed in the previous chapters. In this chapter, we discuss how to form the observation equations.

Whereas the basic principle of GPS was described as in Chapter 1, this chapter goes into more detail. Section 1 of this chapter describes GPS observations. The handling of biases in GPS observations is discussed in Section 2. The partial derivatives of the observations with respect to the estimated parameters are discussed in Section 3.

5.1 Carrier Phase Observations

A GPS satellite is transmitting electromagnetic signals to the Earth continuously. These signals can be related to the positions of the satellites and the stations, and other parameters. Different measurements can be made on the GPS signals. However, the most powerful measurement for static applications is the carrier beat phase measurement [Wells et al., 1987].

The equation of a GPS carrier beat phase observation can be written as [Wells et al., 1987]

$$- \lambda \phi(t) = \rho(t) + c\{dt(t) - dT(t)\} + d_{trop}(t) - d_{ion}(t) + \lambda N + \varepsilon \quad , \tag{5.1}$$

where

$\phi(t)$	is the carrier beat phase measurement in cycles,
λ	is the carrier wavelength,
$\rho(t)$	is the distance from the satellite to the receiver,
c	is the speed of the light,
$dt(t)$	is the bias of the satellite clock,
$dT(t)$	is the bias of the receiver clock,
$d_{trop}(t)$	is the bias of the tropospheric delay,
$d_{ion}(t)$	is the bias of the ionospheric delay,
N	is the integer carrier beat phase ambiguity,
ε	is the random measurement noise in a carrier phase measurement.

To simplify the data processing, a single difference observation between receivers is formed by taking the difference of two phase observations from two receivers (but the same satellite) of the same epoch. A double difference observation is then formed by differencing between two single difference observations (referred to different satellites), i.e.,

$$- \nabla\Delta\lambda\phi(t) = \nabla\Delta\rho(t) + \nabla\Delta d_{trop}(t) - \nabla\Delta d_{ion}(t) + \lambda \nabla\Delta N + \nabla\Delta\varepsilon \quad , \tag{5.2}$$

where

∇	represents the difference between two satellites,
Δ	represents the difference between two stations.

The above two conventions are used throughout the remainder of the thesis.

The advantage of the double difference is to greatly reduce the effects of errors associated with the misalignment between receiver clocks, and satellite clocks. Therefore, the double difference observations also make data processing easier. [Wells et al., 1987]. The effect of clock biases will be further discussed in Section 2.

5.2 Bias Handling

The biases in GPS positioning are orbital biases, satellite clock bias, receiver clock bias, station coordinate bias, cycle ambiguities of the carrier beat phase observations, ionospheric effect, and tropospheric delay. They are discussed in the following subsections.

5.2.1 Orbital Bias

The orbital bias arises from the uncertainties of the predicted broadcast ephemeris. The bias can be reduced largely in relative positioning by forming difference observations between receivers. This is effective for short baseline positioning, but for a long baseline, forming difference observations does not completely remove the effect of orbital bias. Therefore, the more effective way to handle orbital bias in static positioning is to improve the accuracy of the orbits of the GPS satellites with the approach of post-processing, i.e., estimating orbital elements and certain dynamical parameters. To improve the accuracy of the satellite orbit determination, a spatially large network of GPS receivers is required.

In our orbit improvement model, six initial Keplerian orbital elements and two dynamical elements (one for the direct radiation component and another for the y-bias component) for each satellite are estimated in the data processing.

5.2.2 Satellite Clock Bias

The satellite clock bias is the offset of satellite clock time with respect to GPS time. Since the difference in the times of emission of the signals from a satellite to the two receivers forming a double difference observation is small, the drift of the satellite clock in the period between the times of emission of the signals received simultaneously at the two receivers is negligible. Therefore, the effect of the bias is almost completely removed in double difference observations as stated earlier. The higher order terms of a satellite clock offset are negligible in double difference observations.

5.2.3 Receiver Clock Bias

The receiver clock bias is the offset of the receiver clock time with respect to GPS time. Although a GPS receiver is supposed to synchronize itself to GPS time at the start of observations, the synchronization is not perfect. Furthermore, the receiver clock will drift after synchronization. Just as in the case of the satellite clock bias, however, the receiver clock bias can be reduced in double difference observations.

The remaining effect of the receiver clock misalignments still has to be taken into account. For some receivers, (e.g., Texas Instruments TI 4100), the recorded GPS observation epochs are tagged at receiver clock times, and observations received at the same epoch according to the values of the receiver clock times (but by different receivers) are not at the same instant of time according to GPS time. However, our integrated *a priori* orbits are tagged in GPS time and the observation equations should be established according to GPS time if the integrated orbits are used in data processing. To compensate for this effect, the observations tagged at epochs of receiver clock times are converted to those tagged at epochs of GPS time. The conversion equation used is,

$$\lambda\phi|_{t_{GPS}=T_R} = \lambda\phi_{|T_R} + \left[(\rho|_{t_{GPS}=T_R-\Delta t}^{o}) - (\rho|_{t_{GPS}=T_R}^{o})\right] \, , \tag{5.3}$$

where

T_R is the receiver clock time,

t_{GPS} is the GPS time,

$\lambda\phi_{|T_R}$ is the recorded phase observation at the receiver clock time T_R,

$\lambda\phi|_{t_{GPS}=T_R}$ is the converted phase observation at the GPS time of the value T_R,

Δt is the clock offset of the receiver with respect to GPS time,

ρ° is the signal propagation distance computed from the broadcast ephemeris or

     an *a priori* orbit. $\rho|_{t_{GPS}=T_R}^{o}$ is ρ^{o} corresponding to the GPS time of the value

     T_R; $\rho|_{t_{GPS}=T_R-\Delta t}^{o}$ is ρ^{o} corresponding to the GPS time of the value $T_R - \Delta t$.

In the above equation, Δt can be computed as follows:

$$\Delta t = \rho^{o}/c - P - c\,(a_0 + a_1\,(t - t_0) + a_2\,(t - t_0)^2) \, , \tag{5.4}$$

where

P is the pseudorange measurement,

t_0 is the ephemeris reference epoch,

c is the speed of the light,

a_0, a_1, and a_2 are the coefficients of the satellite clock offset (from GPS time)

     obtained from the broadcast navigation messages.

Rigorously speaking, the above equation should be computed at the reception epoch. However, one microsecond accuracy is sufficient for computing equation (5.3), even if an observation of the precision of one millimeter is required. This means the above equation can also be computed at an epoch close to the reception epoch. Also, the ionospheric effect is negligible for computing equation (5.3), since it is normally much below one microsecond.

For an ideal synchronization and a good receiver clock, there should be no problem of misalignment. However, large misalignments of a receiver clock with GPS time (larger than one millisecond) do exist. An example of such a misalignment is illustrated in Section 7.3.

5.2.4 Carrier Beat Phase Ambiguities

A carrier beat phase measurement is based on the phase alignment of the receiver's local oscillator with the incoming carrier signal, but the number of integer cycles representing the perfect cycle synchronization is unknown since one cycle of the carrier cannot be distinguished from any other. This unknown cycle count is called the cycle ambiguity. The cycle ambiguity is designated as an unknown parameter and estimated as a real value in the adjustment process.

Ideally, if the estimated real-valued ambiguities are accurate enough, cycle ambiguities should be rounded off to the nearest integers and then the data readjusted to the final result with the ambiguities held fixed at the integer values. However, the integer character of the cycle ambiguity can not always be employed because of the insufficient accuracy of its corresponding real-value estimation. The longer the length of a baseline, the more difficult it is to fix the ambiguities, since the positioning of a longer baseline is more affected by biases. In our processing of the standard data set, the ambiguities are estimated as real values (see Chapter 7).

5.2.5 Station Coordinate Bias

The stations whose coordinates are held fixed to establish a coordinate system in data processing are called fiducial points. Any errors in the coordinates of these points will

affect the accuracy of the orbit determination and, in turn, affect the accuracy of positioning of other sites in a network. This problem is handled by selecting well-known stations (e.g., VLBI stations; see Chapter 7) as fiducial coordinates. In this way, the effect of the uncertainties of the fixed stations is much smaller than the effects of other unmodelled biases.

5.2.6 Ionospheric Effect

The ionospheric effect is the phase delay of a GPS signal, caused by the free electrons in the upper layer of the atmosphere resulting from the ionization of atoms and molecules by solar radiation. At the GPS frequencies, the ionospheric delay may vary from more than 150 m (at midday, during the period of maximum sunspot activity, with the satellite near the horizon of the observer) to less than 5 m (at night, during the period of minimum sunspot activity, with the satellite at the zenith) [Wells et al.,1987]. The ionospheric phase delay can be expressed as [Wells et al.,1987]

$$d\rho_{ion} = - a_{ion} \, N_T \, / \, f^2 \quad .$$
(5.5)

where

N_T is the total electron content along the propagation path in electrons/m^2,

a_{ion} is a constant.

In equation (5.5), higher order terms have been neglected. The dispersive nature of the ionosphere as evidenced by equation (5.5) can be used to good advantage. For the dual frequency GPS observations, a linear combination can be formed to eliminate the ionospheric delay

$$- \frac{c^2}{f2^2 - f1^2} \left(\frac{\nabla \Delta \phi 2}{\lambda 2} - \frac{\nabla \Delta \phi 1}{\lambda 1} \right) = \nabla \Delta \rho + \nabla \Delta d_{trop} + \frac{c^2}{f2^2 - f1^2} \left(\frac{\nabla \Delta N2}{\lambda 2} - \frac{\nabla \Delta N1}{\lambda 1} \right) + \epsilon' \quad ,$$
(5.6)

where

$\lambda 1, \lambda 2$ represent the carrier wavelengths corresponding to L1 and L2 carriers,

f1, f2   represent the frequencies corresponding to L1 and L2 carriers.

$\phi 1$, $\phi 2$ represent the phase observations corresponding to L1 and L2 carriers,

N1, N2   represent the integer ambiguities corresponding to L1 and L2 carriers,

ε' is the observation noise in the ionospheric free combination.

5.2.7 Tropospheric Effect

The tropospheric delay is caused by the refraction of a GPS signal in the lower atmosphere (the bulk of the troposphere is below a height of about 10 km) and is independent of the frequency of the GPS carrier. To account for this delay, a tropospheric model has been used [Janes et al.,1990]. Hopfield's tropospheric model is currently implemented [Vanicek et al., 1985a]. The model requires surface meteorological data.

The surface meteorogical data may not be able to represent the atmospheric conditions along the signal path, or may even suffer from blunder errors. A parameter estimation approach is adopted to handle this problem, that is to say, a nuisance parameter for each station per observation window (a continuous observation period; a typical observation window is about three to seven hours) is designated for the tropospheric delay, and this parameter is the scale correction for the modelled tropospheric delay.

By designating an estimated tropospheric scale correction, the tropospheric model can be written as

$$d_{trop} = (1 + s_{trop})\, d_{trop}^{\circ} \; , \tag{5.7}$$

where

d_{trop} is the tropospheric delay.

s_{trop} is the estimated tropospheric scale parameter,

$d_{trop}{}^\circ$ is the approximate tropospheric delay from the surface weather data and the tropospheric model.

5.3 Partial Derivatives with Respect to the Unknown Parameters

The observations can be expressed as functions of the various parameters governing the behaviour of the observations. Some parameters are well-known and are treated as constants while others are not known or are not known exactly and are treated as unknowns and are solved for in the data processing. To simplify the mathematical procedure, the equations are usually linearized around the approximate values of the unknowns. The linearization requires the partial derivatives with respect to the unknown parameters. The discussion of these partials is the topic of this section. For a general discussion on adjustment, see Mikhail [1976].

To simplify the notation to be used in the following subsections, let us assume that the baseline consists of stations 1 and 2, and the satellites in a double difference observation are satellites 1 and 2.

The single difference between satellites for receiver i is defined as,

$$\nabla \lambda \phi_i = \lambda \phi_i{}^2 - \lambda \phi_i{}^1 \ , \quad i = 1, 2 \ ; \tag{5.8}$$

The single difference between stations for satellite k is defined as

$$\Delta \lambda \phi^k = \lambda \phi_2{}^k - \lambda \phi_1{}^k \ , \quad k = 1, 2 \ . \tag{5.9}$$

The double difference observation is defined as

$$\nabla \Delta \lambda \phi = \Delta \lambda \phi^2 - \Delta \lambda \phi^1 \ , \tag{5.10}$$

or equivalently

$$\nabla \Delta \lambda \phi = \nabla \lambda \phi_2 - \nabla \lambda \phi_1 \ . \tag{5.11}$$

67

Similar definitions are valid for the other terms in equation (5.2), and these conventions are used throughout this section.

The partials in the following subsections are obtained by taking derivatives of equations (5.1), and (5.2) or equation (5.6), depending on whether an observation is a direct carrier beat phase or an ionospheric free combination of the two carriers.

5.3.1 Satellite Orbit Parameters

Partial derivatives of the phase measurement with respect to the satellite orbit parameters are derived as follows (they are the same for the L1 and L2 observations, and the ionospheric free combination):

$$\frac{\partial \ell}{\partial \kappa'} = \pm \left(\Delta \frac{\partial \rho}{\partial \mathbf{r}} \right) \cdot \frac{\partial \mathbf{r}}{\partial \kappa'} \, , \qquad (5.12)$$

where

ℓ is a double difference observation,

κ' is the partitioned vector formed by the initial state vector and the dynamical parameters of a satellite,

$\mathbf{r}$ is the position vector of the satellite,

ρ is the geometric distance from a receiver at the time of signal reception to the satellite at the time of signal transmission and can be expressed as

$$\rho = |\mathbf{R} - \mathbf{r}| \, , \qquad (5.13)$$

$\mathbf{R}$ is the position vector of the receiver.

The positive sign in equation (5.12) is for the second satellite; the negative sign is for the first satellite.

The partial derivatives of $\mathbf{r}$ with respect to κ have been discussed in Chapter 4. The partial derivatives of ρ with respect to $\mathbf{r}$ can be derived from equation (5.13) as follows:

$$\frac{\partial \rho}{\partial \mathbf{r}} = \frac{-(\mathbf{R} - \mathbf{r})^T}{\rho (1 + \frac{\dot{\rho}}{c})} \; , \tag{5.14}$$

where

$\dot{\rho}$ is the derivative of the distance with respect to GPS time.

The term $\dot{\rho}/c$ is due to the difference in the signal reception time and signal transmission time, and the relative motion between the satellite and the receiver. However, this term is small and the partials needn't be computed to such an accuracy. Therefore, in our present software implementation, a simplified equation is used, i.e.,

$$\frac{\partial \rho}{\partial \mathbf{r}} = \frac{-(\mathbf{R} - \mathbf{r})^T}{\rho} \; . \tag{5.15}$$

5.3.2 Station Parameters

The partial derivatives with respect to station coordinates for a double difference observation (whether it is L1, L2, or the ionospheric free combination) are,

$$\frac{\partial \ell}{\partial \mathbf{R}} = \pm \nabla \frac{(\mathbf{R} - \mathbf{r})^T}{\rho (1 + \frac{\dot{\rho}}{c})} \; . \tag{5.16}$$

Again as with equation (5.15), the above equation may be simplified as,

$$\frac{\partial \ell}{\partial \mathbf{R}} = \pm \nabla \frac{(\mathbf{R} - \mathbf{r})^T}{\rho} \; . \tag{5.17}$$

The positive sign in the above two equations is for the second station; the negative sign is for the first station.

5.3.3 Tropospheric Scale Parameters

The partial of the double difference observation with respect to the tropospheric scale parameter is derived as

$$\frac{\partial \ell}{\partial s_{trop}} = \pm \nabla d_{trop}^{o} \quad .$$

(5.18)

The positive sign in the above equation is for the partial with respect to the second station; the negative sign is with respect to the first station.

5.3.4 Carrier Phase Ambiguity

Although a carrier beat phase ambiguity is an integer number by definition, it is designated as an unknown real number and is solved for in the adjustment process. The partial of a single frequency observation (L1 or L2) with respect to an ambiguity parameter is very straight forward:

$$\frac{\partial \ell}{\partial \nabla \Delta N} = \pm \lambda \quad .$$

(5.19)

Here, the positive sign is for the second satellite, and the negative sign is for the first satellite.

For the ionospheric free combination "observable", the term $\dfrac{\nabla \Delta N2}{\lambda 2} - \dfrac{\nabla \Delta N1}{\lambda 1}$ in equation (5.6) multiplied by $77 \lambda 1$ is defined as the ambiguity parameter (note that $60 \lambda 2 = 77 \lambda 1$). The result of this multiplication is

$$\nabla \Delta N = 77 \, \nabla \Delta N1 - 60 \, \nabla \Delta N2 \quad ,$$

(5.20)

where N is the ambiguity parameter for the ionospheric free combination observable.

The partial with respect to an ambiguity parameter for an ionospheric free combination observation as expressed in equation (5.20) is

$$\frac{\partial \ell}{\partial \nabla \Delta N} = \pm \frac{77}{2329} \lambda 1 \quad . \tag{5.21}$$

Here, as with equation (5.19), the positive sign is for the second satellite, and the negative sign is for the first satellite.

As we can see from equation (5.20), an ambiguity parameter for the ionospheric free combination is an integer which is a harmonic combination of the L1 and L2 ambiguity parameters. However, because of the effect of the other biases and the observation noises, an estimated real valued ambiguity parameter can not always to be rounded to an integer. Furthermore, an ambiguity parameter for the ionospheric free combination alone cannot resolve the two ambiguity parameters for the L1 and L2 carriers. As mentioned earlier, in our present data processing, the ambiguity parameters are estimated as real values and no attempt has been made to round them to integer values.

We believe that the accuracy of our model is approximately 0.05 ppm + a few centimeters. This is borne out by the results we have obtained from processing a standard data set (see Chapter 7). The 0.05 ppm may mostly come from the force modelling, since our force model of a GPS satellite is at about the meter level. The "a few centimeters" comes mostly from residual tropospheric delay, since the zenith tropospheric delay varies with time whereas we estimate it as a constant value over a period of time. However, the accuracy of horizontal positioning should be better than vertical positioning. From our test results, horizontal positioning should be 1-3 times better than vertical positioning (see Chapter 7).

CHAPTER 6

COMPUTATIONAL ALGORITHMS AND
SOFTWARE IMPLEMENTATION

To realize and test the mathematical model described in the previous chapters, a software package has been developed. The software development is partially based on the GPS DIfferential POsitioning Program (DIPOP) package of the Department of Surveying Engineering of the University of New Brunswick, and the new software is called DIPOP-E (Enhanced version of DIPOP). DIPOP-E's main-processor significantly differs from the main-processor of DIPOP due to a much more sophisticated model although DIPOP-E inherits most features of DIPOP (DIPOP 2.0).

The first section of this chapter begins with a brief introduction of the history of DIPOP, followed by the overall structure of DIPOP-E. The comparisons of DIPOP-E with DIPOP 2.0 are made in Sections 2 and 3. Next, the auxiliary software accompanying DIPOP-E is described in Section 4. The final section describes some of the computational algorithms developed for DIPOP-E.

6.1 Introduction of DIPOP-E

6.1.1 Brief History of DIPOP

DIPOP is a program package developed by researchers of the Department of Surveying Engineering at the University of New Brunswick for estimating relative station positions from the carrier phase observations of the Global Positioning System satellites.

The first version of DIPOP, documented by Santerre et al. [1985] and Vanicek et al. [1985a] was developed on the Department of Surveying Engineering's HP-1000 minicomputer in 1984 and 1985 under a Department of Supplies and Services contract with the Canadian Geodetic Survey. The software was tested for two years during which time the package was modified extensively and a second generation version, DIPOP 2.0, was released subsequently in 1987 [Santerre et al., 1987]. More recently, version 2.1 has been released, which is able to process data from a variety of receivers using the same pre-processor programs [Kleusberg et al., 1989].

DIPOP has been widely used by the research staff and students of the Department, and distributed to many universities, government agencies and private companies in Canada and all over the world. Some examples of the use of DIPOP for GPS data processing are: the Ottawa Macrometer[TM] V -1000 and TI 4100 tests [Vanicek et al., 1985a, 1985b; Kleusberg et al., 1985]; the Ste-Foy Macrometer[TM] V-1000 [Moreau et al., 1985] and TI 4100 campaigns; two hundred township corner survey marks positioned by Usher Canada Ltd., using the Macrometer[TM] V1000; part of the Spring 1985 High Precision Baseline Test [Langley et al., 1986a]; and the TI 4100 Juan de Fuca Strait [Kleusberg and Wanninger, 1987] and Port Alberni networks [Georgiadou, 1987; Kleusberg and Georgiadou, 1988].

In 1986, Parrot started work on the addition to DIPOP of a short arc orbit improvement capability. This work was completed about the beginning of 1989 [Parrot, 1989].

In a parallel and essentially independent effort, a study was started in 1988 to develop an orbit improvement algorithm for multi-day orbital arcs. The preliminary model and its implementation in a prototype program were reported briefly by Chen and Langley [1989]. Subsequent improvement and testing have been carried out. The resulting program

package has been christened DIPOP-E. The testing of DIPOP-E and the results obtained are shown in the next chapter. But first, in the following sections, the work involved in the software implementation is described.

6.1.2 DIPOP-E Data Flow

Figure 6.1 shows a macro view of differences between DIPOP-E and DIPOP 2.0. Software components with the white shadow " ⬭ " are the same as in DIPOP; software components with the shadow " ⬭ " have only small differences with DIPOP; software components with the shadow " ⬭ " have many differences with DIPOP; software components with the shadow " ⬭ " have significant differences with DIPOP; and software components with the shadow " ⬭ " are new. More details are given below.

All versions of DIPOP, up to and including DIPOP 2.1, were divided into three parts: the pre-processor, the main-processor and the post-processor. DIPOP-E is divided into only two parts: the pre-processor and the main-processor. The functions of the post-processor have been incorporated into the main-processor. The pre-processor is primarily the same as in DIPOP 2.0, except for some minor modifications which were made due to the new features in DIPOP-E's main-processor and to improve its operational efficiency. (As stated at the beginning of this chapter, DIPOP-E inherits most of the features of DIPOP 2.0 and all comparisons below are made with respect to this version). The most significant differences are in the main-processor. The source code of DIPOP-E's main-processor takes up around 600 Kbytes (partially commented) of disk space, whereas those of the main-processor and post-processor together for DIPOP 2.0 (with comments) are close to 200 Kbytes.

74

The procedure for using DIPOP-E is also sketched in Figure 6.1. The first step in processing data is to check whether the dimensions of the large arrays in the compiled programs are sufficient. If they are not, the array dimensions must be re-defined. This is done manually for the pre-processor and automatically for the main-processor using auxiliary program MPDIM.

Secondly, the data files and the control file for the pre-processor must be prepared. We can then run the pre-processor. The data output by the pre-processor becomes the input data for the main-processor.

In the third step, the main-processor reads in its command file and the output data from the pre-processor. The main-processor is then run to produce the final results. When processing involves an orbit improvement, the approximate initial state vector for each satellite involved has to be available before the execution of the main-processor. This is realized by running the program called GNKPL.

Fourthly, the residuals from the main-processor are examined, and cycle slips remaining in the data are determined, checked, and corrected.

Fifthly, the corrected observations are used as the input data of the main-processor and re-processed. Steps 3 to 5 are repeated until satisfactory residuals are obtained. The output results from the main-processor then become the final results we are pursuing. Usually, only one or two iterations through the main-processor are required.

The software controlling the above tasks is described in the following subsections. We concentrate on the new features in the software. For further details on the DIPOP approach in processing GPS data, see Santerre et al. [1985, 1987].

The goal of the following sections is to outline the new features of DIPOP-E by comparing it with DIPOP 2.0.

PROCEDURE OF OPERATION

RAW DATA

DECODER

DATA

COMMAND FILE → PRE-PROCESSOR

MPDIM ← No — Enough Dim.?

Yes

GNKPL ← COMMAND FILE

Recompile Main-processor

COMMAND FILE → MAIN-PROCESSOR

New
Significant Differences
Many Differences
Minor Differences
The Same

CPLOT

Cycle Slip Free ? — No

Yes

FINAL OUTPUT DATA
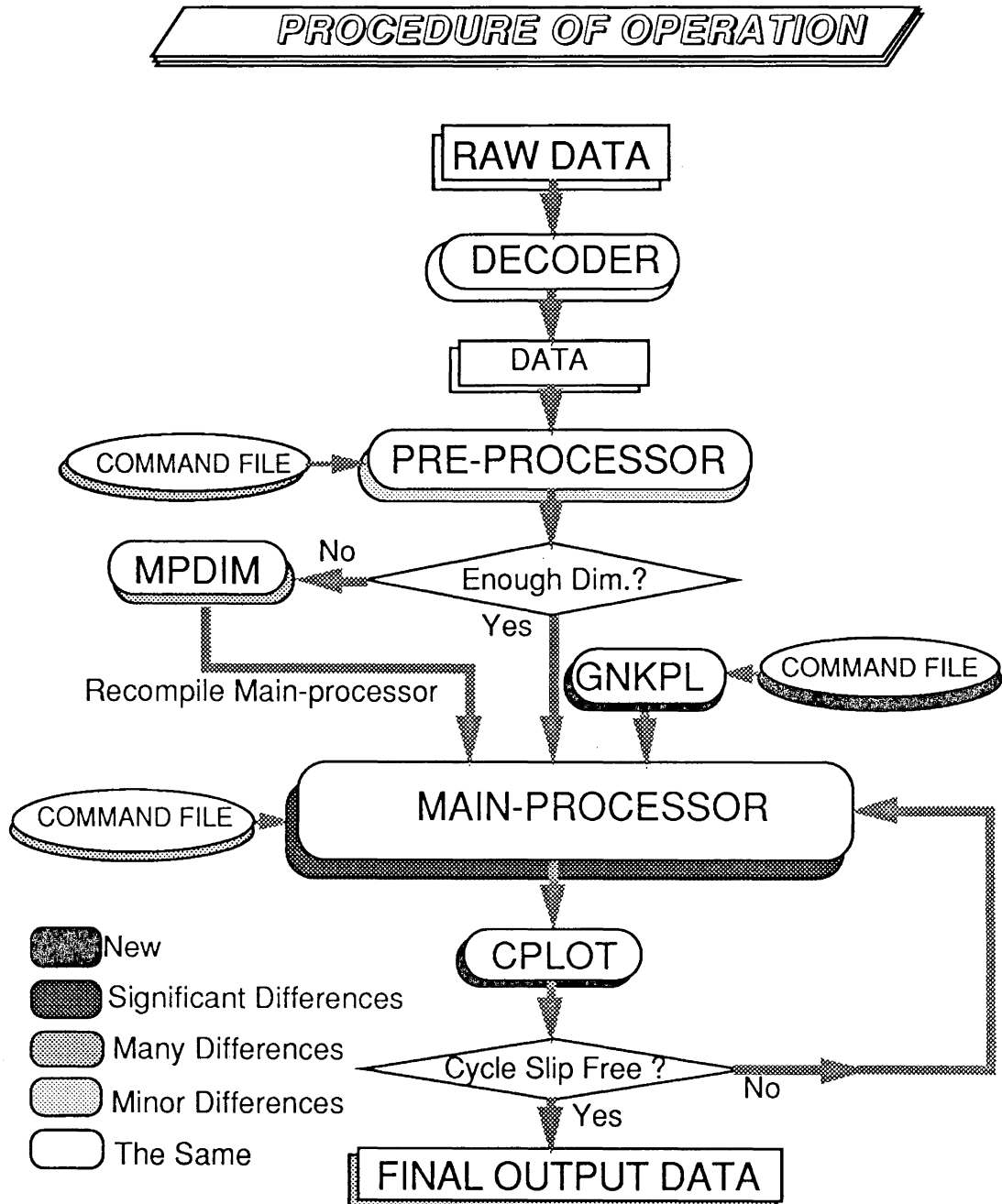
Figure 6.1   DIPOP-E data flow.

76

6.2 Pre-Processor

The first step in the data processing is to run the pre-processor. The primary functions of the pre-processor are to eliminate cycle slips and obviously bad data, and to form double difference phase observations and the ephemeris file for input to the main-processor (which is discussed in Section 3 of this chapter).

The pre-processor consists of programs PREGE and PREDD. The basic performance of the pre-processor of DIPOP 2.0 is described in subsection 1, the new features of the pre-processor of DIPOP-E are discussed in subsection 2.

6.2.1 Pre-processor in DIPOP 2.0

The first program, PREGE, is used in the first stage of preprocessing to eliminate obvious data errors and to detect and correct cycle slips in the one-way phase measurements. The output of PREGE is the input to PREDD for further processing. The second program, PREDD, first forms inter-station carrier phase single differences for pre-selected baselines and then forms double differences. PREDD detects and corrects cycle slips more precisely than PREGE. The "cleaned" carrier phase observations and the satellite coordinates are written to the output file which is the basic input file for the main-processor.

Earlier versions of the pre-processor had different programs for models of different GPS receivers. However, in the latest standard version DIPOP 2.1, the same software package, PREGE and PREDD, can process the data of different receivers [Kleusberg et al., 1989]. Most recently, the capability to handle data from Ashtech receivers has been implemented [Doucet, 1989].

77

For more details on DIPOP's pre-processor, see Santerre et al. [1987] and Kleusberg et al. [1989].

6.2.2 Pre-processor in DIPOP-E

Compared with DIPOP 2.0's pre-processor, the new features in DIPOP-E are as follows:

- It can use initial conditions to compute a satellite orbit; that is, it contains an orbital integration algorithm. This is very useful when the available broadcast ephemeris records are incomplete.

- An *a priori* orbit can be improved using the positions from the broadcast ephemerides as pseudo-observables.

- It has a different command file (also called a control file) structure and has an optional batch processing mode, which makes data processing more efficient and convenient (see Appendix I for a sample command file).

- It can convert the observation time tags to the GPS time scale. The conversion is carried out so that the data are consistent with the orbit improvement algorithm in the main-processor.

- It can read the data format of the SSG 1.104 Standard GPS Data Set (see Chapter 7) directly.

6.3 Main-processor

The most significant modifications for DIPOP-E are in the main-processor. For comparison, the basic features of MPROC (main-processor) and PPROC (post-processor)

78

in DIPOP 2.0 are outlined briefly in the following subsection, followed by a subsection describing the new features in the main-processor of DIPOP-E.

6.3.1 MPROC and PPROC in DIPOP 2.0

DIPOP 2.0's MPROC essentially performs a sequential least-squares parametric adjustment of the data provided by the pre-processor in single baseline or in network (multiple baselines) mode.

All observations made during a campaign are divided into sessions (a session consists of one observation file). After the observations of a session have been processed, the nuisance parameters (e.g. clock parameters, ambiguity parameters) pertaining to this session are eliminated rigorously from the normal equations of the sequential least-squares adjustment to reduce the memory requirement of the main-processor.

The physical models used in DIPOP are as follows: 1) Hopfield's model is used for the tropospheric refraction correction; 2) the L1 and L2 ionospheric free linear combination is created optionally for dual-frequency receivers; and 3) the relative receiver clock behaviour for the Macrometer™ V-1000 observables is modelled with a zero order (offset) or a first order (offset and drift) algebraic polynomial.

DIPOP 2.0 has a separate program called Post-PROCessor (PPROC). It performs the back substitution to re-evaluate nuisance parameters and their standard deviations for each session; it organizes and prints out the final and *a priori* results of stations and baselines, and other corresponding information.

For more details of the program features, see Vanicek et al. [1985a] and Santerre et al. [1985, 1987].

6.3.2 Main-processor in DIPOP-E

The data processing procedure in the main-processor of DIPOP-E is greatly different from that in DIPOP 2.0. A flow chart describing its basic operations is shown in Figure 6.2.

The essential feature is the multi-day orbital integration and adjustment. Also, a tropospheric scale parameter for each station is estimated for each observation window. Thus, computational burden increases and more memory is required. As described in Figure 6.2, a modified data processing procedure was implemented in DIPOP-E and many model components were improved.

As stated earlier, in DIPOP-E, there is no longer a separate post-processor program. It has become a subroutine of the main-processor. Originally, the post-processor had been separated from the main-processor because of memory limitations on the HP 1000 minicomputer on which DIPOP was initially developed. Such limitations do not exist on more modern computers. The change we made was intended to save the user's interfacing time.

Beside the above changes, other new features in DIPOP-E are:

- A modified command file for the station adjustment to accommodate the new features. It includes: options for improving orbit, estimating tropospheric delay scale parameters, setting masking angles, modelling vertical solid Earth tidal displacement (including the restoration of the permanent tide); various input, output and intermediate files; different data inputs. In addition, it is easy to add lines of comments anywhere in the command file (except in the session by session information area; see Appendix I), which possibly makes the command file self-explanatory.
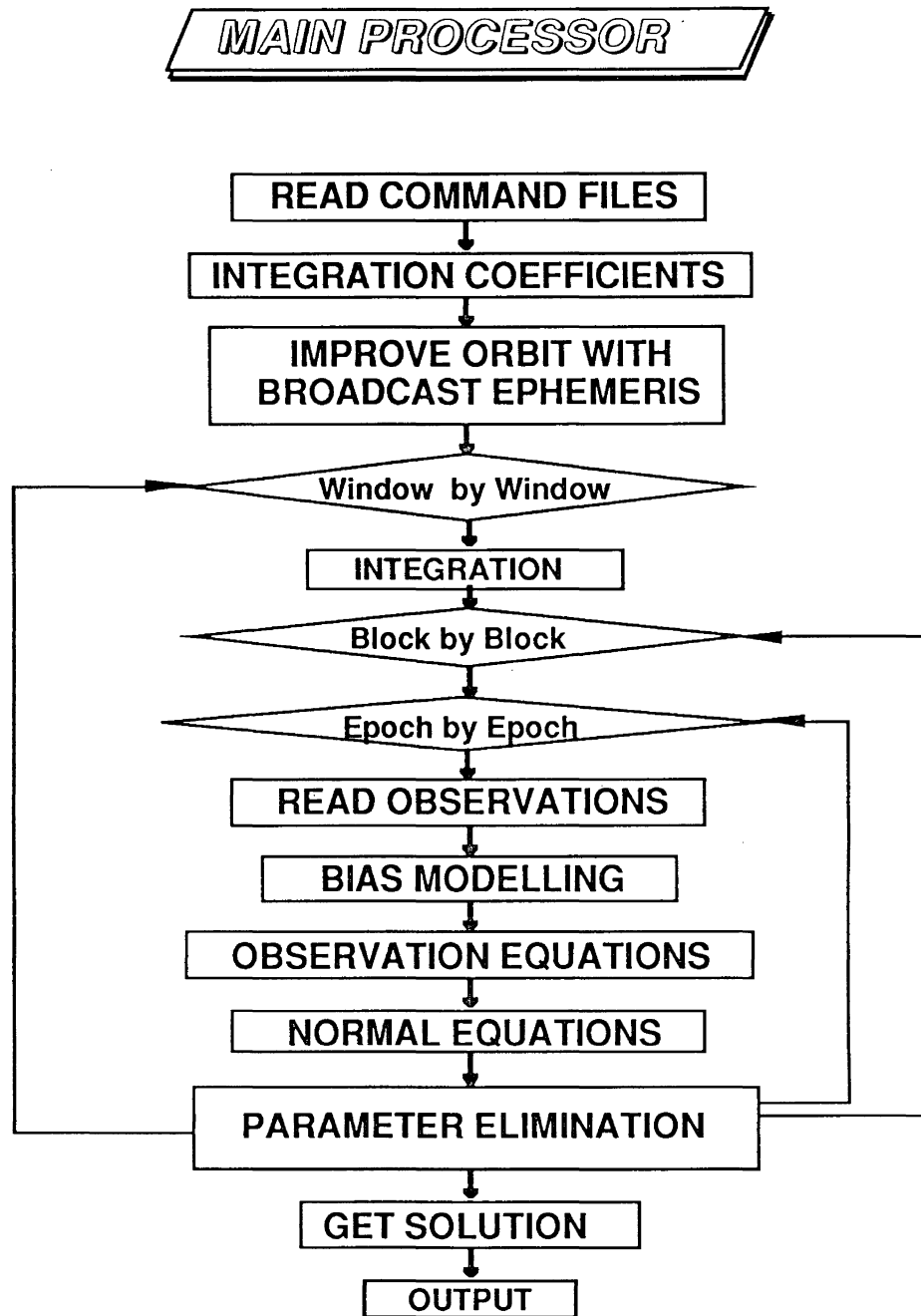
Figure 6.2   DIPOP-E's main-program flow chart

81

- A new command file for the control of the orbital integration and adjustment. It provides information or options for: satellites, force models, time scale and Earth orientation, orbit improvement with the broadcast ephemeris, integration, etc. (See Appendix II for an example of a command file).

- In DIPOP 2.0, the computation of residuals could be performed for only a single observation file at a time. For a multi-session, multi-baseline solution, the residuals cannot be obtained. In DIPOP-E, the residuals can be computed in all cases, whether for only a few selected files or for all processed files.

- A fast algorithm for determining the variance and covariance of the baseline components and a fast subroutine for the computation of the error propagation (see Section 6.5).

- A fast algorithm for computing the normal equation (see Section 6.5).

- Improved reporting of output for the station coordinates and the baseline components. The tabulated format has reduced the number of pages of output and made the output more readable.

- More extensive output (for example, tropospheric delay scale parameters, orbital adjustment results).

- Optional batch processing mode.

6.4 Auxiliary Software

As shown in Figure 6.1, there are three auxiliary programs associated with DIPOP-E: MPDIM, GNKPL and CPLOT. The program, **GNKPL**, is designed to generate approximate initial Keplerian elements (Chapter 2).

The purpose of **MPDIM** is to set-up the array dimensions for the main-processor to satisfy the need of a particular processing task without the user having to alter the source code directly. The dimension include file of DIPOP-E is considerably different from that of

DIPOP 2.0, because it has to accommodate the more sophisticated main-processor of DIPOP-E.

One of the important tasks of the pre-processor in DIPOP is to remove cycle slips. Although usually the pre-processor can remove most if not all cycle slips, there is no guarantee of that. When there is a perturbed ionosphere, or if the baseline is very long, or when the data rate is low, there are often some cycle slips left in the PREDD output file. Before a final solution can be obtained, the observation residuals should be freed from the remaining cycle slips and this had been achieved previously with the help of RPLOT (a residual plotting program developed at UNB). The cycle slips are detected by plotting the residuals, followed by the manual computation of the size of the cycle slips and then cycle slip corrections are applied to the data using a program called CYCLE. DIPOP 2.0's procedure for the cycle slip correction is:

- Run MPROC for the L1 and L2 observations separately.
- Read the residual file corresponding to the L1 solution.
- Plot the residuals and check for epochs at which there are big jumps.
- Measure the amount of each jump.
- Compute and determine the cycle slip for each jump manually.
- Repeat the above process for the L2 residuals in the case of dual frequency data.
- If there are valid cycle slips, make up a command file for the corresponding observation file and use the program CYCLE to correct the cycle slips.
- Re-run MPROC and plot the residuals to check the success of the cycle slip determination.
- Repeat the above steps if there are still some remaining cycle slips, until there is no detectable cycle slip left.

This process can be tedious and prone to mistakes. A program called **CPLOT** was developed to reduce the demand on the data analyst and to transfer the cycle slip detection and correction process almost entirely to the computer. CPLOT's features include:

- The ability to read in both the residual file and the observation file, and to plot both residuals and the ionospheric delay combination of L1 and L2 phase observations.

- For dual frequency phase observations, the main-processor needs to process only the ionospheric free combination, not the individual L1 and L2 observations.

- The software can calculate the integer number of slipped cycles in a cycle slip.

- The correctness of the cycle slip-determination can be checked by plotting the corrected residuals and the corrected ionospheric delay combination directly without reprocessing the data with the main-processor. Thus, a possibly incorrect determination of a cycle slip can be found immediately after the determination of the cycle slips, and this reduces iterations through the main-processor.

- Plots from different files or from the same file can be overlaid.

- CPLOT makes full use of the Macintosh toolbox: windows, buttons, mouse, menus, and graphics, etc., which makes it very quick and easy to use.

- Cycle slip detection, determination, checking, and correction are all in one application.

- CPLOT can find cycle slips which RPLOT would ignore. Figures 6.3 and 6.4 illustrate two such cases. In Figure 6.3, a cycle slip of satellite 6 occurs at the exact epoch at which the receivers start tracking a new satellite. Before satellite 9 is tracked, double difference observations are formed for satellite pair 3 and 6. After satellite 9 is tracked, double difference observations may be automatically formed for satellite pair 3 and 9 and for satellite pair 9 and 6 in the pre-processors of both DIPOP 2.0 and DIPOP-E. Double difference formation in a residual file is the same as in the corresponding double difference observation file. Because RPLOT can plot directly only what is available in the residual file, it will fail to show the jump at the epoch at which satellite 9 rises.

84

Similarly, as shown in Figure 6.4, a cycle slip associated with satellite 9 occurs at the same epoch at which receivers stop tracking satellite 3. If there are no double difference observations formed by satellite pair 9 and 12 before tracking of satellite 3 ends, RPLOT will fail to show the cycle slip.
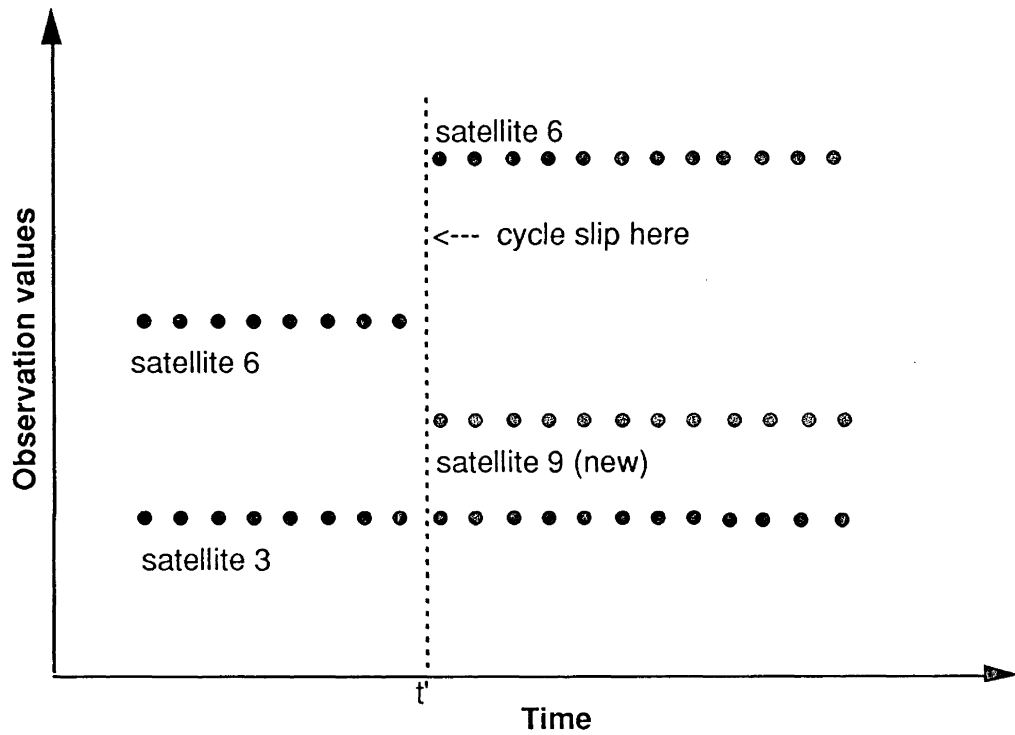
Figure 6.3   Cycle slip can occur at the exact epoch at which receivers start tracking a
            new satellite.

At the moment, CPLOT is more or less at the prototype stage and works only with dual frequency data. For the cycle slip determination, the residuals must be those from the analysis of the linear ionospheric free combination of the L1 and L2 observations. Also, the capability to determine and correct half cycle slips which may be present in data from squaring-type receivers is not implemented yet. More work needs to be done to enhance CPLOT further.
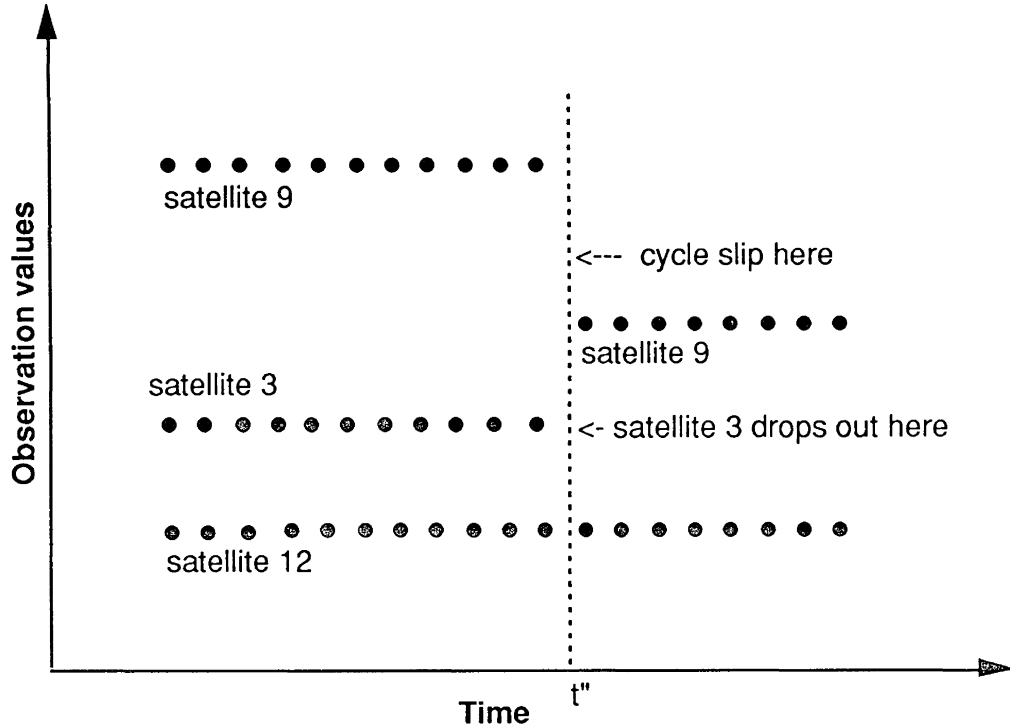
Figure 6.4 Cycle slip can occur at the exact epoch at which receivers stop tracking a satellite.

6.5 Computational Algorithms

As mentioned in Section 6.3.2, the adjustment computation has been sped up in DIPOP-E. We will go into more detail about this topic in this section.

As the number of the points in a network grows, the average computation time per observation file increases greatly, since the computation for the normal equations dominates the computational effort for a large network. The computation time can be reduced significantly, however, if we consider the sparseness of the design matrix. As we know, each double difference observation is related only to the coordinates of two stations, the orbital parameters of two satellites, and the associated nuisance parameters. The partial derivatives of the observation with respect to other parameters in the adjustment are zero.

86

Certain operations on the normal equations corresponding to these zeros can be skipped, and thereby the computational efficiency improves significantly.

As an illustration of the reduction in computation time due to these improvements, we compared the processing time for one session of the SSG 1.104 data set (described in Section 1 of Chapter 7) using DIPOP 2.1 and DIPOP-E on a Macintosh II computer without using its floating point coprocessor (DIPOP 2.1 uses the same adjustment algorithm as DIPOP 2.0). For the session of 3 January, involving 18 stations and about 2 Mbytes worth of double difference observations, DIPOP 2.1 required 34 minutes to process the data in the main-processor followed by an additional 14 minutes for the post-processor. The same data was processed by DIPOP-E using the same set of estimated parameters in 13 minutes total. The relative difference in computational speed will be even greater if more stations are involved. It should be pointed out that this comparison is of total processing time including the time required for the reading of the observation data from the disk and the computation of the observation equations.

The speeding up in the covariance propagation subroutine is achieved by designing a different computational procedure. It is described as follows:

The law of the covariance propagation is written as:

$$Q_{zz} = A_{zx} \, Q_{xx} \, A_{zx}^T \, , \tag{6.1}$$

where

Q_{xx} represents the covariance matrix of a vector of variables,

Q_{zz} represents the covariance matrix of a vector of functional variables,

A_{zx} represents the matrix of the linear mapping function.

DIPOP 2.0 computes each element of the covariance matrix separately, except each symmetrical pair is computed only once due to their equality. In DIPOP 2.0, the following equation is used to compute Q_{zz}:

$$q^z_{ij} = \sum a_{im} \, q^x_{mn} \, a_{nj} \quad , \tag{6.2}$$

where

q^z_{ij} represents an element of Q_{zz},

a_{im}, a_{nj} represent elements of A_{zx},

q^x_{mn} represents an element of Q_{xx}.

As the dimension of matrices increases, the computation using equation (6.2) increases in the power of 4. The number of multiplications involved in equation (6.2) is (exclusive of the integer operations for subscript housekeeping),

$$z \, (z + 1) \, x^2 \, . \tag{6.3}$$

Here z and x represent the dimensions of the corresponding covariance matrices.

The computation operations can be reduced significantly by simply using the associative characteristics of matrix multiplication, i.e.,

$$Q_{zz} = (A_{zx} \, Q_{xx}) \, A_{zx}^T \, . \tag{6.4}$$

The operational procedure is first to compute the product, $A_{zx} \, Q_{xx}$, in equation (6.4), and then to multiply the resultant matrix with matrix A_{zx}^T. Using this method, the number of multiplications required is

$$z \, x^2 + \frac{1}{2} z \, (z + 1) \, x \quad . \tag{6.5}$$

A further saving of the computation time comes from the computation of covariances of baselines. In DIPOP 2.0, the covariance matrix computation of a baseline is carried out

in the following steps: 1) Write the baseline components as a function (linear combination) of all station coordinates (even if a station not forming the baseline is also included, and the linear coefficient corresponding to the station is zero in the linear combination); 2) Use the above function and the law of the covariance propagation (equation (6.2)) to compute the covariance of the baseline components.

This computation can be simplified, using the following formula:

$$Q_{bb} = Q_{11} + Q_{22} - Q_{12} - Q_{21} \ , \tag{6.6}$$

where

Q_{bb} is the covariance of the baseline components,

Q_{11} is the covariance of the coordinates of one station forming the baseline,

Q_{22} is the covariance of the coordinates of the other station forming the baseline,

Q_{12}, Q_{21} is the covariance between coordinates of the two stations.

As we can see, there is no multiplication involved in the computation of equation (6.6).

PREGE, PREDD, the main-processor, and GNKPL are all command driven programs. A command file specifies the control data and controls for different performances. Sample command files are listed in Appendices I through III.

To close this chapter, it should be noted that DIPOP-E is currently implemented with the MacFORTRAN/020 implementation of ANSI FORTRAN 77, and also care should be taken with the data type DIPOP-E can handle. DIPOP-E's main-processor can handle the data which DIPOP 2.0's main-processor can handle, but DIPOP-E's main-processor cannot handle binary format. DIPOP-E's preprocessor can only handle TI 4100 data format. DIPOP-E's main-processor and DIPOP's pre-processor are compatible if there is no orbital improvement involved. However, if the orbit improvement is required and the

drift of receiver clock cannot be ignored, the direct using of the output of DIPOP's pre-processor will result in coordinates absorbing the bias of receiver clocks. Also DIPOP's main-processor has the capability to estimate receiver clock coefficients for Macrometer™ (almost extinct) V1000 type data which has no pseudorange observations, but the capability of estimating the receiver clock coefficients hasn't been implemented in DIPOP-E's main-processor yet.

CHAPTER 7

ANALYSIS OF A STANDARD GPS DATA SET

To test the model and the associated software implementation, a standard GPS data set (see Section 7.1) has been analyzed. This chapter shows the results of this test. Section 1 of this chapter describes the standard data set. Section 2 discusses the data processing approach and Section 3 presents results of the test.

7.1 Description of the Data Set

In December 1986 and January 1987, a five-year campaign was initiated in central and southern California to monitor tectonic motion west of the San Andreas fault by repeated measurements of a geodetic network surveyed using the Global Positioning System satellites [Bock, 1988]. Three five-day experiments constituted the first epoch measurements. A different subset of the network was surveyed in each experiment. Five days were deemed sufficient to detect possible blunders and to assess the short-term repeatability of the GPS determined baselines. The third experiment (3 to 7 January) was the most ambitious of the campaign, involving fourteen receivers in California and five receivers at other sites in North America (see Figure 7.1 and Table 7.1). The data collected during the third experiment comprised the standard data set and was put together and disseminated by International Association of Geodesy (IAG) Special Study Group (SSG) 1.104.
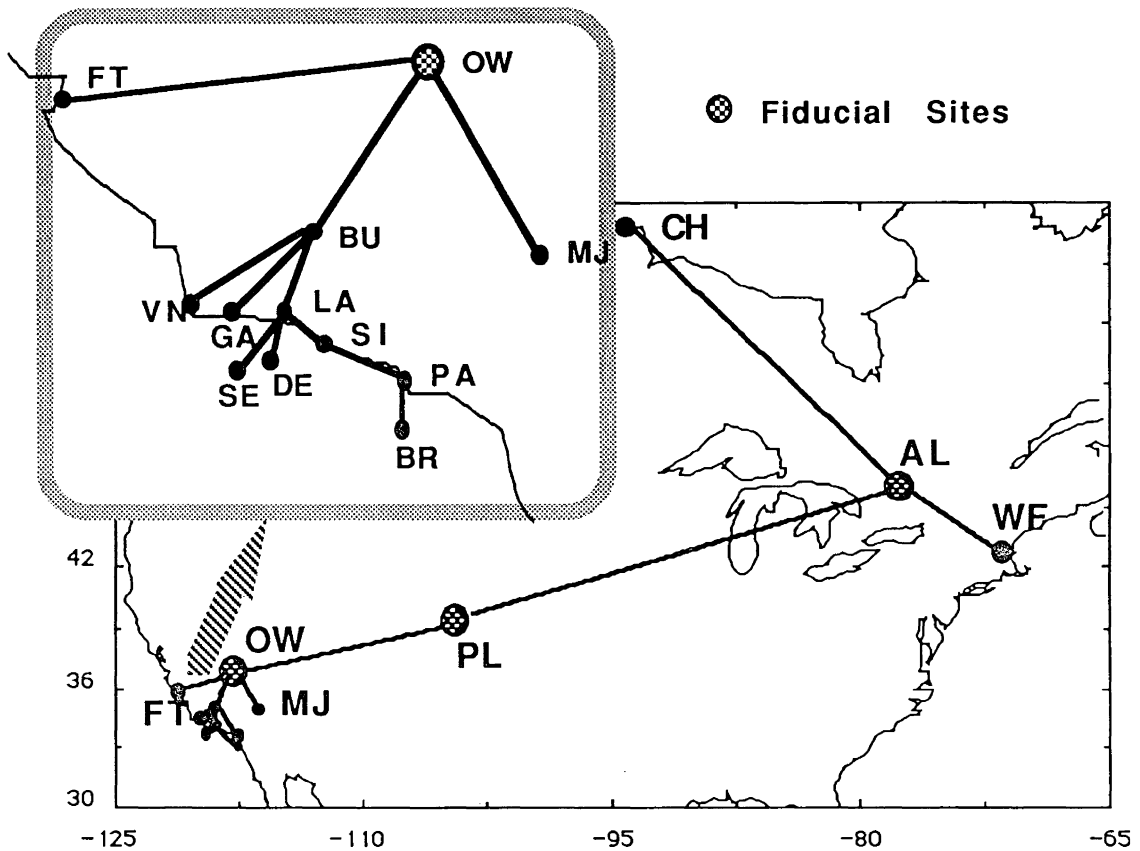
Figure 7.1 Network of the standard data set

As stated by Bock [1988], the network of this experiment was designed to span a wide-range of spatial scales. It includes 9 sites of local tectonic interest (in southern California) with baseline lengths ranging from 30 to 200 kilometres. These are distributed primarily along the California coastline and on three off-shore islands (Santa Rosa, Santa Cruz, and Santa Catalina). One of these sites is located at Buttonwillow east of the San Andreas and was chosen so as to lie near the centre of a set of regional sites located at Owens Valley, Ft. Ord, Palos Verdes, Vandenburg and Mojave. The local and regional sites provide a mix of baseline lengths of 30-500 kilometres in length. The regional sites have been surveyed by VLBI measurements so that their relative positions are accurately known. The baseline from Owens Valley to Mojave is particularly important for calibration purposes since it does not appear to be deforming at a level of more than a few millimetres

a year. Sites outside California at locations in Massachusetts (Westford), Colorado (Platteville), Ontario (Algonquin), and Manitoba (Churchill), provide baseline separations of 1200 to 4200 km.

All observations were performed with Texas Instruments TI 4100 GPS receivers. The TI 4100 is a code-correlating receiver and provides time-tagged L1 and L2 carrier-beat-phases and P-code pseudoranges. For this experiment, a 30-second sampling rate was used over a daily schedule of 7.5 hours. The TI 4100 has only four channels so all "visible" satellites cannot be tracked throughout their entire passes. A schedule was designed to provide maximum tracking on the five satellites (PRN 3, 6, 9, 11, and 13) that together provided the best sky coverage (see Figure 7.2). A sixth satellite (PRN 12) was tracked for only 1.4 hr. The observations took place entirely at night when effects of ionospheric refraction were at a minimum [Bock, 1988]. All 19 sites were occupied with 15 to 16 sites per day. At Vandenburg on Jan. 6, there was another station VNDN7880 which was occupied, but the data at two minute intervals were not available for the station. Also, the data from a station at Austin, Texas was not usable. This station is not shown in Figure 7.1.

Figure 7.2 shows the sky distribution of the GPS satellites during the measurement period (The plot was drawn with the program MacGEPSAL which was developed at UNB). The curves represent the tracks of the satellites, the arrows represent the directions of motion of the satellites (arrows also mark the hours), and the numbers on the curves correspond to satellite PRNs. Since Platteville is located at a central area of the observation network and Jan. 5 was in the middle of the observation period, Figure 7.2 may be assumed to represent the satellite sky distribution of the whole observation period of the entire network. As seen from the figure, the satellite tracks extend mostly in a north-south direction.

Time: 1987 5/15/ 0 0

Ephemerides file: GPS.NOV.1986 2

SATELLITE TYPE
GPS Constellatn 7 Satlites

EPHEMERIDES
NASA Prediction Bullet 11/1986

LATITUDE
40 d 10 m 0 s

LONGITUDE
-104 d 42 m 0 s

MASK ANGLE
5.0 deg

BEGIN YEAR DAY/ H/ M
1987 5/ 7/ 0

END YEAR DAY/ H/ M
1987 5/15/ 0

INCREMENT
10 minutes

Elevation

30
60
90
270
90
0
180

Azimuth
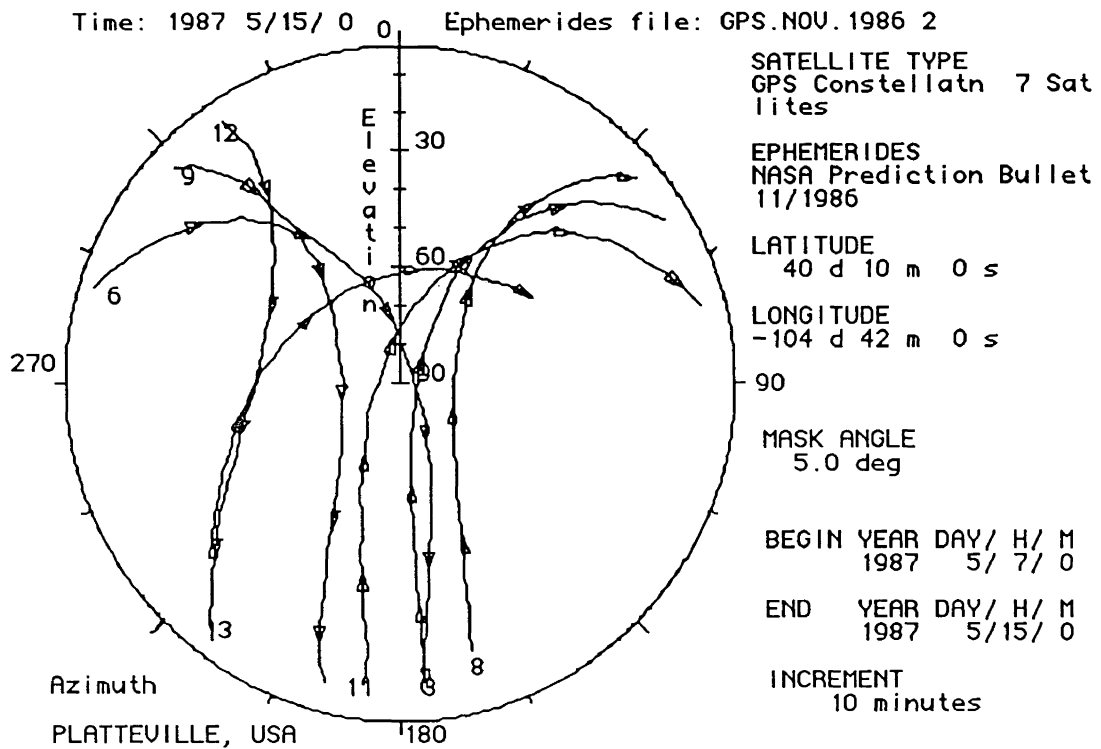
PLATTEVILLE, USA

Figure 7.2 Sky distribution of the GPS satellites on Jan. 5, 1987 at the station Platteville.

7.2 Data Processing Approach

A number of different options had to be considered in processing the data, and these included the selection of the reference stations (fiducial points), *a priori* orbits, data sample rate, the formulation of the double difference observations, etc. The choices made are described below.

Reference stations: A fiducial point approach was used for the data processing. The coordinates of a few well-positioned stations were held fixed to establish an Earth-fixed coordinate system, and satellite orbits, coordinates of other stations, and other parameters were free in the data adjustment processing. This approach is called the fiducial point approach. It was decided by IAG SSG 1.104 that three stations were to be held fixed:

Algonquin, Platteville, Owens Valley. The coordinates of these stations had been established by very long baseline interferometry with formal uncertainties of about 1 cm [Bock, 1988]. Although considered as estimated parameters, the coordinates at these stations were fixed in the data processing by weighting them at 0.1 mm.

A Priori **orbits:** The approximate initial conditions of the satellites were estimated from broadcast ephemerides with program GNKPL. However, these initial conditions are very poor, since in the program (GNKPL): 1) there was no rigorous coordinate system transformation between the coordinate system corresponding to the ephemerides and the coordinate system of the initial conditions (see Chapter 2); 2) no orbital integration was involved; 3) healthy ephemerides at the initial epoch were not always available; 4) the broadcast ephemerides were not very accurate. The positions from these initial state vectors had biases of hundreds (even thousands) of meters after a few day's integration.

Before the final adjustment with the dual frequency phase observations, the integrated orbits were fitted into satellite positions from the broadcast ephemerides at fifteen minute intervals to speed up the convergence in the main-processor. Since the broadcast ephemerides had maximum deviations of approximately 50-60 m in the coordinate system defined by the recommended fiducial points of SSG 1.104, the *a priori* orbits fitted from the broadcast ephemerides had a bias of the same amount. However, the orbital constraints for the final adjustment were assigned almost arbitrarily. A list of the orbital constraints used in our final adjustment is as follows (the angles are in radians):

a (in m)	e	i (in rad.)	Ω (in rad.)	ω (in rad.)	τ (in sec.)
50.0	2.000E-6	2.000E-6	4.000E-6	4.000E-9	0.1,

and the constraints for the solar radiation pressure parameters are as follows:

direct radiation: 2.0D-8 (in m/sec^2),

y-bias radiation: 2.0D-9. (in m/sec^2).

The argument of perigee was assigned a high constraint due to its low separability from the time of perigee passage (since the orbit of a GPS satellite is near circular).

The large deviation of the broadcast ephemerides in the fiducial coordinate system was confirmed by the processing of the observation data, using satellite orbits computed directly from the broadcast ephemerides. When the broadcast ephemerides were used, the relative positioning accuracies were only about 3 ppm. Even if the broadcast ephemerides had approximately 20 m accuracy, the corresponding accuracy of the relative positioning should be less than about 1 ppm in this campaign. Therefore, this large deviation can be explained only by a difference in the coordinate systems of the broadcast ephemerides and the distributed station positions. The distributed station positions are in the SV-4 coordinate system [Bock, 1988].

The Earth orientation data: UT1-UTC and the polar motion data were obtained from an IRIS bulletin [IAG, 1987], and they were given at intervals of five days. Three sets of Earth orientation data (at 0^h UTC on Dec. 30, 1986, Jan. 4 and 9, 1987) were used to interpolate the values at any epoch between these three tabulated epochs. The polynomial interpolation is implemented in DIPOP-E to obtain the Earth orientation values at any epoch.

The Earth's gravity field: The GEM L2 [Lambeck and Coleman, 1983] gravitational field was used in the orbital adjustment process. In our data processing, the gravitational field up to order and degree eight was used.

Positions of the Sun and the Moon: We use Bernese subroutines "SUN" and "MOON" [Santerre et al., 1985] to compute the positions of the Sun and the Moon. The ephemeris time required to call subroutines is replaced with TDT time (see Chapter 2). To save computational effort, the positions of the Sun and the Moon are computed at a certain interval from the two subroutines and then the positions of the Sun and the Moon are

approximated with polynomials. The positions of the Sun and the Moon are then computed from these polynomials. In this data processing, the positions computed from the subroutines "SUN" and "MOON" are at intervals of 18 minutes.

Computation of the positions of the satellites: Since a numerical method is used in our model, the positions from orbital integration are obtained at epochs spaced by a certain time interval. The interval used in this data processing was 120 seconds and the order of the integrator was 9 (these values were somewhat arbitrarily selected but a test has been made that showed they provided orbits precise enough for this data processing). To compute positions at any epoch, a polynomial approximation of the integrated positions of the satellites is used in our software for each particular period of time (called segmentation, see Appendix II). The order of the polynomial used in this data processing was 11 and the length of the segmentation was two hours.

Data sampling rate: The raw observation data recording interval was 30 seconds. However, due to the large volume of the input data for the main-processor and the limited disk space of the Macintosh computer, only the two minute decimated data (also distributed by the SSG 1.104) was used in the data processing.

PREGE processing: The processing in this step for the most part was successful. However, there were a few observation files which failed to be processed properly. The failure of the two observation files of the station Austin on Jan. 6 and Jan. 7 were caused by abnormal L1 observation records (all L1 observation records were "***********"). There were no observations in the data file at two minute intervals on Jan. 3 for the station Solimar. The processing of the data file on Jan. 5 for the station Palos Verdes failed. The cause of this failure was unclear.

97

Table 7.1 Stations used in the formation of daily double difference observations and the eccentricities of the stations*

Abbreviation & Stations	Day:	Jan.			
Units of the eccentricities in meters	3	4	5	6	7
AL ALGONQUIN (ALGORMA)	1.399	1.399	1.399	1.399	1.399
AU AUSTIN (AUSTIN GPS)					
BR BRUSH (SANTA CATALINA)	1.656	1.656	1.656	1.708	1.708
BU BUTTONWILLOW	1.483	1.287	1.319	1.460	1.389
CF CHAFFEE	1.421				
CH CHURCHILL	1.454	1.454	1.454	1.454	1.454
DE DEVILS PEAK		1.496	1.496	1.496	1.496
FT FORT ORD (NCMN1981)	1.372	1.773	1.740	1.754	1.746
GA GAVIOTA PEAK	1.374	1.426	1.411		
LA LA CUMBRE	1.319	1.374	1.297	1.366	1.308
MJ MOJAVE (MOJAUTEX)				0.000	0.000
ML MILLER CADT					1.491
OW OWENS VALLEY (OVRO7114)	1.387	1.890	1.890	1.890	1.890
PA PALOS VERDES (PVER7268)	1.332			1.447	1.475
PL PLATTEVILLE (PLAT7258)	1.682	1.682	1.682	1.682	1.682
SE SOLEDAD (S. ROSA IS)	1.418	1.418	1.418	1.418	1.418
SI SOLIMAR		1.457	1.343	1.410	1.315
VN VANDENBURG (VNDNRM1)	1.264	1.263	1.260	1.260	1.260
WF WESTFORD (WESTGPS)	0.000	0.000	0.000	0.000	

*Note: In DIPOP-E data processing, a station name has to be represented by an abbreviation consisting of two letters.

The stations from which observation data were used in forming double difference observations each day are shown in Table 7.1. A station for which an eccentricity value is

98

given in the table formed double difference observations with another station on the same day. Some station names differ from location names and they follow location names in parentheses. As discussed in Chapter 2, there are usually upward offsets between ground station coordinates and the antenna phase centers of receivers (the offset is called eccentricity). The measured upward eccentricities of the stations supplied with the data are listed in Table 7.1; the horizontal eccentricities for all stations are zero.

PREDD processing: The output data from PREGE were the input data of PREDD. Since there were insufficient ephemeris records in the data set for observations on Jan. 7, integrated *a priori* orbits were used for PREDD processing for that day. The observations recorded at the receiver epochs were converted to the GPS epoch to be used in the main-processor. Some baselines failed to be processed with the program output message of "error array dimension too small." A closer look over the summary files of PREDD showed that when the above case happens, cycle slips occur at almost all epochs. This can be due to problems in the observation data, or problems with PREDD. To handle this problem, alternative double difference observations were formed (for context, see below).

Criteria for double difference formulation: Generally speaking, the criteria used in forming baselines in the data processing were ease of cycle slip fixing and minimization of data gaps as a result of the pre-processing. Thus, shorter baselines and baselines having minimal data gaps were preferred. Table 7.2 lists the baselines forming double difference observations on individual days in our data processing, and the lengths of the baselines are also listed; notice that the baseline formulations had some differences on different days. See Table 7.1 for the abbreviations used in the tables, figures, and in our data processing. It should be noticed that the criteria were only loosely applied and our double difference formation was not the optimized one. The cells filled with shading mean that the corresponding baselines formed double difference observations for the corresponding day.

Table 7.2 Daily baseline formation

Baselines	Lengths (m)	Day: Jan.				
		3	4	5	6	7
PL AL	2240379	▨	▨	▨	▨	▨
AL CH	1221697	▨	▨	▨	▨	▨
PL OW	1779016	▨	▨	▨	▨	▨
AL WF	642550	▨	▨	▨	▨	
OW FT	316122	▨	▨	▨		▨
OW MJ	245873				▨	▨
BU BR	238895					▨
OW BU	226240	▨	▨	▨	▨	▨
BU PA	204822				▨	▨
BU VN	145547				▨	▨
BR DE	145307		▨	▨	▨	
CF BR	131037	▨				
GA BU	123698	▨	▨	▨		
BU LA	104483				▨	▨
LA SE	70287				▨	▨
GA DE	64859		▨	▨		
GA SE	61720	▨	▨	▨		
LA DE	52030				▨	▨
LA ML	47417					▨
GA LA	44551	▨	▨	▨		
LA CF	41269	▨				
LA SI	40495		▨	▨	▨	▨
GA VN	38803	▨	▨	▨		
BR PA	37354	▨				

Main-processor: The output data of PREDD were the input data of the main-processor. A tropospheric delay scale parameter was estimated for each station per observation window. The observation windows of the standard data set were mostly seven hours. The

100

initial "integer" phase ambiguities were estimated as real numbers. Station coordinates, the six Keplerian elements describing the initial condition of the orbit of each satellite, together with the two solar radiation parameters per satellite, were estimated from all data while the fiducial points were held fixed. In the computation of the daily repeatability, the satellite orbits from the 5 day solution were held fixed and observations of a particular day were used to estimate the receiver coordinates.

A long smooth orbit arc for each satellite is used in the five day solution. That is, only one set of initial Keplerian elements and solar radiation parameters for each satellite were used for all five days in the five day solution. The short arc approach, which estimates a set of initial Keplerian elements for each observation window, can be regarded as a specific case of our model. The analysis of the data using the short arc approach, i.e., estimating Keplerian elements daily as a daily solution, using DIPOP-E, hasn't been made.

Table 7.3 is a set of initial Keplerian orbital elements and solar radiation parameters obtained from our data processing. Table 7.3(a) was obtained from orbital improvement of the broadcast ephemerides spanning five days. Table 7.3(b) was obtained from the solutions of processing the phase observations of the 5 days.

Correcting remaining cycle slips: As stated in Chapter 6, PREDD does not always eliminate cycle slips completely. To solve this problem, the utility software, CPLOT, was used to go over the residuals, and to determine and correct the cycle slips remaining in the double difference observations. In this data processing, two iterations of the cycle slip correction loop were involved as depicted in Figure 6.1. In the first iteration, the main-processor processed the data from the direct PREDD output, CPLOT was used to go over the observation data and the residuals and only very large cycle slips were corrected in this iteration. In the second iteration, the main-processor used the data from the first iteration,

and CPLOT determined all fixable cycle slips. The data from the second iteration were used for our final data processing.

Table 7.3 (a) Orbital elements and solar radiation parameters (from broadcast ephemerides)

PRN	9	12	3
Orbit Elements			
a (in meters)	0.265623221E+08	0.265591212E+08	0.265843473E+08
e	0.121493179E-01	0.881303605E-02	0.117557166E-01
i (in radians)	0.111643370E+01	0.110775781E+01	0.110795382E+01
Ω (in radians)	0.157521546E+01	0.157118107E+01	0.535396978E+00
ω (in radians)	0.117183847E+01	0.983537482E+00	0.369656315E+01
τ (in seconds)	0.553454950E+06	0.544005236E+06	0.522894181E+06
direct radiation (in meter/sec^2)	0.891610110E-07	0.872821172E-07	0.101445458E-06
y-bias radiation (in meter/sec^2)	0.434894417E-09	0.432685055E-10	0.104120531E-08
PRN	6	11	13
Orbit Elements			
a (in meters)	0.265612212E+08	0.265594496E+08	0.265595858E+08
e	0.442318000E-02	0.114892253E-01	0.305436881E-02
i (in radians)	0.111981356E+01	0.109871593E+01	0.109386909E+01
Ω (in radians)	0.157277318E+01	0.545947666E+00	0.537835376E+00
ω (in radians)	0.207932408E+01	0.268846616E+01	0.284746474E+00
τ (in seconds)	0.554837350E+06	0.533103765E+06	0.556490887E+06
direct radiation (in meter/sec^2)	0.887474911E-07	0.984374639E-07	0.896995176E-07
y-bias radiation (in meter/sec^2)	0.164099767E-09	0.325393558E-09	0.679359018E-09

Table 7.3 (b) Orbital elements and solar radiation parameters (from phase observations).

PRN	9	12	3
Orbit Elements			
a (in meters)	0.265623261E+08	0.265591489E+08	0.265843487E+08
e	0.121493911E-01	0.881343351E-02	0.117557431E-01
i (in radians)	0.111643361E+01	0.110775774E+01	0.110795390E+01
Ω (in radians)	0.157521289E+01	0.157117860E+01	0.535399656E+00
ω (in radians)	0.117180498E+01	0.983411606E+00	0.369656238E+01
τ (in seconds)	0.553454727E+06	0.544006091E+06	0.522894181E+06
direct radiation (in meter/sec^2)	0.970236713E-07	0.883548939E-07	0.864471184E-07
y-bias radiation (in meter/sec^2)	0.401788084E-09	0.438007097E-09	0.572105432E-09
PRN	6	11	13
Orbit Elements			
a (in meters)	0.265612205E+08	0.265594507E+08	0.265595419E+08
e	0.442294421E-02	0.114892375E-01	0.305333824E-02
i (in radians)	0.111981352E+01	0.109871589E+01	0.109386909E+01
Ω (in radians)	0.157277045E+01	0.545950257E+00	0.537837448E+00
ω (in radians)	0.207931852E+01	0.268847361E+01	0.283902650E+00
τ (in seconds)	0.554837317E+06	0.533103710E+06	0.556496647E+06
direct radiation (in meter/sec^2)	0.991089023E-07	0.882286156E-07	0.909213821E-07
y-bias radiation (in meter/sec^2)	0.569593192E-09	0.262118160E-09	0.273451000E-09

The number of remaining cycle slips after PREDD processing was dependent on both the length of the corresponding baseline and data quality of the two stations forming the double difference observations. Observations of a longer baseline had more cycle slips than those of shorter baselines. Observations contaminated more by ionospheric effect also had more cycle slips. For example, a double difference data file involving the station Churchill had more than 20 cycle slips. However, short baselines had only a couple of

cycle slips or had no cycle slips. We did not fix the cycle slips for which the real estimations were very close to half cycles.

Tropospheric effect: A tropospheric scale correction was estimated for each station per observation window. However, the *a priori* values and the constraint (0.8) were almost arbitrarily set.

Correlation between observations: no correlations are included in our model and software. Therefore, all correlations were ignored in our data processing.

7.3 The Results

Numerous internal tests were made for many parts of the model and the software implementation (and they are too trivial to be presented here), but the most convincing test was in using the real data. In this section, the results from analyzing the standard data set are presented. Five aspects are examined: the formal uncertainties (or formal errors, or standard deviations) directly from the results of the adjustment; the daily repeatabilities; the comparisons with the distributed station coordinates; and the comparisons of the results with those obtained completely independently by another research group. In the last subsection, miscellaneous results of the test are given.

7.3.1 Station Coordinates and Formal Uncertainties

Table 7.4 shows the Cartesian coordinates and formal uncertainties of the stations using the data from all five days. The three fiducial stations have formal uncertainties of 0 mm (after truncation), since we had high constraints on them in our adjustment (discussed in the previous section).

Table 7.4 Geocentric coordinates of stations from five days' data processing

station coordinates in meters and standard deviation (formal uncertainties) in millimeters						
Stations	X	STD	Y	STD	Z	STD
PL	-1240708.269	0	-4720454.201	0	4094481.781	0
AL	918127.499	0	-4346061.915	0	4561984.26	0
OW	-2410422.594	0	-4477802.462	0	3838686.837	0
CH	-236417.055	17	-3307612.019	19	5430055.694	9
WF	1492232.869	7	-4458091.779	9	4296046.017	8
BU	-2554674.248	3	-4534923.658	4	3674025.614	3
GA	-2647055.561	5	-4548316.947	5	3592861.563	4
LA	-2608883.252	5	-4571283.202	5	3592440.503	4
SE	-2656791.895	6	-4582160.484	6	3542173.98	5
CF	-2583875.903	6	-4598589.286	7	3574215.914	6
BR	-2535535.775	7	-4688425.847	7	3491976.597	5
DE	-2628754.245	6	-4592961.077	6	3549517.938	5
FT	-2697026.914	3	-4354393.146	3	3788077.727	3
SI	-2584758.154	6	-4597954.754	6	3573827.375	5
PA	-2525452.92	7	-4670035.5	8	3522886.861	6
VN	-2678071.783	5	-4525451.627	6	3597427.484	4
MJ	-2356214.783	5	-4646733.83	6	3668460.524	4
ML	-2648983.13	7	-4545991.937	9	3593264.396	7

The formal uncertainties of the ellipsoidal station coordinates are shown in Figure 7.3. As seen from the figure, for the station coordinates, the formal uncertainties of the latitude components range from 0.88 to 0.50 as large as the formal uncertainties of the longitude components and the formal uncertainties of the longitude components range from 1.06 to 0.40 as large as the formal uncertainties of the height components.
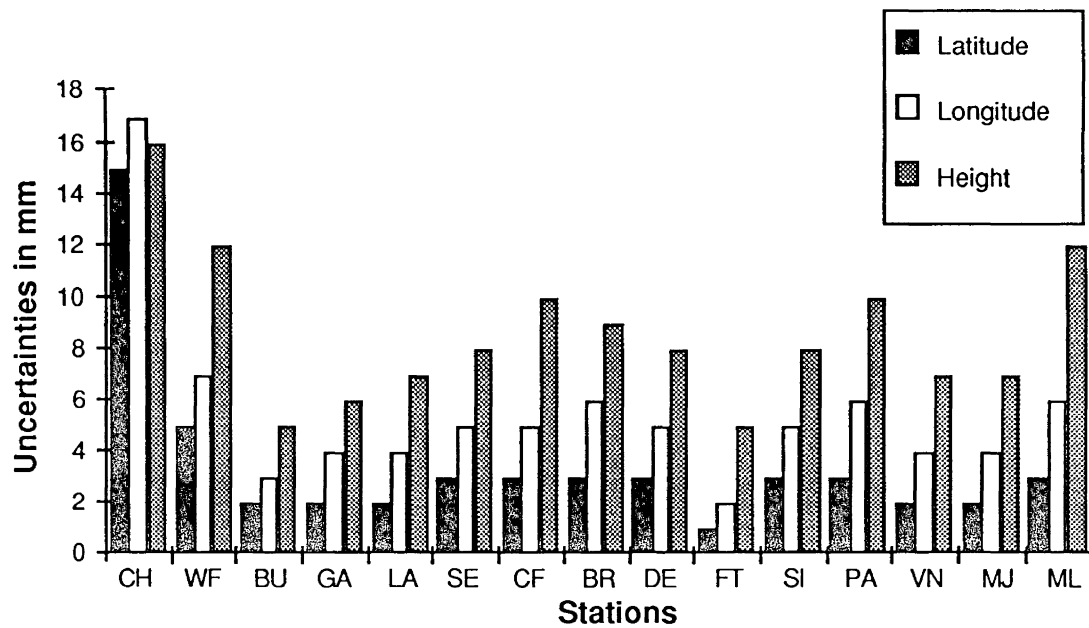
Figure 7.3 Formal uncertainties of the geodetic coordinate components of the stations

Figure 7.4 illustrates the formal uncertainties of ellipsoidal baseline components from the five day solution. The baselines are in order of lengths. Similarly to Figure 7.3, the formal uncertainties of the latitude components range from 0.88 to 0.33 as large as the formal uncertainties of the longitude and the longitude components range from 1.06 to 0.40 of the height components. All formal uncertainties of the components were below 20 mm and most of the components were below 10 mm.
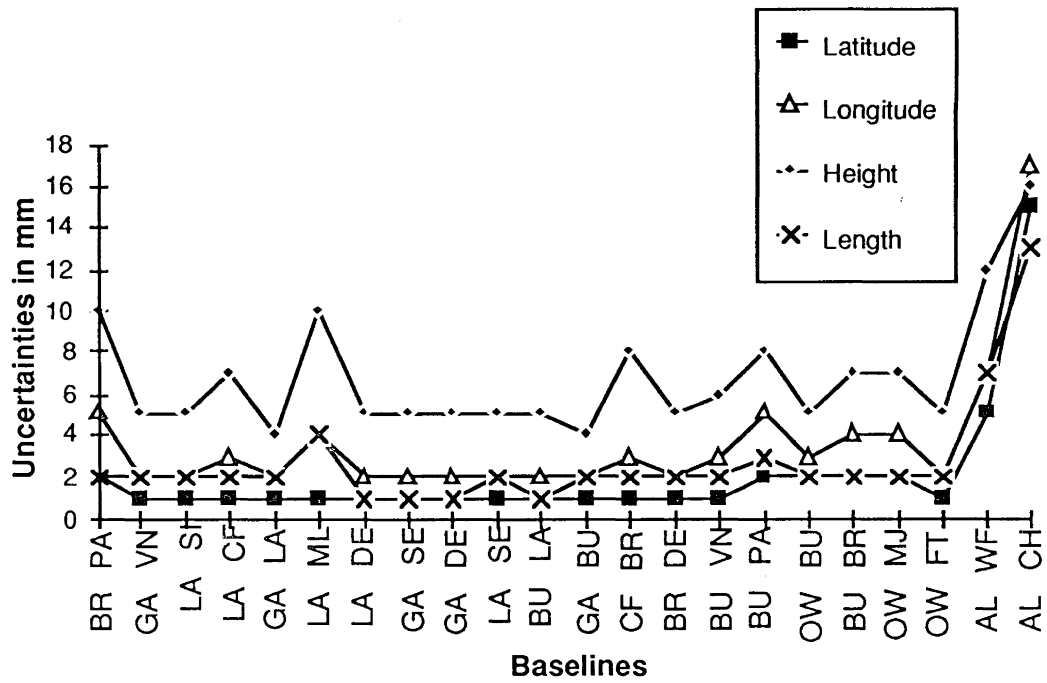
Figure 7.4 (a) Formal uncertainties of the geodetic coordinate components of the
baselines (in mm)
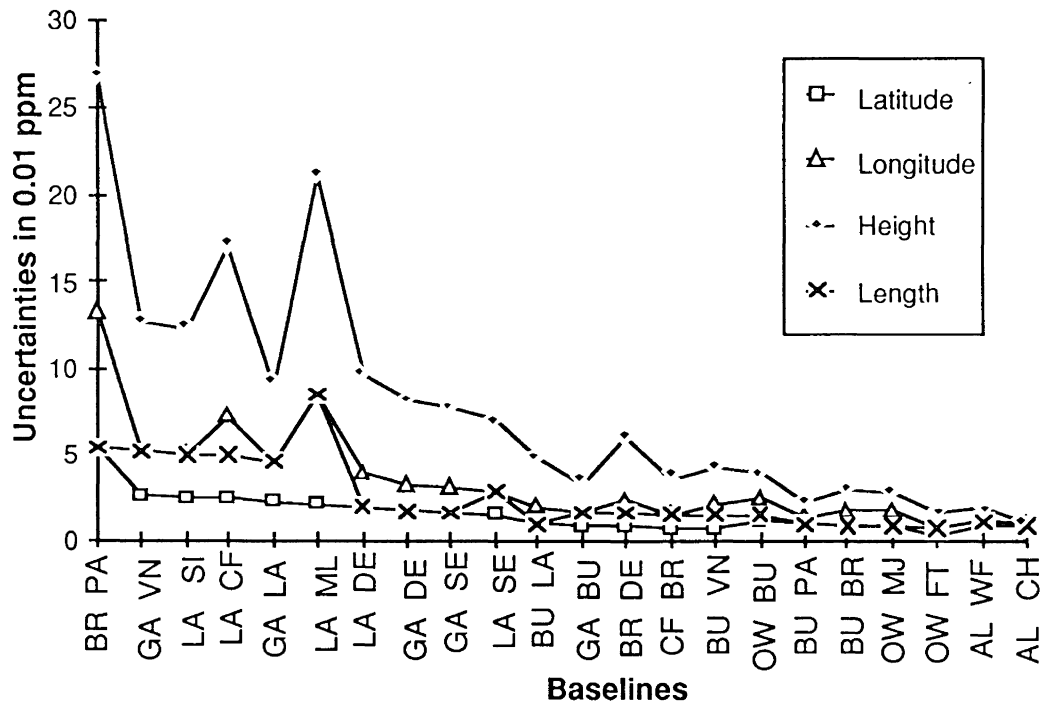
Figure 7.4 (b) Formal uncertainties of the geodetic coordinate components of the
baselines (in ppm)

107

The poorer results on the longitude components can be explained by the sky distribution of the GPS satellites during the campaign: as seen from Figure 7.2, the tracks of the six observed satellites (PRN 3, 6, 9, 11, 12, and 13) are favorable in the latitude direction. The poor formal uncertainties of the station Churchill (CH) results from its being further away from the fiducial points than the other stations.

The formal uncertainties tend to be overly optimistic. Although the relative sizes of the formal uncertainties can reflect the relative strengths of the station geometry and data spans, they do not reflect the effect of unmodelled biases (or systematic effects) and data quality for individual stations or baselines.
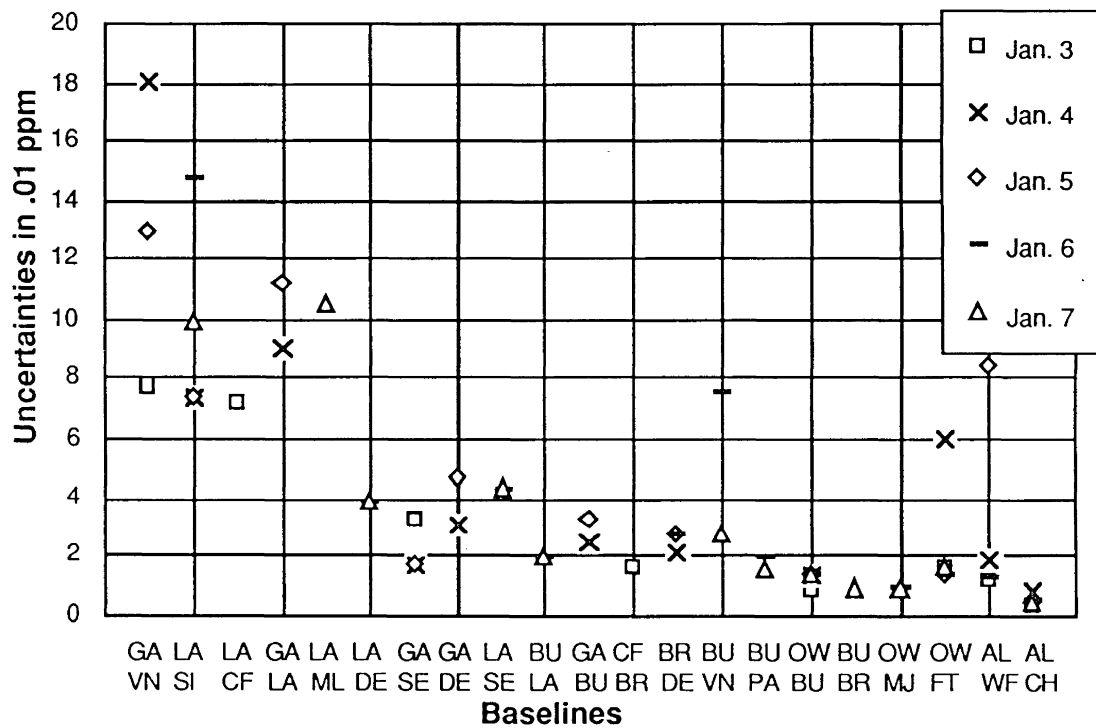
Figure 7.5 Formal errors of daily baseline length determination.

The formal uncertainties for the lengths of daily solutions are shown in Figure 7.5. They are useful in analyzing the effects of the geometry of the baselines. The baseline

108

"BR-PA" is not shown in the figure due to its outstanding large values of formal uncertainties and we will discuss more about this in the next subsection.

7.3.2 Daily Repeatabilities

One of the methods used to test the software was the comparison of station coordinates from daily solutions. The orbits obtained from the five day solution were used and held fixed during the processing to get daily solutions. The daily results were assessed by comparing them with the five day solution and they are plotted in Figures 7.6 to 7.10. The repeatabilities of the lengths of the baselines for all 5 individual days are overlaid in Figure 7.11. The differences shown in all six figures are with respect to the results from the 5 day solution.

As seen from the figures, the best results are for the latitude components, and the baseline lengths second best, followed by the longitude components and at last the height components. This characteristic behaviour coincides with the results of section 7.3.2 and can be explained, in part, by the sky distribution of the GPS satellites during the whole observation period. However, the sizes of the differences are larger than those of the formal uncertainties and this indicates there are some systematic effects remaining in the results.

There are two clear "outliers" for the baseline results: the baseline BR-PA on 3 January (day 3) and the baseline BU-VN on 6 January (day 6). The poor results for these baselines are due to short observation periods. For baseline BR-PA on day 3, only observations for satellites 3, 6, and 11 were available: observation period of 76 minutes for the satellite pair 3-6; observation period of 38 minutes for the satellite pair 6-11. Similarly for BU-VN on day 6, there is a large data gap and only observations at the beginning and the end of the observation session are available.

109

As seen by comparing Figure 7.5 with Figure 7.11, large formal uncertainties in lengths normally correspond to large daily length differences. Large "singled out" differences in heights (but not in other components) for some baselines are most likely caused by tropospheric effects or less likely by antenna height measurement errors (not confirmed).

Overall lower accuracy for the short baselines is mostly caused by effects other than orbital errors, possibly by unmodelled residual tropospheric delays. Only two minute samples were used and possibly some unfixable cycle slips or bad data had been input to the main-processor. Also, there was a reported antenna height measurement error at Ft. Ord on day 3 [Bock, 1988] and we have not accounted for this in our processing.

Repeatability reflects the positioning accuracy for a single day solution. Therefore, the five day solution should be better than the daily solutions for each of 5 days.
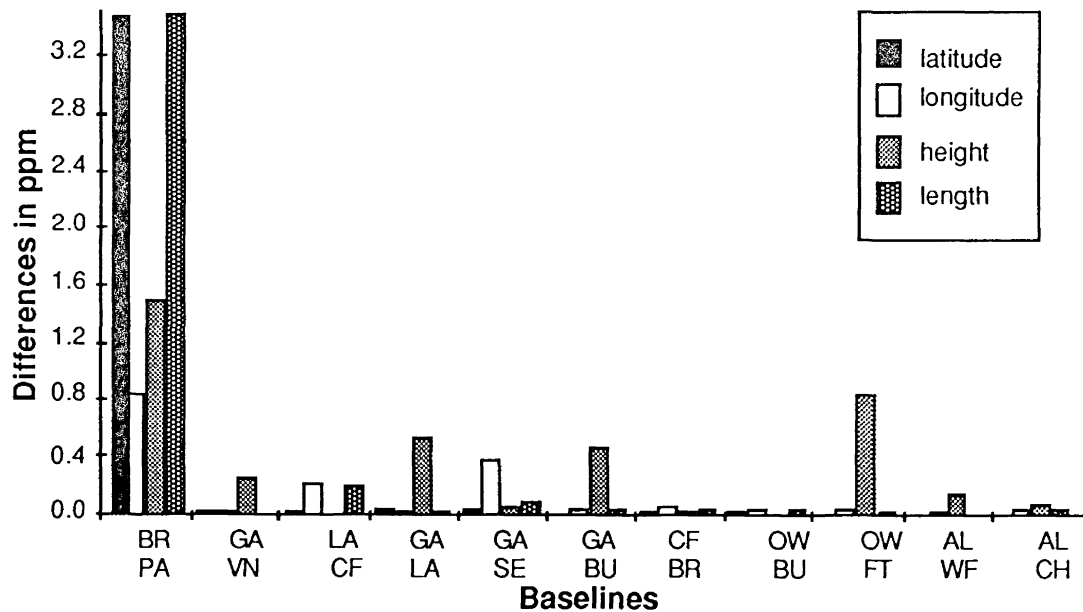
Figure 7.6 Comparison of baseline components for 3 January with the 5-day solution.
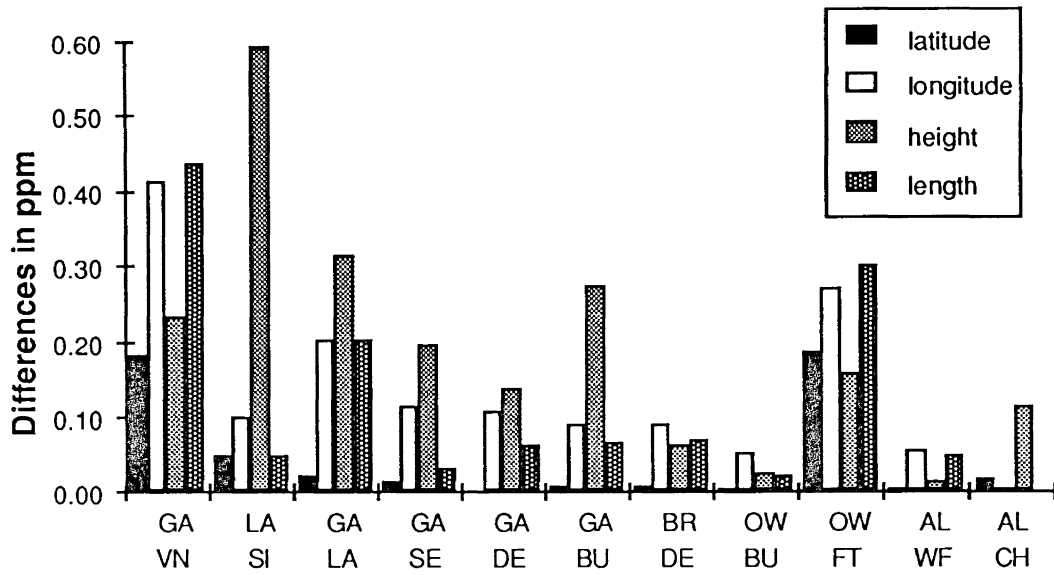
Figure 7.7 Comparison of baseline components for 4 January with the 5-day solution.
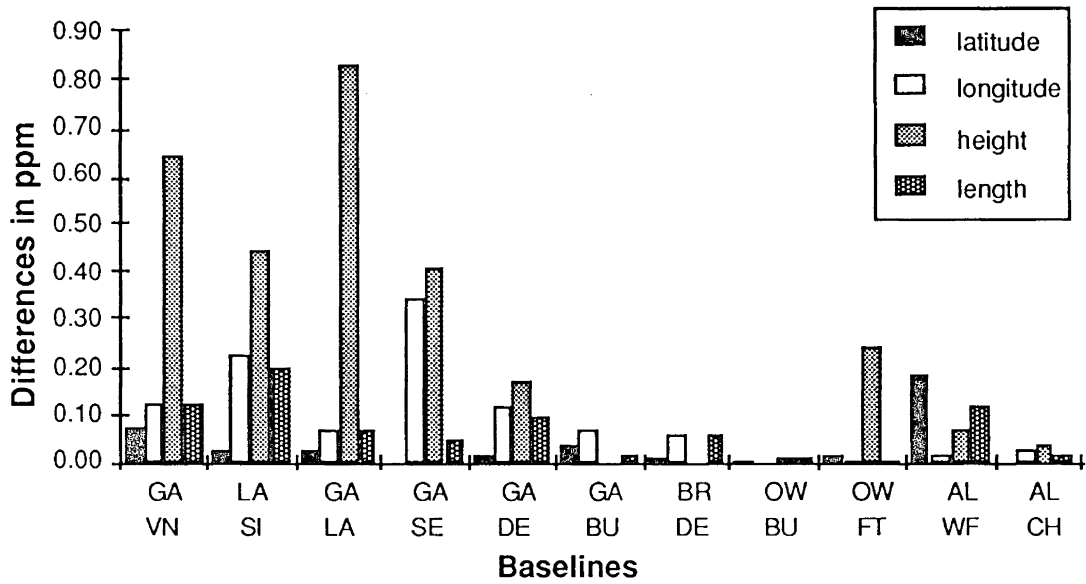
Figure 7.8 Comparison of baseline components for 5 January with the 5-day solution.

111
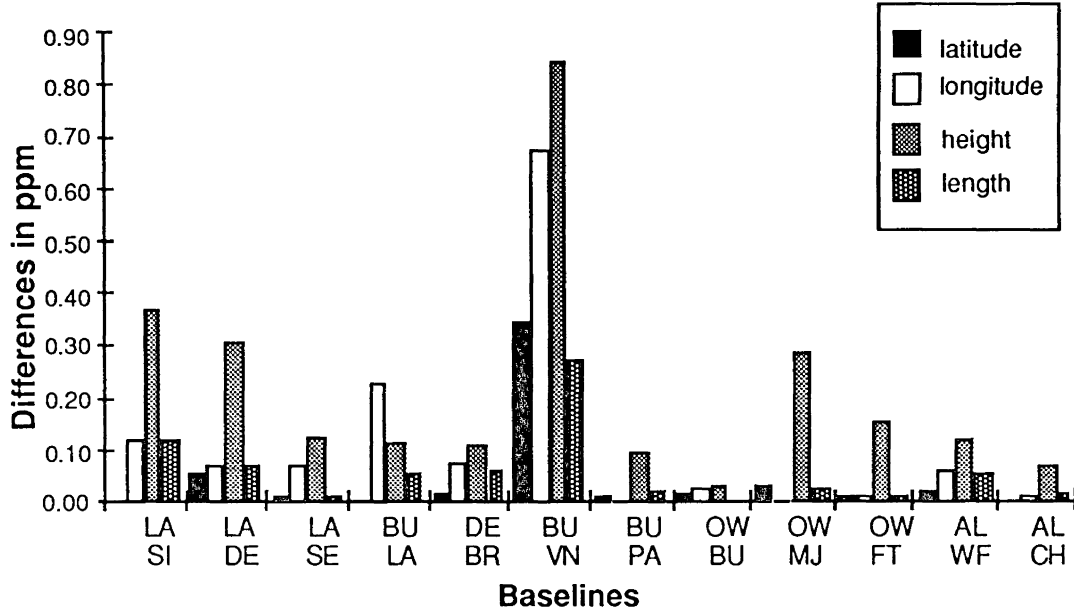
Figure 7.9 Comparison of baseline components for 6 January with the 5-day solution.
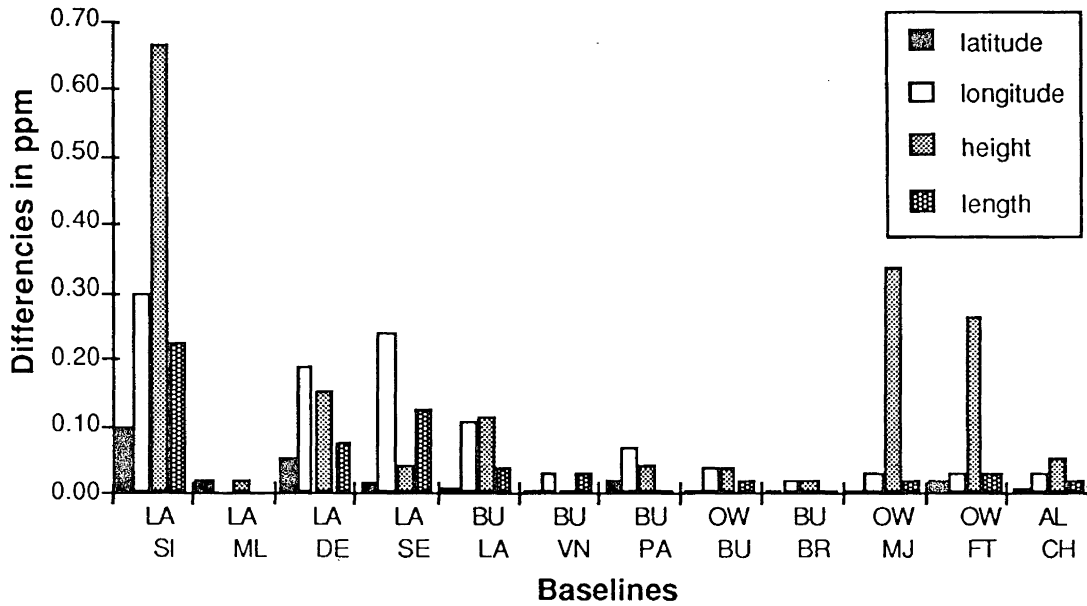
Figure 7.10 Comparison of baseline components for 7 January with the 5-day solution.

112

Differences in .01 ppm

45
40
35
30
25
20
15
10
5
0

□ Jan. 3
✕ Jan. 4
◇ Jan. 5
— Jan. 6
△ Jan. 7

GA LA LA GA LA LA GA GA LA BU GA CF BR BU BU OWBU OW OWAL AL
VN SI CF LA ML DE SE DE SE LA BU BR DE VN PA BU BR MJ FT WF CH
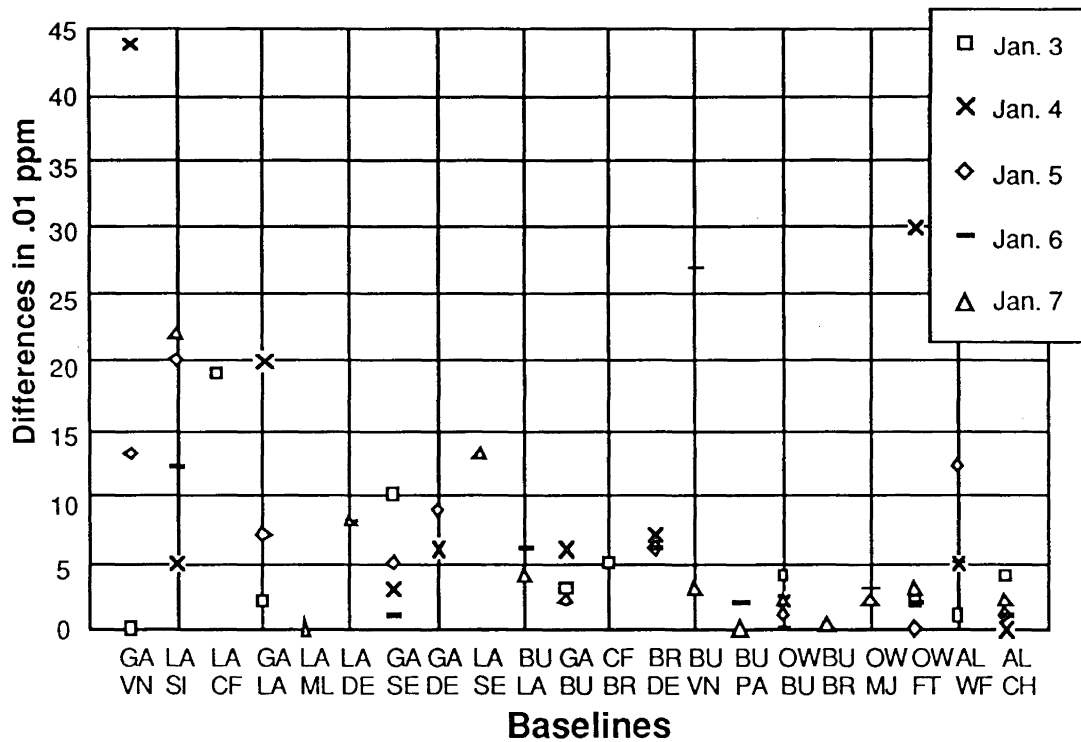
Baselines

Figure 7.11 Daily repeatabilities of baseline lengths for all 5 daily solutions.

7.3.3 Comparison with an Independent Solution

Another method to test the model and the software is to compare our results with the results of another research group. A particular solution obtained by the Astronomical Institute of the University of Bern was used for the comparison [Beutler, 1989]. The Bernese results are taken from the solution file called UPFXT307. The results in this file were obtained using updated orbits from a previous solution, and tropospheric delay parameters were estimated along with the station coordinates. The initial phase ambiguities were fixed to integer values. The same set of fiducial stations were used by the Bernese group, but because we expressed the coordinates of these stations in a different coordinate system, it was necessary to use a seven parameter Helmert similarity transformation in order to compare our results. Only local and regional stations are compared.

The results of the comparison are depicted in Table 7.5 and Figure 7.12. Table 7.5 contains the transformation parameters and Figure 7.12 shows the residual differences after the transformation. The comparison was made using Cartesian coordinates. The agreement between the two solutions is quite good. The differences range from 0.2 mm to 21.8 mm. The r.m.s. of the residuals after the transformation was only 8.5 mm. The residual differences between the two solutions are due to a number of factors. For example, we may have carried out the orbital integrations differently; we probably formed different site and satellite combinations for the double differences; the ambiguities were fixed in the Bernese solution whereas we estimated them as real numbers; the Bernese group used the 30 second data whereas we used the two minute decimated data.

Table 7.5 Results of comparison with Bernese solution.

NUMBER OF PARAMETERS	7	
NUMBER OF COORDINATES	42	
r.m.s. OF TRANSFORMATION	8.5 mm	
PARAMETERS:	VALUES	FORMAL ERRORS
TRANSLATION IN		
X	0.000 m	0.002 m
Y	14.058 m	0.002 m
Z	-0.012 m	0.002 m
ROTATION AROUND		
X-AXIS	0° 0' 0.48"	0.00 "
Y-AXIS	0° 0' 0.00"	0.00 "
Z-AXIS	0° 0' 0.31"	0.00 "
SCALE FACTOR	-0.04 mm/km	0.01 mm/km

The small differences between our solution and the Bernese solution show the fixing of initial ambiguities has only a small impact on the results of analyzing this data set. This

is primarily due to the relatively long observation windows (almost seven hours). However, for short observation windows, the fixing of initial ambiguities is still very important, since the ambiguity fixing will improve the geometrical strength of the observation equations.
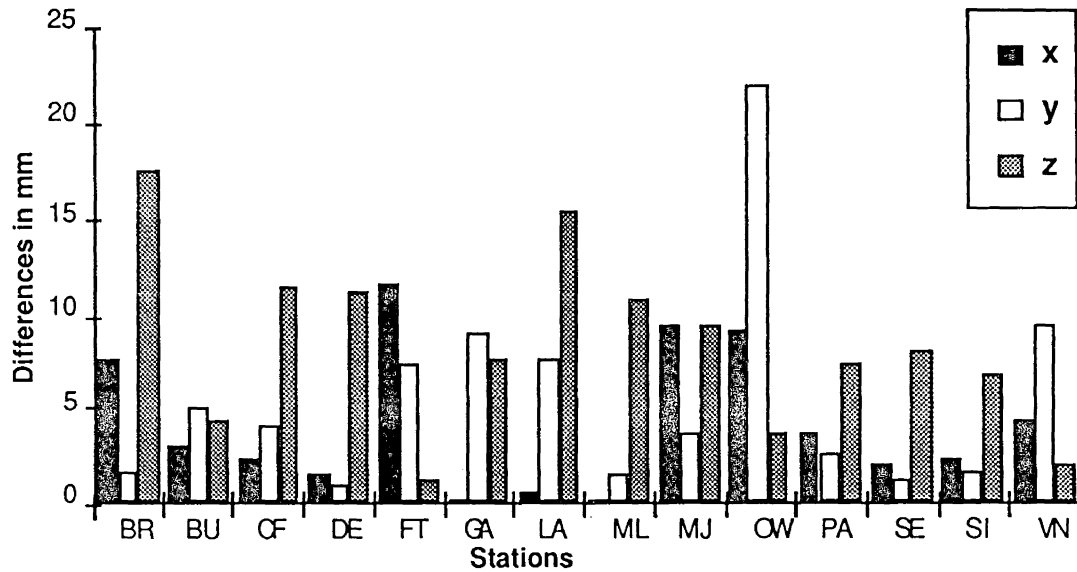
Figure 7.12 Residuals from the comparison of our results with those of the Bernese group after applying a Helmert similarity transformation.

7.3.4 Comparison with the Distributed Coordinates

Another test made was to compare our results with previously determined coordinates of the stations. The coordinates accompanying the distributed data were compared with our 5 day solution. The coordinates of the fiducial sites and the regional sites were accurately known from earlier VLBI observations. The VLBI stations are Algonquin, Owens Valley, Platteville, Palos Verdes, Fort Ord, Mojave, and Vandenburg. However, we didn't get the station coordinates for the station Fort Ord from the distributed standard data set, so the comparison for the station Ford Ord was excluded.

Figure 7.13 Differences with respect to the distributed coordinates in mm.

116
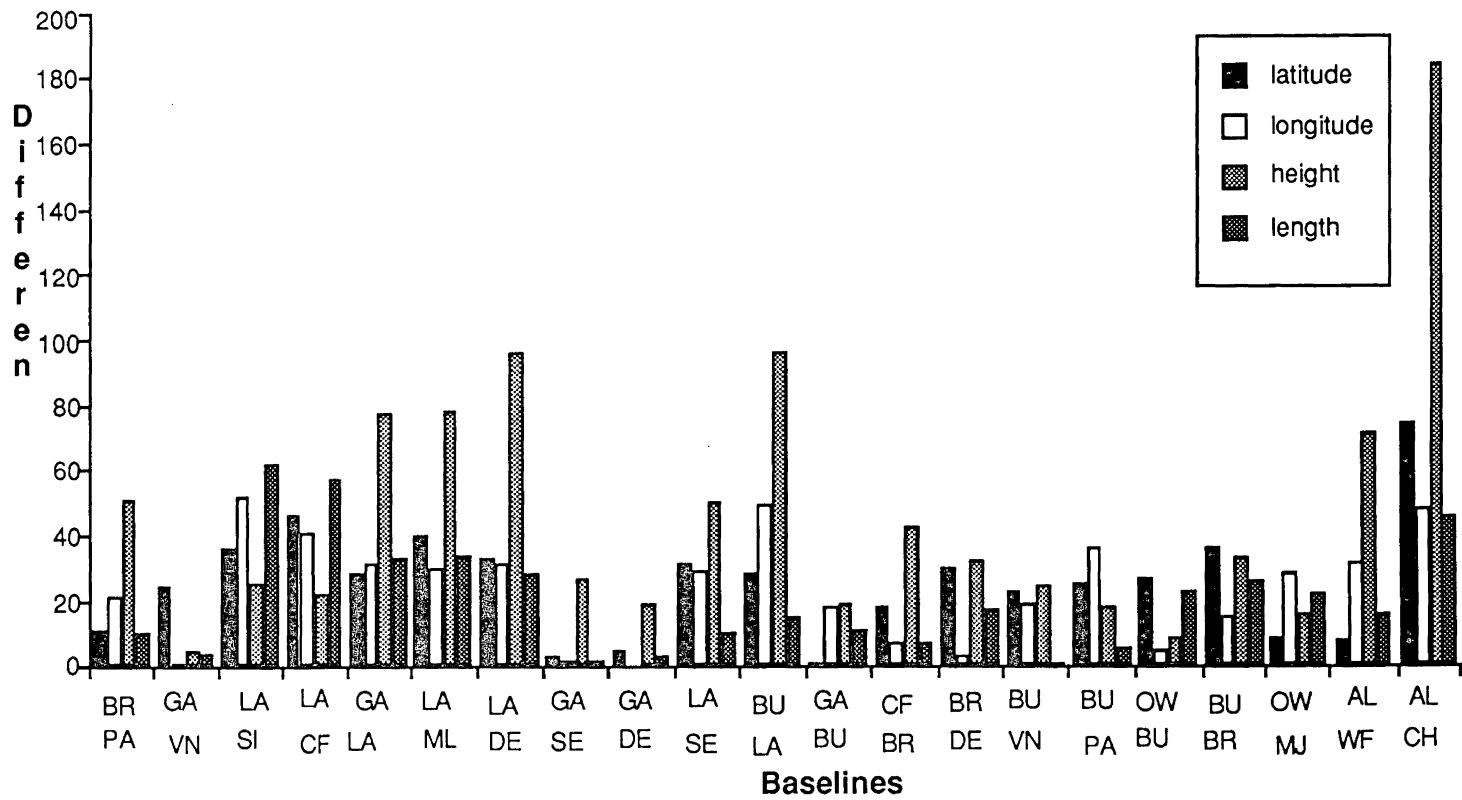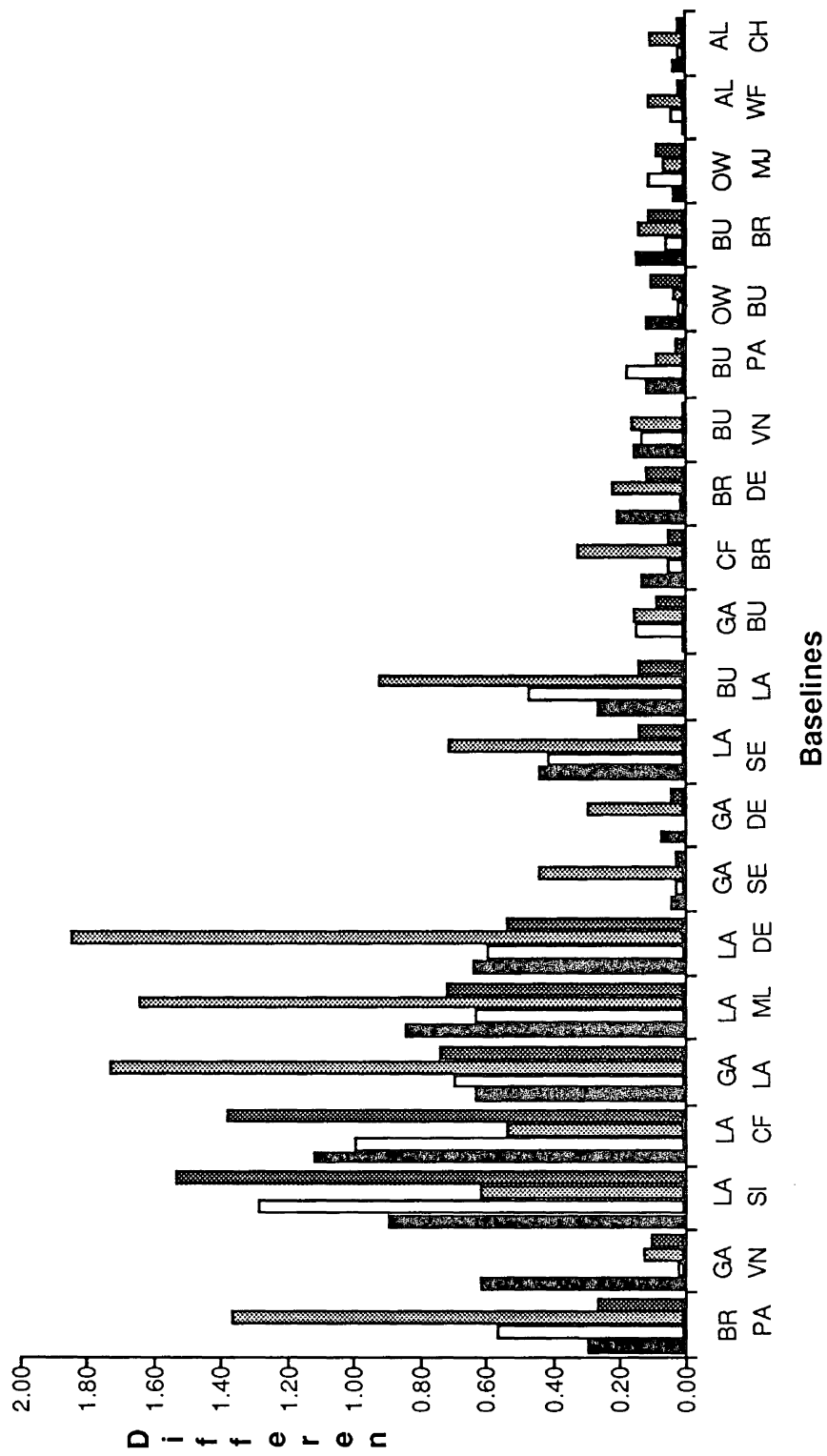
Figure 7.14 Differences with respect to the distributed coordinates in ppm.

Figure 7.13 and Figure 7.14 depict the differences of the ellipsoidal baseline components between the five day solution and the distributed coordinates. As seen from the figures, the sizes of the differences for baseline components are (from the best to worst): latitude components, baseline lengths, longitude components, and height components. These differences are not really dependent on the lengths of the baselines. The comparison also indicates that something other than the satellite orbits affects the results of this testing. As discussed in Section 2 of this chapter, these large differences for the short baselines come from the unmodelled tropospheric effect, missing satellites, and remaining cycle slips. Another cause for the larger differences could be that the distributed station coordinates of the local sites are somehow less accurate. As discussed previously, the poorer results of the station Churchill are due to its being further away from the fiducial stations and also poorer cycle slip fixing of the observations relating to this station.

7.3.5 Analysis of Residuals

Residuals may reveal whether there are unmodelled bias effects in our solution. They can also reflect abnormal observations. As a typical example, shown in Figure 7.15, are the residuals from our processing for satellite pair 9-11 of baseline Buttonwillow - Palos Verdes on 7 January.

The top figure shows the residuals obtained without considering the difference of the receiver clock time with respect to GPS time in time tagging the observations. The bottom figure shows the residuals obtained by taking this time difference into account using the measured pseudoranges. There is a clear improvement.

118
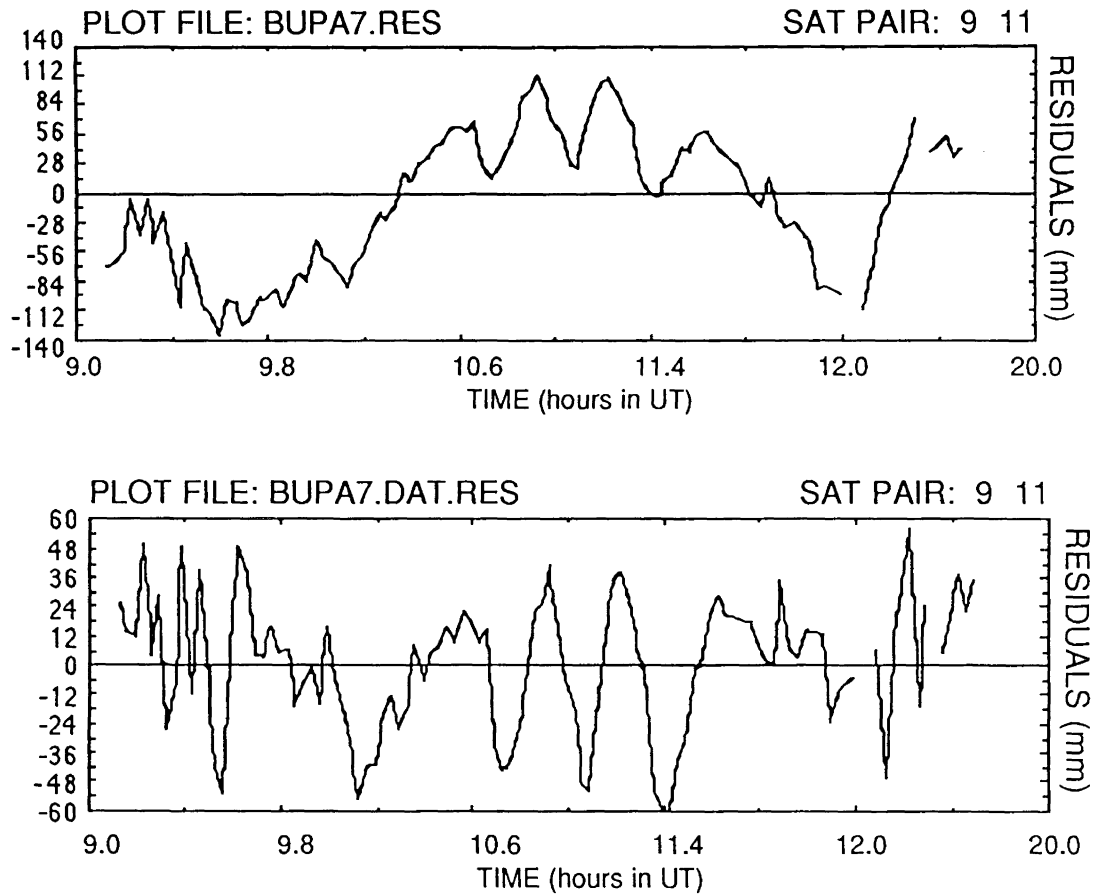
Figure 7.15 Double difference residuals for the satellite pair 9-11 for the baseline
Buttonwillow - Palos Verdes on 7 January.

7.3.6 Miscellaneous Results

We made many tests of our model and software. These tests included the tidal perturbation on the GPS satellite orbits, effect of different values for the Earth's gravitational constant GM, penumbral effect of solar radiation pressure, receiver clock offsets, etc. They are briefly described below.

For the test of the solid body tidal perturbation on the orbits of the GPS satellites and subsequently on positioning, two different processings were carried out: one was the

processing of five days' data by considering the tidal perturbation on the orbits; the other processing without considering the tidal perturbation. The differences of the positions from the two processings were below the formal uncertainties of the positioning. The difference on the height component for the station Churchill was close to 1 cm, a few millimeters (or even zero) for other stations.

Different gravitational values of GM were used to process the standard data set. The difference in the solutions caused by the two different GM values (WGS 84 value: GM = 3.986005D14; and the distributed value of the standard data set: GM = 3.98600443D14 were used) is below the formal uncertainty values. The maximum difference is close to 3 mm considering all stations; there are no differences for most stations.

The penumbral effect of the solar radiation pressure was examined for this standard data set. The penumbral effect means that the solar radiation pressure on a satellite disappears gradually instead of suddenly when the satellite moves into the Earth's shadow or moves out of the shadow. In our model and software development, the penumbral effect is not considered (see Section 3.3.1).

Our integrator tends to smooth the sudden change of the solar radiation model and integrations using different step sizes smooth the sudden change of the radiation model differently. If the penumbral effect were significant in this data analysis, the results from integrations using different step sizes should differ significantly as well. To test the penumbral effect, we used different steps (i.e., step sizes of 60, 120 and 240 seconds) for the integration of the orbits since the orbits obtained with different integration steps were affected by the penumbral effect differently. The result of the test is: there are no differences in the station coordinates of five day solutions using different step sizes of integrators.

The drift of the receiver clock at Buttonwillow on Jan. 6 is plotted in Figure 7.16. The drift was computed using equation (5.4). As shown, the drift is linear to within a precision of 5 microseconds during the observation period of nearly seven hours. Table 7.6 lists the maximum clock offsets (with respect to the GPS time) of the receivers during the observation period on Jan 6. As seen from the table, the receiver clocks at the stations Algonquin and Owens Valley had small offsets; the receiver clock at the stations Buttonwillow, Vandenburg and Palos Verdes had large offsets with respect to the GPS time.
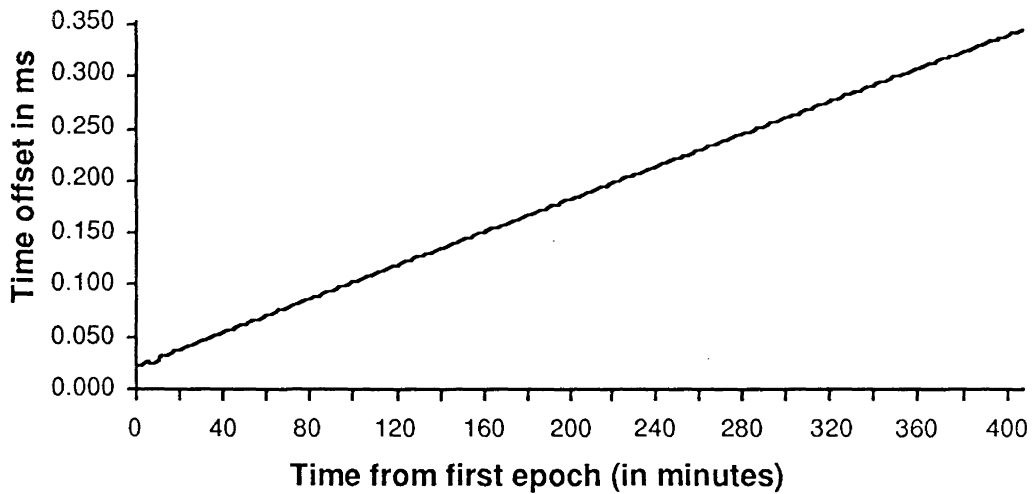
Figure 7.16   The drift of the receiver clock at Buttonwillow on Jan. 6, 1987.

Table 7.6   The maximum clock offsets of the receivers on Jan. 6, 1987.

Stations	Offsets (in ms)	Stations	Offsets (in ms)
LA	.00019	SI	.00089
SE	-.00009	AL	.00002
VN	-.00113	CH	-.00043
WF	0.00000	FT	.00061
OW	0.00000	DE	-.00018
MJ	.00002	PL	.00013
BU	.00035	BR	-.00021
PA	-.00154		

7.4 Summary of Results

From our analysis of the SSG data set, it can be concluded that the formal uncertainties tend to be overly optimistic. The daily repeatabilities show that the latitude component and baseline length determination were mostly better than 0.1 ppm. For the regional and continental stations, 0.05 ppm level repeatabilities were achieved for the lengths of baselines. The comparison of our 5 day solution with the solution of the Bernese group showed that the r.m.s. difference is only 8.5 mm. The worse results for the short baselines may be due to the residual tropospheric effects as no observed meteorological data have been used in the data processing. Comparison with the distributed coordinates also shows consistency at the 0.1 ppm level. Worse results were obtained for short baselines, partially due to the troposphere, and partially due to the lesser accuracies of the distributed local station coordinates (as they were not VLBI stations). Our results for these stations seem to be better than the distributed coordinates. Latitude components were better determined due to the sky distribution of the satellites.

CHAPTER 8

SUMMARY AND RECOMMENDATIONS

This chapter gives a summary of the orbit improvement model, its software implementation and the results of the testing. Finally, some suggestions are made for the further improvement of the model and the software.

A GPS orbit improvement model and its associated software have been developed. The model includes the coordinate system transformations, modeling of the forces acting on a GPS satellite, integration technique, computational algorithms, and the establishment of double difference observation equations.

The geocentric inertial (space-fixed) coordinate system is used for the equations of motion of the GPS satellites whereas the Earth-fixed coordinate system is used for observation equations. The coordinate system transformation between these two systems includes a rigorous description of the effects of nutation and precession using the J2000.0 system of constants and models. The tidal variations of UT1 are also incorporated.

A single continuous orbital arc for each satellite is used in the orbital adjustment. The advantage of the long arc approach is that a more realistic orbit can be obtained as long as the force model is correct. The trajectories of the satellites are obtained by numerical integration. The integration technique used is a multi-step predictor-corrector method. Typically an integrator of the order of 9 or 10 is used. In addition to the parameters describing the orbits, two parameters associated with the solar radiation pressure model are estimated for each satellite. The partial derivatives with respect to the two solar radiation parameters are computed using the same numerical integration technique as that used for the

123

orbits of the satellites. The partial derivatives with respect to initial state vectors are obtained by assuming the satellite orbits to be ellipses described by the initial state vectors.

The vertical displacements of the ground stations due to the solid Earth tide are modelled. And the offsets between the centres of mass of the GPS satellites and the phase centres of their antennas are also taken into account.

The modelling of the forces acting on the GPS satellites includes the gravitational perturbations of the Earth to degree and order 8 using the GEM L2 gravity field, the effect of the Moon and the Sun, the effect of solar radiation pressure and the effect of the solid Earth tide. As already mentioned, the solar radiation pressure on a satellite is described by two parameters which are estimated in the least squares adjustment procedure.

Double difference phase observations are used as input for the adjustment, and the observation time tags are converted from receiver time to GPS time using the observed pseudoranges. Note that the double differencing *a priori* removes, or greatly reduces, the effects of the satellite and receiver clock errors.

The ionospheric effect is removed almost entirely by forming ionospheric free linear combinations of the L1 and L2 observations. The tropospheric delay is modelled using a modified Hopfield's model in conjunction with a scale correction for each station and each observing window. The scale correction is estimated in the adjustment process. Optionally, the satellite orbital elements and the two solar radiation pressure components for each satellite can be estimated. Carrier beat phase ambiguities are estimated as real values. All satellite orbital initial conditions, dynamical parameters in the force modelling of satellites, the troposphere scale parameters and *a priori* station coordinates are weight constrained.

A software package corresponding to the above model has been developed independently in this research at UNB and is called DIPOP-E. The inclusion of DIPOP in the name implies that it is a close relative of the original software DIPOP 2.0. Its pre-processor is basically the same model except some modifications have been made to accommodate the new features in the main-processor of DIPOP-E. The main-processor has significant differences with respect to DIPOP 2.0, but its software development has contributions from DIPOP 2.0. Nevertheless, most of DIPOP 2.0's subroutines have been used in direct or modified ways, although the new main-processor is more than three times as large as the main-processor and post-processor of DIPOP 2.0 together. Besides the new model features, there are many new program features implemented in DIPOP-E.

A prototype graphical utility program called CPLOT has been developed. It may be used to go over the residuals and the observations, and to detect, estimate, verify and correct remaining cycle slips that the pre-processor has failed to. Although it is still in a primitive stage, experiments on the SSG 1.104 standard data show a great improvement in solving the remaining cycle slip problem compared with the previous method in terms of both efficiency and capability.

The fast processing speed of the software is achieved by considering the sparseness of the design matrix and by designing appropriate computational algorithms. The improvement of processing speed is especially significant for large networks.

The model and its associated software were tested with the SSG 1.104 standard data set. The results were examined from five different aspects: the formal uncertainties; the daily repeatabilities; the comparison with the results of the Bernese group; the comparison with the distributed coordinates accompanying the SSG data set; the plotting of the residual files.

All of above tests show that the most accurate results were for the latitude components, followed by the baseline lengths, the longitude components, and finally height components. This phenomenon is due in large part to the sky distribution of the GPS satellites. The optimistic results of formal uncertainties show that there are some remaining systematic biases in the model. The daily repeatabilities show that the latitude component and baseline length determination were mostly better than 0.1 ppm. For the regional and continental stations 0.05 ppm level repeatabilities were achieved for the lengths of baselines. The worse results for the short baselines are primarily due to the residual tropospheric effects as no observed meteorological data have been used in the data processing. Comparison with the Bernese group shows that both models (and software) can achieve a similar level of accuracy. Comparison with the distributed coordinates also shows consistency at the 0.1 ppm level. Worse results were obtained for short baselines, partially due to the troposphere, and partially due to the lesser accuracies of distributed local station coordinates (as they were not VLBI stations).

The plots of the residuals show that it is sensible to convert the phase observations from the receiver clock time to GPS time for coded receivers to achieve better than 0.1 ppm accuracies.

From this research, suggestions may be made in two aspects: one is in the modelling and the other is in the software.

As far as the modelling is concerned, the suggestions are as follows:
• The better modelling of the troposphere should be investigated. In our data analysis, the *a priori* values and constraints were set almost arbitrarily. Therefore, the setting of these *a priori* values and constraints should be studied. Hopfield's mapping function for the tropospheric delay is not the optimal one and better mapping functions should be studied. The tropospheric scale parameters are estimated for each station per observation window

in our software. In the case of long observation periods, a stepwise approach of tropospheric scale parameter estimation should be implemented in our software (i.e., estimating a new tropospheric parameter at each station every hour or two).

- The modelling of the forces acting on the satellites should also be refined. An improved model would include the effects of: albedo, the ocean tides, the gravitation field of the planets, and the effects of relativity. The disk effect of solar radiation should also be considered for completeness of the solar radiation effect.

- A better coordinate system transformation should also be considered. Test should be made on the use of observed daily values of Earth orientation data rather than interpolated 5-day values. Also, tests should be made using a more up-to-date nutation model.

- An automatic ambiguity fixing method should also be developed and this is especially important for the short observation windows.

- We haven't considered any correlations in our model. The effect of mathematical and physical correlations should be investigated.

- Station displacement caused by ocean tide loading is not considered in our model and it should be implemented in any further development.

As far as the software is concerned, the following is recommended:

- The refined models described above should be implemented.

- The capability of processing different types of data should be implemented. DIPOP-E's main-processor can handle the data which DIPOP 2.0's main-processor can handle, but DIPOP-E's main-processor cannot handle in binary format. DIPOP-E's pre-processor can only handle TI 4100 data. DIPOP-E's main-processor and DIPOP's pre-processor are compatible if there is no orbital improvement involved. However, if orbit improvement is required and the drift of receiver clocks cannot be ignored, the direct using of the output of DIPOP's preprocessor will result in the bias of the receiver clock mapping in solving for coordinates.

- The utility software CPLOT should be refined. Such refinements should include: a neat output, reports (or prevention) of misuse by users, cycle slip correction for single frequency receivers, and cycle slip correction for squaring-type receivers.

REFERENCES

Arsenault, T. (1982). "Computer program library user's guide." Department of Surveying Engineering Technical Report No. 86, University of New Brunswick, Fredericton, Canada.

Bock, Y. (1988). "Availability of Standard GPS Data Set." GPS Bulletin, Global Positioning System Subcommission VIII, International Coordination of Space Techniques for Geodesy and Geodynamics, of IAG and IUGG, Vol. 1, No. 2, pp. 1-6.

Beutler, G., D.A. Davidson, R.B. Langley, R. Santerre, P. Vanicek, D.E. Wells (1984). "Some theoretical and practical aspects of geodetic positioning using carrier phase difference observations of GPS satellites." Department of Surveying Engineering Technical Report No. 109, University of New Brunswick, Fredericton, Canada.

Beutler, G. (1989). Personal communication. Astronomical Institute, University of Bern, Switzerland.

Buffett, B.A. (1985). "A short arc orbit determination for the Global Positioning System." M.Sc. thesis, Department of Surveying Engineering, The University of Calgary, Alberta, Canada.

Boucher, C. (1988). Definition and realization of terrestrial reference system. International Association of Geodesy, Special Study Group 5.123.

Chen, D.S. and R.B. Langley (1989). "A long arc approach to GPS satellite orbit improvement." Paper presented at the Canadian Geophysical Union 16th Annual General Meeting, McGill University, Montreal, May.

Decker, B.L. (1986). "World Geodetic System 1984." *Proceedings of the Fourth International Geodetic Symposium on Satellite Positioning*, Vol. 1, pp. 69-92.

Doucet, K. (1989). Personal communication. Department of Surveying Engineering, University of New Brunswick, Fredericton, Canada.

Fliegel, H.F., W.A. Fees, W.C. Layton and N.W. Rhodus (1985). "The GPS radiation force model." *Proceedings of First International Symposium on Precise Positioning with the Global Positioning System - Positioning with GPS-1985,* U.S. Dept. of Commerce, NOAA, Rockville, Md., pp. 113-120.

Gaposchkin, E.M. (1973). "1973 Smithsonian Standard Earth (III)." Smithsonian Astrophysical Observatory, Special Report 353. ED.

Georgiadou, Y. (1987). "Results of the Port Alberni GPS Survey 1986." Internal Report, Geophysics Divsision, Geological Survey of Canada, Ottawa, Ontario.

IAG (International Association of Geodesy) (1987). "IRIS Earth Orientation Bulletin" no. 35, International Radio Interferometric Surveying (IRIS).

Janes, H.W., R.B. Langley, S.P. Newby (1990). "Analysis of tropospheric delay prediction models: comparisons with ray-tracking and implications for GPS relative positioning (a summary)." *Proceedings of Second International Symposium on Precise Positioning with the Global Positioning System - GPS'90*, Ottawa, Canada, Sept. 3-7.

Kaplan, G.H. (1981). "The IAU resolutions on astronomical constants, time scales, and the fundamental reference frame." Circular No. 163, U.S. Naval Observatory, Washington, D.C.

Kaula, W.M. (1966). *Introduction to Satellite Geodesy*. Blaisdell, Waltham, Mass.

Kleusberg, A., R.B. Langley, R. Santerre, P. Vanicek, D.E. Wells and G.Beutler (1985). "Comparison of surveying results from different types of GPS receivers." *Proceedings of First International Symposium on Precise Positioning with the Global Positioning System - Positioning with GPS* U.S. Dept. of Commerce, NOAA, Rockville, Md., pp. 579-592.

Kleusberg, A. and L. Wanninger (1987). "Analysis of the Juan de Fuca GPS Survey 1986." Department of Surveying Engineering Technical Report No. 127, University of New Brunswick, Fredericton, Canada.

Kleusberg, A. and Y. Georgiadou (1988). "Establishment of crustal deformation networks using GPS: A case study." *CISM Journal ACSGC*, Winter, Vol. 42, No. 4, pp. 341-351.

Kleusberg, A., Y. Georgiadou, F. V. D. Heuvel and P. Héroux (1989). "Single and dual frequency GPS data preprocessing with DIPOP 2.1." Department of Surveying Engineering Technical Memorandum TM-21, University of New Brunswick, Fredericton, Canada.

Lambeck, K. and R. Coleman (1983). "The earth's shape and gravity field: a report of progress from 1958 to 1982." Geophys. J. R. Astr. Soc., 74, pp. 25-54.

Lambert, J.D. (1973). *Computational Methods in Ordinary Differential Equations*. John Wiley & Sons, New York.

Landau, H. and D. Hagmaier (1986). "Analysis of the required force-modelling for NAVSTAR/GPS satellites." GPS Research 1985 at the Institute of Astronomical and Physical Geodesy, Universität der Bundeswehr Munchen, pp. 193-208.

Langley, R.B., G. Beutler, D. Delikaraoglou, B. Nickerson, R.Santerre, P. Vanicek and D.E. Wells (1984). "Studies in the application of the Global Positioning System to differential positioning." Department of Surveying Engineering Technical Report No. 108, University of New Brunswick, Fredericton, Canada.

Langley, R.B., D. Parrot, A. Kleusberg, R. Santerre, D.E. Wells and P. Vanicek (1986a). "DIPOP: An iterative software package for precise positioning with GPS." Paper

presented at the American Congress on Surveying and Mapping, Spring Convention, Washington, D.C., 16-21 March.

Langley, R.B., D. Parrot, R. Santerre, P. Vanicek and D.E. Wells (1986b). "The spring 1985 GPS high-precision baseline test: preliminary analyses with DIPOP." *Proceedings of the Fourth International Geodetic Symposium on Satellite Positioning*, Vol. 2, pp. 1073-1088.

Langley, R.B. (1988a). "Special Studies in Geodesy: SE4242.", Lecture Notes, Department of Surveying Engineering, University of New Brunswick, Fredericton, New Brunswick, Canada.

Langley, R.B. (1988b). Personal communication. Department of Surveying Engineering, University of New Brunswick, Fredericton, Canada.

Laurence, G.T. (1985). *Celestial Mechanics*. John Wiley & Sons, New York.

Melchoir, P. (1983). *The Tides of the Planet Earth*. 2nd ed., Pergamon Press, New York.

Mikhail, E.M. (1976). *Observations and Least Squares*. University Press of America, Washington, D.C.

Moreau, R., G. Beutler, J.G. Leclerc, B. Labrecque, R.B. Langley and R. Santerre (1985). "Comparison of phase-difference processing and network solution methods." *Proceedings of First International Symposium on Precise Positioning with the Global Positioning System - Positioning with GPS-1985*, U.S. Dept. of Commerce, NOAA, Rockville, Md., pp. 557-556.

Nautical Almanac Office, United States Naval Observatory, H.M. Nautical Almanac Office, Royal Greenwich Observatory (1987). *The Astronomical Almanac for the Year 1987*. U.S. Government Printing Office, Washington, D.C.

Parrot, D. (1989). "Short arc orbit improvement for GPS satellites." M.Sc.E. thesis, Department of Surveying Engineering Technical Report No. 143, University of New Brunswick, Fredericton, Canada.

Remondi, B.W. (1989). "GPS broadcast orbits versus precise orbits: a comparison study." International Coordination of Space Techniques for Geodesy and Geodynamics (CSTG), GPS Bulletin, Vol. 2, No. 6. pp. 8-22.

Rizos, C. and A. Stolz (1985). "Force modelling for GPS satellite orbits." *Proceedings of First International Symposium on Precise Positioning with the Global Positioning System - Positioning with GPS-1985*, U.S. Dept. of Commerce, NOAA, Rockville, Md., pp. 87-96.

Santerre, R., A. Kleusberg and G. Beutler (1985). "DIPOP: Software documentation." Department of Surveying Engineering Technical Memorandum TM-6, University of New Brunswick, Fredericton, Canada.

Santerre, R. (1987). Personal communication. Department of Surveying Engineering, University of New Brunswick, Fredericton, Canada.

Santerre, R., M.R. Craymer, A. Kleusberg, R.B. Langley, D. Parrot, S.H. Quek, P. Vanicek, D.E. Wells and F. Wilkins (1987). "Precise relative positioning with DIPOP 2.0." Paper presented at the IUGG XIX General Assembly, Vancouver, Canada, 9-22 August.

Sovers, O.J. and J.S. Border (1988). Observation Model and Parameter Partials for the JPL Geodetic GPS Modeling Software GPSOMC." JPL Publication 87-21, Rev. 1, Jet Propulsion Laboratory, Pasadena, California, December 15, 1988.

Vanicek, P., A. Kleusberg, R.B. Langley, R. Santerre and D.E. Wells (1985a). "DIPOP Differential POsitioning Program package for the Global Positioning System." Department of Surveying Engineering Technical Report No. 115, University of New Brunswick, Fredericton, Canada.

Vanicek, P., G. Beutler, A. Kleusberg, R.B. Langley, R. Santerre and D.E. Wells (1985b). "On the elimination of biases in processing differential GPS observations." *Proceedings of First International Symposium on Precise Positioning with the Global Positioning System - Positioning with GPS-1985*, U.S. Dept. of Commerce, NOAA, Rockville, Md., pp. 315-324.

Vanicek, P. and J. Krakiwsky (1986). *Geodesy, the Concepts*. 2nd rev. ed., North-Holland, Amsterdam, The Netherlands.

Velez, C.E., and J.L. Maury (1970). "Derivation of Newtonian-type integration coefficients and some applications to orbit calculations." NASA Technical Note TN D-5958, Goddard Space Flight Center, Greenbelt, Md.

Wahr, J.M. (1981). "The forced nutations of an elliptical, rotating, elastic and oceanless earth." Geophys. J.R. Astr. Soc., vol. 64, pp. 705-727.

Wanless, B. (1985). "A prototype multi-station, multi-pass satellite data reduction program." M.Sc. thesis, Department of Surveying Engineering, The University of Calgary, Alberta, Canada.

Wells, D.E., N. Beck, D. Delikaraoglou, A. Kleusberg, E.J. Krakiwsky, G. Lachapelle, R.B. Langley, M. Nakiboglu, K.P. Schwarz, J.M. Tranquilla and P. Vanicek (1987). *Guide to GPS Positioning*. Canadian GPS Associates, Fredericton, N.B., Canada.

Yoder, C.F. (1981). "Tidal variations of the Earth's rotation." J. Geophys. Res. vol. 86, pp. 881-891.

132

APPENDIX I

COMMAND FILE FOR PRE-PROCESSOR

I.1 Command File for PREGE

An example of the command file of DIPOP-E's PREGE, is as follows (it is from the processing of SSG 1.104 data):

```
****   command file for PREGE   ****
Chen 1/4:f026.mac80
HD20:CHEN:dat:SSGDAT:AL6.PGE
HD20:CHEN:dat:SSGDAT:AL6.PGESUM
CC
120.0
100
(-
Chen 1/4:f027.mac80
HD20:CHEN:dat:SSGDAT:AL7.PGE
HD20:CHEN:dat:SSGDAT:AL7.PGESUM
CC
120.0
100
(-
. . . . . . . . .
. . . . . . . . .
. . . . . . . . .
(-
```

The above command file is explained as follows:

- line 1: is the comment line
- line 2: is the input file name
- line 3: is the output file name
- line 4: is the summary file name of the processing
- line 5: is the data format
   <UN> for UNB (University of New Brunswick) format:
   <SU> for short UNB format
   <GS> for GSC (Geodetic Survey of Canada)
   <CC> data format of SSG 1.104 distributed data
- line 6: decimating sampling time interval of observations

- line 7: is the debugging level that controls the amount of output information to the computer screen and the summary file
- line 8: separates control information for the processing of the next observation file from the previous one with the separator "(-"
- line 9 through 15: information for the processing of the next observation file
- ....
- ....
- ....
- the final line: "(-"

I.2 Command File for PREDD

This section lists a command file of PREDD used to process the standard data set (Chapter 7). The file listed in this section was used for PREDD processing of the data on Jan. 3, 4, and 5. The format of the input is explained as follows:

- A file name should be less than 45 characters in length.

- Don't add any extra lines.

- Following the lines of the header which begin with the character '*', the following four lines are for the processing of the whole data set:

- Summary file name.

- Use the orbits integrated from initial conditions? Y/N. It has to be 'Y' if an integrated orbit is to be used for data processing or for ephemeris output to a double difference observation file.

- Command file name for the integration.

- An integer number to specify debugging output level.

- The line '..' following the above inputs is used for separation.

- A blank line followed by a line beginning with the characters '(-' means input for data processing of a whole window begins.

- Input a line of comment, and 7 input lines follow:

- GPS week and time (in seconds) at the beginning of the window; GPS week and time (in seconds) at the end of the window.

- Ephemeris file name for the observations of this window.

- Whether it is required to convert observations time tagged in receiver clock time to observations time tagged in GPS time: 1: yes; 0: no. If the outputs are used for DIPOP's main-processor and orbit improvement in the main-processor is required, specify 1.

- If integrated orbit is used for data processing: 1: yes; 0: no.

- Broadcast ephemeris format. The format of broadcast ephemeris is specified in the same manner as the format of an observation file format is specified in PREGE's command file (see Appendix I.1).

- Output the improved ephemeris to double difference observation files (output files of PREDD): 1: yes; 0: no.

- Day number.

• Input a comment line, and then, station coordinate and output file name from PREGE follow:

- An integer to indicate the sequence, station name (an abbreviation consisting of two characters); station coordinates in Cartesian (x, y, and z), or in spherical (latitude, longitude, and radius), or geodetic (latitude, longitude, and height) components. Free format is used, but no space between sign and its corresponding value.

- PREGE's output file name for the above station for the observation period.

- Followed by the coordinates and input observation files of other stations in forming double difference observations for the observation period. All stations used in forming double difference observations for the period have to be input.

- The characters '-1' indicate the end of the station input for the observation period.

• Input a comment line followed by information for baseline by baseline processing:

- information for each baseline processing begins with a blank line.

- Two station names forming a baseline; a comment (usually the sequence of the baseline).

I.3

- File name for the output of double difference observations for the baseline.

- Maximum number of single differences. This is determined by the dimensions of PREDD's arrays and disk and memory capacity of the computer.

- Debugging output level (0 - 100) for the processing of the baseline.

- Relative coordinate improvement (Y/N).

- Number of frequencies (1 or 2). Notice: not implemented yet, specify 2 at the moment.

- Receiver model (1 = WM101 or TRIMBLE, 2 = TI4100). Notice: not implemented yet, specify 2 at the moment.

- Cycle slip detection threshold (cm.). Notice: not implemented yet.

- Input control for processing the other baselines of the same observation period.

• The control information for the processing of the next observation window is similar to the above. That is, immediately following the last input of the last baseline of the previous observation window, a new window begins with a blank line, and a line beginning with the character '(-'.

```
...........
...........
...........
```

```
**************** COMMAND FILE FOR DIPOP-E's PREDD ********************
*          a file name should be less than 45 characters in length
*
*                                                                   *
*             INFORMATION COMMON FOR THE WHOLE SESSION
*
*----+----1----+----2----+----3----+----4----+----5----+----6----+----7-
HD20:CHEN:DAT:PRE.OUT:PREDD:PREDD345.SUM      ! SUMMARY FILE NAME
N                                             ! USE INITIAL CONDITION AS ORBY/N
HD20:CHEN:MPR9:ORBIN.CMD                       ! INTEGRATION COMMAND FILE
7                                             ! DEBUG LEVEL

.................................................................................

(-                                             ! Line for separation
C Orbital session 1: The beginning and the ending time of the window
364    5.440E+05 364 5.75000D5
HD20:CHEN:dat:SSG:EPH:f018.mac80
1      ! CONVERT OBSERVATIONS FROM RECEIVER TO GPS TIME TAG   ?
0      ! USE INTEGRATED ORBIT FOR DATA PROCESSING                 ?
CC     ! BROADCAST EPHEMERIS FORMAT                          ?
0      ! OUTPUT THE IMPROVED EPHEMERIS TO OBSERVATION FILES  ?
03     ! DAY NUMBER
```

```
0      ! OUTPUT THE IMPROVED EPHEMERIS TO OBSERVATION FILES  ?
03     ! DAY NUMBER
*************  STATION COORDINATES & PREGE OUTPUT FILES   *************
01 AU      30 18 42.10142 -97 45 22.74673    193.6146
CHEN 4/4:SSG.PGEO:D3:AU3.PGE
02 AL      45 57 21.24086 -78 04 16.92058    200.7782
CHEN 4/4:SSG.PGEO:D3:AL3.PGE
03 BU      35 23 54.58426 -119 23 38.45992    56.6232
CHEN 4/4:SSG.PGEO:D3:BU3.PGE
04 BR      33 24 25.24661 -118 24 17.47639   450.4823
CHEN 4/4:SSG.PGEO:D3:BR3.PGE
05 CF      34 18  2.22346 -119 19 51.44183   309.0608
CHEN 4/4:SSG.PGEO:D3:CF3.PGE
06 CH      58 45 32.96074 -94 05 18.08572   -15.0920
CHEN 4/4:SSG.PGEO:D3:CH3.PGE
07 DE      34 01 44.81445 -119 47 03.87717   706.5085
CHEN 4/4:SSG.PGEO:D3:DE3.PGE
08 GA      34 30  6.51289 -120 11 55.66095   715.3075
CHEN 4/4:SSG.PGEO:D3:GA3.PGE
09 FT      36 40 11.23    -121 46 23.56        4.59
CHEN 4/4:SSG.PGEO:D3:FT3.PGE
10 LA      34 29 39.86912 -119 42 50.01971   1166.6846
CHEN 4/4:SSG.PGEO:D3:LA3.PGE
11 MJ      35 19 53.59722 -116 53 17.35652    906.4217
CHEN 4/4:SSG.PGEO:D3:MJ3.PGE
12 ML      34 30 36.38716 -120 13 46.81878     87.1912
CHEN 4/4:SSG.PGEO:D3:ML3.PGE
13 OW      37 13 57.21511 -118 17 37.65749   1179.9443
CHEN 4/4:SSG.PGEO:D3:OW3.PGE
14 PA      33 44 37.53928 -118 24 12.78803     71.3572
CHEN 4/4:SSG.PGEO:D3:PA3.PGE
15 PL      40 10 58.05604 -104 43 34.84730   1503.2569
CHEN 4/4:SSG.PGEO:D3:PL3.PGE
16 SE      33 57  3.08619 -120  6 20.43013   445.3571
CHEN 4/4:SSG.PGEO:D3:SE3.PGE
17 SI      34 17 54.01834 -119 20 33.67370    -9.7644
CHEN 4/4:SSG.PGEO:D3:SI3.PGE
18 VN      34 33 22.54778 -120 36 58.31415    -9.6181
CHEN 4/4:SSG.PGEO:D3:VN3.PGE
19 WF      42 36 47.95645 -71 29 36.02332     88.3462
CHEN 4/4:SSG.PGEO:D3:WF3.PGE
-1
********  INFORMATION RELATED TO A PARTICULAR BASELINE   **********

PL   AL   1
HD20:CHEN:DAT:PRE.OUT:PREDD:D3:PLAL03.dat
5000          ! MAXIMUM NUMBER OF SINGLE DIFFERENCES (100 - 5000)
50            ! DEBUGGING LEVEL  (0 - 100)
N             ! RELATIVE COORDINATE IMPROVEMENT (Y/N)
2             ! NUMBER OF FREQUENCIES ( 1 OR 2 )
2             ! RECEIVER MODEL ( 1 = WM101 OR TRIMBLE, 2 = TI4100 )
10            ! CYCLE SLIP DETECTION THRESHOLD (CM.)

PL   OW   2
HD20:CHEN:DAT:PRE.OUT:PREDD:D3:PLOW3.dat
5000          ! MAXIMUM NUMBER OF SINGLE DIFFERENCES (100 - 5000)
50            ! DEBUGGING LEVEL  (0 - 100)
N             ! RELATIVE COORDINATE IMPROVEMENT (Y/N)
```

```
2                 ! NUMBER OF FREQUENCIES ( 1 OR 2 )
2                 ! RECEIVER MODEL ( 1 = WM101 OR TRIMBLE, 2 = TI4100 )
10                ! CYCLE SLIP DETECTION THRESHOLD (CM.)


AL   CH   3
HD20:CHEN:DAT:PRE.OUT:PREDD:D3:ALCH03.dat
5000              ! MAXIMUM NUMBER OF SINGLE DIFFERENCES (100 - 5000)
50                ! DEBUGGING LEVEL  (0 - 100)
N                 ! RELATIVE COORDINATE IMPROVEMENT (Y/N)
2                 ! NUMBER OF FREQUENCIES ( 1 OR 2 )
2                 ! RECEIVER MODEL ( 1 = WM101 OR TRIMBLE, 2 = TI4100 )
10                ! CYCLE SLIP DETECTION THRESHOLD (CM.)


AL   WF   4
HD20:CHEN:DAT:PRE.OUT:PREDD:D3:ALWF3.DAT
5000              ! MAXIMUM NUMBER OF SINGLE DIFFERENCES (100 - 5000)
50                ! DEBUGGING LEVEL  (0 - 100)
N                 ! RELATIVE COORDINATE IMPROVEMENT (Y/N)
2                 ! NUMBER OF FREQUENCIES ( 1 OR 2 )
2                 ! RECEIVER MODEL ( 1 = WM101 OR TRIMBLE, 2 = TI4100 )
10                ! CYCLE SLIP DETECTION THRESHOLD (CM.)


PL   WF   4'
HD20:CHEN:DAT:PRE.OUT:PREDD:D3:PLWF3.DAT
5000              ! MAXIMUM NUMBER OF SINGLE DIFFERENCES (100 - 5000)
50                ! DEBUGGING LEVEL  (0 - 100)
N                 ! RELATIVE COORDINATE IMPROVEMENT (Y/N)
2                 ! NUMBER OF FREQUENCIES ( 1 OR 2 )
2                 ! RECEIVER MODEL ( 1 = WM101 OR TRIMBLE, 2 = TI4100 )
10                ! CYCLE SLIP DETECTION THRESHOLD (CM.)


OW   BU   5
HD20:CHEN:DAT:PRE.OUT:PREDD:D3:OWBU3.DAT
5000              ! MAXIMUM NUMBER OF SINGLE DIFFERENCES (100 - 5000)
50                ! DEBUGGING LEVEL  (0 - 100)
N                 ! RELATIVE COORDINATE IMPROVEMENT (Y/N)
2                 ! NUMBER OF FREQUENCIES ( 1 OR 2 )
2                 ! RECEIVER MODEL ( 1 = WM101 OR TRIMBLE, 2 = TI4100 )
10                ! CYCLE SLIP DETECTION THRESHOLD (CM.)


GA   BU   6
HD20:CHEN:DAT:PRE.OUT:PREDD:D3:GABU3.DAT
5000              ! MAXIMUM NUMBER OF SINGLE DIFFERENCES (100 - 5000)
50                ! DEBUGGING LEVEL  (0 - 100)
N                 ! RELATIVE COORDINATE IMPROVEMENT (Y/N)
2                 ! NUMBER OF FREQUENCIES ( 1 OR 2 )
2                 ! RECEIVER MODEL ( 1 = WM101 OR TRIMBLE, 2 = TI4100 )
10                ! CYCLE SLIP DETECTION THRESHOLD (CM.)


GA   LA   7
HD20:CHEN:DAT:PRE.OUT:PREDD:D3:GALA3.DAT
5000              ! MAXIMUM NUMBER OF SINGLE DIFFERENCES (100 - 5000)
50                ! DEBUGGING LEVEL  (0 - 100)
N                 ! RELATIVE COORDINATE IMPROVEMENT (Y/N)
2                 ! NUMBER OF FREQUENCIES ( 1 OR 2 )
2                 ! RECEIVER MODEL ( 1 = WM101 OR TRIMBLE, 2 = TI4100 )
10                ! CYCLE SLIP DETECTION THRESHOLD (CM.)
```

```
GA    SE    8
HD20:CHEN:DAT:PRE.OUT:PREDD:D3:GASE3.DAT
5000            ! MAXIMUM NUMBER OF SINGLE DIFFERENCES (100 - 5000)
50              ! DEBUGGING LEVEL   (0 - 100)
N               ! RELATIVE COORDINATE IMPROVEMENT (Y/N)
2               ! NUMBER OF FREQUENCIES ( 1 OR 2 )
2               ! RECEIVER MODEL ( 1 = WM101 OR TRIMBLE, 2 = TI4100 )
10              ! CYCLE SLIP DETECTION THRESHOLD (CM.)


LA    CF    9
HD20:CHEN:DAT:PRE.OUT:PREDD:D3:LACF3.DAT
5000            ! MAXIMUM NUMBER OF SINGLE DIFFERENCES (100 - 5000)
50              ! DEBUGGING LEVEL   (0 - 100)
N               ! RELATIVE COORDINATE IMPROVEMENT (Y/N)
2               ! NUMBER OF FREQUENCIES ( 1 OR 2 )
2               ! RECEIVER MODEL ( 1 = WM101 OR TRIMBLE, 2 = TI4100 )
10              ! CYCLE SLIP DETECTION THRESHOLD (CM.)


CF    BR    10
HD20:CHEN:DAT:PRE.OUT:PREDD:D3:CFBR3.DAT
5000            ! MAXIMUM NUMBER OF SINGLE DIFFERENCES (100 - 5000)
50              ! DEBUGGING LEVEL   (0 - 100)
N               ! RELATIVE COORDINATE IMPROVEMENT (Y/N)
2               ! NUMBER OF FREQUENCIES ( 1 OR 2 )
2               ! RECEIVER MODEL ( 1 = WM101 OR TRIMBLE, 2 = TI4100 )
10              ! CYCLE SLIP DETECTION THRESHOLD (CM.)


BR    SE    10'
HD20:CHEN:DAT:PRE.OUT:PREDD:D3:BRSE3.DAT
5000            ! MAXIMUM NUMBER OF SINGLE DIFFERENCES (100 - 5000)
50              ! DEBUGGING LEVEL   (0 - 100)
N               ! RELATIVE COORDINATE IMPROVEMENT (Y/N)
2               ! NUMBER OF FREQUENCIES ( 1 OR 2 )
2               ! RECEIVER MODEL ( 1 = WM101 OR TRIMBLE, 2 = TI4100 )
10              ! CYCLE SLIP DETECTION THRESHOLD (CM.)


CF    PA    10''
HD20:CHEN:DAT:PRE.OUT:PREDD:D3:CFPA3.DAT
5000            ! MAXIMUM NUMBER OF SINGLE DIFFERENCES (100 - 5000)
50              ! DEBUGGING LEVEL   (0 - 100)
N               ! RELATIVE COORDINATE IMPROVEMENT (Y/N)
2               ! NUMBER OF FREQUENCIES ( 1 OR 2 )
2               ! RECEIVER MODEL ( 1 = WM101 OR TRIMBLE, 2 = TI4100 )
10              ! CYCLE SLIP DETECTION THRESHOLD (CM.)


BR    PA    11
HD20:CHEN:DAT:PRE.OUT:PREDD:D3:BRPA3.DAT
5000            ! MAXIMUM NUMBER OF SINGLE DIFFERENCES (100 - 5000)
50              ! DEBUGGING LEVEL   (0 - 100)
N               ! RELATIVE COORDINATE IMPROVEMENT (Y/N)
2               ! NUMBER OF FREQUENCIES ( 1 OR 2 )
2               ! RECEIVER MODEL ( 1 = WM101 OR TRIMBLE, 2 = TI4100 )
10              ! CYCLE SLIP DETECTION THRESHOLD (CM.)


GA    VN    12
HD20:CHEN:DAT:PRE.OUT:PREDD:D3:GAVN3.DAT
5000            ! MAXIMUM NUMBER OF SINGLE DIFFERENCES (100 - 5000)
50              ! DEBUGGING LEVEL   (0 - 100)
```

```
N                 ! RELATIVE COORDINATE IMPROVEMENT (Y/N)
2                 ! NUMBER OF FREQUENCIES ( 1 OR 2 )
2                 ! RECEIVER MODEL ( 1 = WM101 OR TRIMBLE, 2 = TI4100 )
10                ! CYCLE SLIP DETECTION THRESHOLD (CM.)


OW    FT     13
HD20:CHEN:DAT:PRE.OUT:PREDD:D3:OWFT3.DAT
5000              ! MAXIMUM NUMBER OF SINGLE DIFFERENCES (100 - 5000)
50                ! DEBUGGING LEVEL   (0 - 100)
N                 ! RELATIVE COORDINATE IMPROVEMENT (Y/N)
2                 ! NUMBER OF FREQUENCIES ( 1 OR 2 )
2                 ! RECEIVER MODEL ( 1 = WM101 OR TRIMBLE, 2 = TI4100 )
10                ! CYCLE SLIP DETECTION THRESHOLD (CM.)


(-
C ORBITAL SESSION 1: The beginning and the ending time of the window
365   2.50D4 365 5.2D4
HD20:CHEN:dat:SSG:EPH:f019.mac80
1        ! CONVERT OBSERVATION FROM RECEIVER TO GPS TIME TAG    ?
0        ! USE INTEGRATED ORBIT FOR DATA PROCESSING             ?
CC       ! BROADCAST EPHEMERIS FORMAT                           ?
0        ! OUTPUT THE IMPROVED EPHEMERIS TO OBSERVATION FILES   ?
04       ! DAY NUMBER                                           ?
********   STATION COORDINATE & PREGE OUTPUT FILE   **********
01 AU      30 18 42.10142   -97 45 22.74673      193.6146
CHEN 4/4:SSG.PGEO:D4:AU4.PGE
02 AL      45 57 21.24086 -78 04 16.92058   200.7782
CHEN 4/4:SSG.PGEO:D4:AL4.PGE
03 BU      35 23 54.58426 -119 23 38.45992    56.6232
CHEN 4/4:SSG.PGEO:D4:BU4.PGE
04 BR      33 24 25.24661 -118 24 17.47639   450.4823
CHEN 4/4:SSG.PGEO:D4:BR4.PGE
05 CF      34 18  2.22346 -119 19 51.44183   309.0608
CHEN 4/4:SSG.PGEO:D4:CF4.PGE
06 CH      58 45 32.96074 -94 05 18.08572   -15.0920
CHEN 4/4:SSG.PGEO:D4:CH4.PGE
07 DE      34 01 44.81445 -119 47 03.87717   706.5085
CHEN 4/4:SSG.PGEO:D4:DE4.PGE
08 GA      34 30  6.51289 -120 11 55.66095   715.3075
CHEN 4/4:SSG.PGEO:D4:GA4.PGE
09 FT      36 40 11.23    -121 46 23.56        4.59
CHEN 4/4:SSG.PGEO:D4:FT4.PGE
10 LA      34 29 39.86912 -119 42 50.01971 1166.6846
CHEN 4/4:SSG.PGEO:D4:LA4.PGE
11 MJ      35 19 53.59722 -116 53 17.35652   906.4217
CHEN 4/4:SSG.PGEO:D4:MJ4.PGE
12 ML      34 30 36.38716 -120 13 46.81878    87.1912
CHEN 4/4:SSG.PGEO:D4:ML4.PGE
13 OW      37 13 57.21511 -118 17 37.65749   1179.9443
CHEN 4/4:SSG.PGEO:D4:OW4.PGE
14 PA      33 44 37.53928 -118 24 12.78803    71.3572
CHEN 4/4:SSG.PGEO:D4:PA4.PGE
15 PL      40 10 58.05604 -104 43 34.84730 1503.2569
CHEN 4/4:SSG.PGEO:D4:PL4.PGE
16 SE      33 57  3.08619 -120  6 20.43013   445.3571
CHEN 4/4:SSG.PGEO:D4:SE4.PGE
17 SI      34 17 54.01834 -119 20 33.67370    -9.7644
CHEN 4/4:SSG.PGEO:D4:SI4.PGE
```

```
18 VN       34 33 22.54778 -120 36 58.31415   -9.6181
CHEN 4/4:SSG.PGEO:D4:VN4.PGE
19 WF       42 36 47.95645 -71 29 36.02332    88.3462
CHEN 4/4:SSG.PGEO:D4:WF4.PGE
-1
*******  INFORMATION RELATED TO A PARTICULAR BASELINE   **********


PL    AL    1
HD20:CHEN:DAT:PRE.OUT:PREDD:D4:PLAL04.DAT
5000          ! MAXIMUM NUMBER OF SINGLE DIFFERENCES (100 - 5000)
50            ! DEBUGGING LEVEL   (0 - 100)
N             ! RELATIVE COORDINATE IMPROVEMENT (Y/N)
2             ! NUMBER OF FREQUENCIES ( 1 OR 2 )
2             ! RECEIVER MODEL ( 1 = WM101 OR TRIMBLE, 2 = TI4100 )
10            ! CYCLE SLIP DETECTION THRESHOLD (CM.)


PL    OW    2
HD20:CHEN:DAT:PRE.OUT:PREDD:D4:PLOW4.DAT
5000          ! MAXIMUM NUMBER OF SINGLE DIFFERENCES (100 - 5000)
50            ! DEBUGGING LEVEL   (0 - 100)
N             ! RELATIVE COORDINATE IMPROVEMENT (Y/N)
2             ! NUMBER OF FREQUENCIES ( 1 OR 2 )
2             ! RECEIVER MODEL ( 1 = WM101 OR TRIMBLE, 2 = TI4100 )
10            ! CYCLE SLIP DETECTION THRESHOLD (CM.)


AL    CH    3
HD20:CHEN:DAT:PRE.OUT:PREDD:D4:ALCH04.DAT
5000          ! MAXIMUM NUMBER OF SINGLE DIFFERENCES (100 - 5000)
50            ! DEBUGGING LEVEL   (0 - 100)
N             ! RELATIVE COORDINATE IMPROVEMENT (Y/N)
2             ! NUMBER OF FREQUENCIES ( 1 OR 2 )
2             ! RECEIVER MODEL ( 1 = WM101 OR TRIMBLE, 2 = TI4100 )
10            ! CYCLE SLIP DETECTION THRESHOLD (CM.)


AL    WF    4   FAIL NOV. 17
HD20:CHEN:DAT:PRE.OUT:PREDD:D4:ALWF4.DAT
5000          ! MAXIMUM NUMBER OF SINGLE DIFFERENCES (100 - 5000)
50            ! DEBUGGING LEVEL   (0 - 100)
N             ! RELATIVE COORDINATE IMPROVEMENT (Y/N)
2             ! NUMBER OF FREQUENCIES ( 1 OR 2 )
2             ! RECEIVER MODEL ( 1 = WM101 OR TRIMBLE, 2 = TI4100 )
10            ! CYCLE SLIP DETECTION THRESHOLD (CM.)


PL    WF    4'  FAIL NOV. 17
HD20:CHEN:DAT:PRE.OUT:PREDD:D4:PLWF4.DAT
5000          ! MAXIMUM NUMBER OF SINGLE DIFFERENCES (100 - 5000)
50            ! DEBUGGING LEVEL   (0 - 100)
N             ! RELATIVE COORDINATE IMPROVEMENT (Y/N)
2             ! NUMBER OF FREQUENCIES ( 1 OR 2 )
2             ! RECEIVER MODEL ( 1 = WM101 OR TRIMBLE, 2 = TI4100 )
10            ! CYCLE SLIP DETECTION THRESHOLD (CM.)


OW    BU    5
HD20:CHEN:DAT:PRE.OUT:PREDD:D4:OWBU4.DAT
5000          ! MAXIMUM NUMBER OF SINGLE DIFFERENCES (100 - 5000)
50            ! DEBUGGING LEVEL   (0 - 100)
N             ! RELATIVE COORDINATE IMPROVEMENT (Y/N)
2             ! NUMBER OF FREQUENCIES ( 1 OR 2 )
```

```
2                ! RECEIVER MODEL ( 1 = WM101 OR TRIMBLE, 2 = TI4100 )
10               ! CYCLE SLIP DETECTION THRESHOLD (CM.)


GA    BU    6
HD20:CHEN:DAT:PRE.OUT:PREDD:D4:GABU4.DAT
5000             ! MAXIMUM NUMBER OF SINGLE DIFFERENCES (100 - 5000)
50               ! DEBUGGING LEVEL   (0 - 100)
N                ! RELATIVE COORDINATE IMPROVEMENT (Y/N)
2                ! NUMBER OF FREQUENCIES ( 1 OR 2 )
2                ! RECEIVER MODEL ( 1 = WM101 OR TRIMBLE, 2 = TI4100 )
10               ! CYCLE SLIP DETECTION THRESHOLD (CM.)


GA    LA    7
HD20:CHEN:DAT:PRE.OUT:PREDD:D4:GALA4.DAT
5000             ! MAXIMUM NUMBER OF SINGLE DIFFERENCES (100 - 5000)
50               ! DEBUGGING LEVEL   (0 - 100)
N                ! RELATIVE COORDINATE IMPROVEMENT (Y/N)
2                ! NUMBER OF FREQUENCIES ( 1 OR 2 )
2                ! RECEIVER MODEL ( 1 = WM101 OR TRIMBLE, 2 = TI4100 )
10               ! CYCLE SLIP DETECTION THRESHOLD (CM.)


GA    SE    8
HD20:CHEN:DAT:PRE.OUT:PREDD:D4:GASE4.DAT
5000             ! MAXIMUM NUMBER OF SINGLE DIFFERENCES (100 - 5000)
50               ! DEBUGGING LEVEL   (0 - 100)
N                ! RELATIVE COORDINATE IMPROVEMENT (Y/N)
2                ! NUMBER OF FREQUENCIES ( 1 OR 2 )
2                ! RECEIVER MODEL ( 1 = WM101 OR TRIMBLE, 2 = TI4100 )
10               ! CYCLE SLIP DETECTION THRESHOLD (CM.)


LA    SI    9
HD20:CHEN:DAT:PRE.OUT:PREDD:D4:LASI4.DAT
5000             ! MAXIMUM NUMBER OF SINGLE DIFFERENCES (100 - 5000)
50               ! DEBUGGING LEVEL   (0 - 100)
N                ! RELATIVE COORDINATE IMPROVEMENT (Y/N)
2                ! NUMBER OF FREQUENCIES ( 1 OR 2 )
2                ! RECEIVER MODEL ( 1 = WM101 OR TRIMBLE, 2 = TI4100 )
10               ! CYCLE SLIP DETECTION THRESHOLD (CM.)


SI    BR    10
HD20:CHEN:DAT:PRE.OUT:PREDD:D4:SIBR4.DAT
5000             ! MAXIMUM NUMBER OF SINGLE DIFFERENCES (100 - 5000)
50               ! DEBUGGING LEVEL   (0 - 100)
N                ! RELATIVE COORDINATE IMPROVEMENT (Y/N)
2                ! NUMBER OF FREQUENCIES ( 1 OR 2 )
2                ! RECEIVER MODEL ( 1 = WM101 OR TRIMBLE, 2 = TI4100 )
10               ! CYCLE SLIP DETECTION THRESHOLD (CM.)


BR    SE    10'
HD20:CHEN:DAT:PRE.OUT:PREDD:D4:BRSE4.DAT
5000             ! MAXIMUM NUMBER OF SINGLE DIFFERENCES (100 - 5000)
50               ! DEBUGGING LEVEL   (0 - 100)
N                ! RELATIVE COORDINATE IMPROVEMENT (Y/N)
2                ! NUMBER OF FREQUENCIES ( 1 OR 2 )
2                ! RECEIVER MODEL ( 1 = WM101 OR TRIMBLE, 2 = TI4100 )
10               ! CYCLE SLIP DETECTION THRESHOLD (CM.)


SI    PA    10''
```

```
HD20:CHEN:DAT:PRE.OUT:PREDD:D4:SIPA4.DAT
5000            ! MAXIMUM NUMBER OF SINGLE DIFFERENCES (100 - 5000)
50              ! DEBUGGING LEVEL   (0 - 100)
N               ! RELATIVE COORDINATE IMPROVEMENT (Y/N)
2               ! NUMBER OF FREQUENCIES ( 1 OR 2 )
2               ! RECEIVER MODEL ( 1 = WM101 OR TRIMBLE, 2 = TI4100 )
10              ! CYCLE SLIP DETECTION THRESHOLD (CM.)

BR    PA    11
HD20:CHEN:DAT:PRE.OUT:PREDD:D4:BRPA4.DAT?
5000            ! MAXIMUM NUMBER OF SINGLE DIFFERENCES (100 - 5000)
50              ! DEBUGGING LEVEL   (0 - 100)
N               ! RELATIVE COORDINATE IMPROVEMENT (Y/N)
2               ! NUMBER OF FREQUENCIES ( 1 OR 2 )
2               ! RECEIVER MODEL ( 1 = WM101 OR TRIMBLE, 2 = TI4100 )
10              ! CYCLE SLIP DETECTION THRESHOLD (CM.)

GA    VN    12
HD20:CHEN:DAT:PRE.OUT:PREDD:D4:GAVN4.DAT
5000            ! MAXIMUM NUMBER OF SINGLE DIFFERENCES (100 - 5000)
50              ! DEBUGGING LEVEL   (0 - 100)
N               ! RELATIVE COORDINATE IMPROVEMENT (Y/N)
2               ! NUMBER OF FREQUENCIES ( 1 OR 2 )
2               ! RECEIVER MODEL ( 1 = WM101 OR TRIMBLE, 2 = TI4100 )
10              ! CYCLE SLIP DETECTION THRESHOLD (CM.)

OW    FT    13
HD20:CHEN:DAT:PRE.OUT:PREDD:D4:OWFT4.DAT
5000            ! MAXIMUM NUMBER OF SINGLE DIFFERENCES (100 - 5000)
50              ! DEBUGGING LEVEL   (0 - 100)
N               ! RELATIVE COORDINATE IMPROVEMENT (Y/N)
2               ! NUMBER OF FREQUENCIES ( 1 OR 2 )
2               ! RECEIVER MODEL ( 1 = WM101 OR TRIMBLE, 2 = TI4100 )
10              ! CYCLE SLIP DETECTION THRESHOLD (CM.)

OW    LA    13'
HD20:CHEN:DAT:PRE.OUT:PREDD:D4:OWLA4.DAT
5000            ! MAXIMUM NUMBER OF SINGLE DIFFERENCES (100 - 5000)
50              ! DEBUGGING LEVEL   (0 - 100)
N               ! RELATIVE COORDINATE IMPROVEMENT (Y/N)
2               ! NUMBER OF FREQUENCIES ( 1 OR 2 )
2               ! RECEIVER MODEL ( 1 = WM101 OR TRIMBLE, 2 = TI4100 )
10              ! CYCLE SLIP DETECTION THRESHOLD (CM.)

GA    DE    14
HD20:CHEN:DAT:PRE.OUT:PREDD:D4:GADE4.DAT
5000            ! MAXIMUM NUMBER OF SINGLE DIFFERENCES (100 - 5000)
50              ! DEBUGGING LEVEL   (0 - 100)
N               ! RELATIVE COORDINATE IMPROVEMENT (Y/N)
2               ! NUMBER OF FREQUENCIES ( 1 OR 2 )
2               ! RECEIVER MODEL ( 1 = WM101 OR TRIMBLE, 2 = TI4100 )
10              ! CYCLE SLIP DETECTION THRESHOLD (CM.)

BR    DE    14'
HD20:CHEN:DAT:PRE.OUT:PREDD:D4:BRDE4.DAT
5000            ! MAXIMUM NUMBER OF SINGLE DIFFERENCES (100 - 5000)
50              ! DEBUGGING LEVEL   (0 - 100)
N               ! RELATIVE COORDINATE IMPROVEMENT (Y/N)
```

```
2              ! NUMBER OF FREQUENCIES ( 1 OR 2 )
2              ! RECEIVER MODEL ( 1 = WM101 OR TRIMBLE, 2 = TI4100 )
10             ! CYCLE SLIP DETECTION THRESHOLD (CM.)

(-
C ORBITAL SESSION 1: The beginning and the ending time of the window
365    11.1D4 365 13.8D4
HD20:CHEN:dat:SSG:EPH:f019.mac80
1        ! CONVERT OBSERVATIONS FROM RECEIVER TO GPS TIME TAG  ?
0        ! USE INTEGRATED ORBIT FOR DAT PROCESSING             ?
CC       ! BROADCAST EPHEMERIS FORMAT                          ?
0        ! OUTPUT THE IMPROVED EPHEMERIS TO OBSERVATION FILES  ?
04       ! DAY NUMBER                                          ?
********  STATION COORDINATE & PREGE OUTPUT FILE   ***********
01 AU      30 18 42.10142  -97 45 22.74673      193.6146
CHEN 4/4:SSG.PGEO:D5:AU5.PGE
02 AL      45 57 21.24086 -78 04 16.92058  200.7782
CHEN 4/4:SSG.PGEO:D5:AL5.PGE
03 BU      35 23 54.58426 -119 23 38.45992     56.6232
CHEN 4/4:SSG.PGEO:D5:BU5.PGE
04 BR      33 24 25.24661 -118 24 17.47639   450.4823
CHEN 4/4:SSG.PGEO:D5:BR5.PGE
05 CF      34 18  2.22346 -119 19 51.44183   309.0608
CHEN 4/4:SSG.PGEO:D5:CF5.PGE
06 CH      58 45 32.96074 -94 05 18.08572   -15.0920
CHEN 4/4:SSG.PGEO:D5:CH5.PGE
07 DE      34 01 44.81445 -119 47 03.87717   706.5085
CHEN 4/4:SSG.PGEO:D5:DE5.PGE
08 GA      34 30  6.51289 -120 11 55.66095   715.3075
CHEN 4/4:SSG.PGEO:D5:GA5.PGE
09 FT      36 40 11.23     -121 46 23.56        4.59
CHEN 4/4:SSG.PGEO:D5:FT5.PGE
10 LA      34 29 39.86912 -119 42 50.01971 1166.6846
CHEN 4/4:SSG.PGEO:D5:LA5.PGE
11 MJ      35 19 53.59722 -116 53 17.35652     906.4217
CHEN 4/4:SSG.PGEO:D5:MJ5.PGE
12 ML      34 30 36.38716 -120 13 46.81878      87.1912
CHEN 4/4:SSG.PGEO:D5:ML5.PGE
13 OW      37 13 57.21511 -118 17 37.65749     1179.9443
CHEN 4/4:SSG.PGEO:D5:OW5.PGE
14 PA      33 44 37.53928 -118 24 12.78803    71.3572
CHEN 4/4:SSG.PGEO:D5:PA5.PGE
15 PL      40 10 58.05604 -104 43 34.84730 1503.2569
CHEN 4/4:SSG.PGEO:D5:PL5.PGE
16 SE      33 57  3.08619 -120  6 20.43013   445.3571
CHEN 4/4:SSG.PGEO:D5:SE5.PGE
17 SI      34 17 54.01834 -119 20 33.67370    -9.7644
CHEN 4/4:SSG.PGEO:D5:SI5.PGE
18 VN      34 33 22.54778 -120 36 58.31415    -9.6181
CHEN 4/4:SSG.PGEO:D5:VN5.PGE
19 WF      42 36 47.95645 -71 29 36.02332    88.3462
CHEN 4/4:SSG.PGEO:D5:WF5.PGE
-1
********  INFORMATION RELATED TO A PARTICULAR BASELINE    ***********

PL   AL   1
HD20:CHEN:DAT:PRE.OUT:PREDD:D5:PLAL05.DAT
5000          ! MAXIMUM NUMBER OF SINGLE DIFFERENCES (100 - 5000)
```

```
50              ! DEBUGGING LEVEL   (0 - 100)
N               ! RELATIVE COORDINATE IMPROVEMENT (Y/N)
2               ! NUMBER OF FREQUENCIES ( 1 OR 2 )
2               ! RECEIVER MODEL ( 1 = WM101 OR TRIMBLE, 2 = TI4100 )
10              ! CYCLE SLIP DETECTION THRESHOLD (CM.)


PL   OW   2
HD20:CHEN:DAT:PRE.OUT:PREDD:D5:PLOW5.DAT
5000            ! MAXIMUM NUMBER OF SINGLE DIFFERENCES (100 - 5000)
50              ! DEBUGGING LEVEL   (0 - 100)
N               ! RELATIVE COORDINATE IMPROVEMENT (Y/N)
2               ! NUMBER OF FREQUENCIES ( 1 OR 2 )
2               ! RECEIVER MODEL ( 1 = WM101 OR TRIMBLE, 2 = TI4100 )
10              ! CYCLE SLIP DETECTION THRESHOLD (CM.)


AL   CH   3
HD20:CHEN:DAT:PRE.OUT:PREDD:D5:ALCH05.DAT
5000            ! MAXIMUM NUMBER OF SINGLE DIFFERENCES (100 - 5000)
50              ! DEBUGGING LEVEL   (0 - 100)
N               ! RELATIVE COORDINATE IMPROVEMENT (Y/N)
2               ! NUMBER OF FREQUENCIES ( 1 OR 2 )
2               ! RECEIVER MODEL ( 1 = WM101 OR TRIMBLE, 2 = TI4100 )
10              ! CYCLE SLIP DETECTION THRESHOLD (CM.)


AL   WF   4
HD20:CHEN:DAT:PRE.OUT:PREDD:D5:ALWF5.DAT
5000            ! MAXIMUM NUMBER OF SINGLE DIFFERENCES (100 - 5000)
50              ! DEBUGGING LEVEL   (0 - 100)
N               ! RELATIVE COORDINATE IMPROVEMENT (Y/N)
2               ! NUMBER OF FREQUENCIES ( 1 OR 2 )
2               ! RECEIVER MODEL ( 1 = WM101 OR TRIMBLE, 2 = TI4100 )
10              ! CYCLE SLIP DETECTION THRESHOLD (CM.)


PL   WF   4'
HD20:CHEN:DAT:PRE.OUT:PREDD:D5:PLWF5.DAT
5000            ! MAXIMUM NUMBER OF SINGLE DIFFERENCES (100 - 5000)
50              ! DEBUGGING LEVEL   (0 - 100)
N               ! RELATIVE COORDINATE IMPROVEMENT (Y/N)
2               ! NUMBER OF FREQUENCIES ( 1 OR 2 )
2               ! RECEIVER MODEL ( 1 = WM101 OR TRIMBLE, 2 = TI4100 )
10              ! CYCLE SLIP DETECTION THRESHOLD (CM.)


OW   BU   5
HD20:CHEN:DAT:PRE.OUT:PREDD:D5:OWBU5.DAT
5000            ! MAXIMUM NUMBER OF SINGLE DIFFERENCES (100 - 5000)
50              ! DEBUGGING LEVEL   (0 - 100)
N               ! RELATIVE COORDINATE IMPROVEMENT (Y/N)
2               ! NUMBER OF FREQUENCIES ( 1 OR 2 )
2               ! RECEIVER MODEL ( 1 = WM101 OR TRIMBLE, 2 = TI4100 )
10              ! CYCLE SLIP DETECTION THRESHOLD (CM.)


GA   BU   6
HD20:CHEN:DAT:PRE.OUT:PREDD:D5:GABU5.DAT
5000            ! MAXIMUM NUMBER OF SINGLE DIFFERENCES (100 - 5000)
50              ! DEBUGGING LEVEL   (0 - 100)
N               ! RELATIVE COORDINATE IMPROVEMENT (Y/N)
2               ! NUMBER OF FREQUENCIES ( 1 OR 2 )
2               ! RECEIVER MODEL ( 1 = WM101 OR TRIMBLE, 2 = TI4100 )
```

```
10                    ! CYCLE SLIP DETECTION THRESHOLD (CM.)

GA    LA    7
HD20:CHEN:DAT:PRE.OUT:PREDD:D5:GALA5.DAT
5000              ! MAXIMUM NUMBER OF SINGLE DIFFERENCES (100 - 5000)
50                ! DEBUGGING LEVEL   (0 - 100)
N                 ! RELATIVE COORDINATE IMPROVEMENT (Y/N)
2                 ! NUMBER OF FREQUENCIES ( 1 OR 2 )
2                 ! RECEIVER MODEL ( 1 = WM101 OR TRIMBLE, 2 = TI4100 )
10                ! CYCLE SLIP DETECTION THRESHOLD (CM.)

GA    SE    8
HD20:CHEN:DAT:PRE.OUT:PREDD:D5:GASE5.DAT
5000              ! MAXIMUM NUMBER OF SINGLE DIFFERENCES (100 - 5000)
50                ! DEBUGGING LEVEL   (0 - 100)
N                 ! RELATIVE COORDINATE IMPROVEMENT (Y/N)
2                 ! NUMBER OF FREQUENCIES ( 1 OR 2 )
2                 ! RECEIVER MODEL ( 1 = WM101 OR TRIMBLE, 2 = TI4100 )
10                ! CYCLE SLIP DETECTION THRESHOLD (CM.)

LA    SI    9
HD20:CHEN:DAT:PRE.OUT:PREDD:D5:LASI5.DAT
5000              ! MAXIMUM NUMBER OF SINGLE DIFFERENCES (100 - 5000)
50                ! DEBUGGING LEVEL   (0 - 100)
N                 ! RELATIVE COORDINATE IMPROVEMENT (Y/N)
2                 ! NUMBER OF FREQUENCIES ( 1 OR 2 )
2                 ! RECEIVER MODEL ( 1 = WM101 OR TRIMBLE, 2 = TI4100 )
10                ! CYCLE SLIP DETECTION THRESHOLD (CM.)

SI    BR    10
HD20:CHEN:DAT:PRE.OUT:PREDD:D5:SIBR5.DAT
5000              ! MAXIMUM NUMBER OF SINGLE DIFFERENCES (100 - 5000)
50                ! DEBUGGING LEVEL   (0 - 100)
N                 ! RELATIVE COORDINATE IMPROVEMENT (Y/N)
2                 ! NUMBER OF FREQUENCIES ( 1 OR 2 )
2                 ! RECEIVER MODEL ( 1 = WM101 OR TRIMBLE, 2 = TI4100 )
10                ! CYCLE SLIP DETECTION THRESHOLD (CM.)

BR    SE    10'
HD20:CHEN:DAT:PRE.OUT:PREDD:D5:BRSE5.DAT
5000              ! MAXIMUM NUMBER OF SINGLE DIFFERENCES (100 - 5000)
50                ! DEBUGGING LEVEL   (0 - 100)
N                 ! RELATIVE COORDINATE IMPROVEMENT (Y/N)
2                 ! NUMBER OF FREQUENCIES ( 1 OR 2 )
2                 ! RECEIVER MODEL ( 1 = WM101 OR TRIMBLE, 2 = TI4100 )
10                ! CYCLE SLIP DETECTION THRESHOLD (CM.)

SI    BR    10
HD20:CHEN:DAT:PRE.OUT:PREDD:D5:SIBR5.DAT
5000              ! MAXIMUM NUMBER OF SINGLE DIFFERENCES (100 - 5000)
50                ! DEBUGGING LEVEL   (0 - 100)
N                 ! RELATIVE COORDINATE IMPROVEMENT (Y/N)
2                 ! NUMBER OF FREQUENCIES ( 1 OR 2 )
2                 ! RECEIVER MODEL ( 1 = WM101 OR TRIMBLE, 2 = TI4100 )
10                ! CYCLE SLIP DETECTION THRESHOLD (CM.)

GA    VN    12
HD20:CHEN:DAT:PRE.OUT:PREDD:D5:GAVN5.DAT
```

I.14

```
5000            ! MAXIMUM NUMBER OF SINGLE DIFFERENCES (100 - 5000)
50              ! DEBUGGING LEVEL   (0 - 100)
N               ! RELATIVE COORDINATE IMPROVEMENT (Y/N)
2               ! NUMBER OF FREQUENCIES ( 1 OR 2 )
2               ! RECEIVER MODEL ( 1 = WM101 OR TRIMBLE, 2 = TI4100 )
10              ! CYCLE SLIP DETECTION THRESHOLD (CM.)


OW    FT    13
HD20:CHEN:DAT:PRE.OUT:PREDD:D5:OWFT5.DAT
5000            ! MAXIMUM NUMBER OF SINGLE DIFFERENCES (100 - 5000)
50              ! DEBUGGING LEVEL   (0 - 100)
N               ! RELATIVE COORDINATE IMPROVEMENT (Y/N)
2               ! NUMBER OF FREQUENCIES ( 1 OR 2 )
2               ! RECEIVER MODEL ( 1 = WM101 OR TRIMBLE, 2 = TI4100 )
10              ! CYCLE SLIP DETECTION THRESHOLD (CM.)


OW    LA    13'
HD20:CHEN:DAT:PRE.OUT:PREDD:D5:OWLA5.DAT
5000            ! MAXIMUM NUMBER OF SINGLE DIFFERENCES (100 - 5000)
50              ! DEBUGGING LEVEL   (0 - 100)
N               ! RELATIVE COORDINATE IMPROVEMENT (Y/N)
2               ! NUMBER OF FREQUENCIES ( 1 OR 2 )
2               ! RECEIVER MODEL ( 1 = WM101 OR TRIMBLE, 2 = TI4100 )
10              ! CYCLE SLIP DETECTION THRESHOLD (CM.)


GA    DE    14
HD20:CHEN:DAT:PRE.OUT:PREDD:D5:GADE5.DAT
5000            ! MAXIMUM NUMBER OF SINGLE DIFFERENCES (100 - 5000)
50              ! DEBUGGING LEVEL   (0 - 100)
N               ! RELATIVE COORDINATE IMPROVEMENT (Y/N)
2               ! NUMBER OF FREQUENCIES ( 1 OR 2 )
2               ! RECEIVER MODEL ( 1 = WM101 OR TRIMBLE, 2 = TI4100 )
10              ! CYCLE SLIP DETECTION THRESHOLD (CM.)


BR    DE    14'
HD20:CHEN:DAT:PRE.OUT:PREDD:D5:BRDE5.DAT
5000            ! MAXIMUM NUMBER OF SINGLE DIFFERENCES (100 - 5000)
50              ! DEBUGGING LEVEL (0 - 100)
N               ! RELATIVE COORDINATE IMPROVEMENT (Y/N)
2               ! NUMBER OF FREQUENCIES ( 1 OR 2 )
2               ! RECEIVER MODEL ( 1 = WM101 OR TRIMBLE, 2 = TI4100 )
10              ! CYCLE SLIP DETECTION THRESHOLD (CM.)
```

APPENDIX II

COMMAND FILES FOR MAIN-PROCESSOR OF DIPOP-E

II.1 Command File for the Adjustment

```
*
*    | | | | | | | | |   CONTROL FILE FOR MAIN-PROCESSOR OF DIPOP-E   | | | | | | | | |
*
* Syntax for inputs:
* 1. all the lines beginning with the character '*' or "#" are the
*    comment lines and they are skipped in processing the file.
*    Don't start a line beginning with '*' or '#', if it isn't a comment.
* 2. a comment line (as described above) can be added anywhere in
*    the control file except in the input area for the
*    observation files
* 3. a input line will begin with: '==>', or 'n ==>', or without any special
*    sign, where n means that this line corresponds
*    to the preceding comment with the same number 'n'.
* 4. the characters following '!' (including '!') in a input line
*    function as comments and are ignored.
* 5. lines beginning with '=======',  '--------', '++++++++', are
*    title lines or separation lines for different input areas (or
*    blocks) and can not be changed arbitrarily
* 6. the maximum number of characters in an input line is 200.
* 7. DIPOP-E's command file cannot be used for DIPOP's command file,
*    (of any version) and vice versa.
*
*_____
*
VERSION                              : 3.00
```

```
* ========= PART 1. FILE NAMES CREATED IN THE PROCEDURE (A64) ======
#1. MAIN-PROCESSOR ERROR, DEBUG, AND SUM              FILE NAME ?
#2. FINAL OUTPUT                                      FILE NAME ?
#3. RESIDUAL                                          FILE NAME ?
#4. DISCREPANCY                                       FILE NAME ?
#5. FINAL SOLUTION & COV. FOR NEXT RUNNING,           FILE NAME ?
*    NOT IMPLEMENTED
#6. FIRST  TEMPORARY                                  FILE NAME ?
#7. SECOND TEMPORARY                                  FILE NAME ?
#8. THIRD  TEMPORARY                                  FILE NAME ?
#9. FORTH  TEMPORARY                                  FILE NAME ?
#10 FIFTH  TEMPORARY                                  FILE NAME ?
*
* Caution: you should give different names for these
* intermediate files
*-------------------------------------------------------------------
1 ==> HD20:CHEN:MPR9:OUT:OMSK25:ALLC2.DBG
2 ==> HD20:CHEN:MPR9:OUT:OMSK25:allc2.MPR
3 ==> HD20:CHEN:MPR9:OUT:TEST
4 ==> HD20:CHEN:MPR9:OUT:SSG.DIS
5 ==> HD20:CHEN:MPR9:OUT:SSG0304.FIN
6 ==> HD20:CHEN:MPR9:OUT:SSG0304.TRO
7 ==> HD20:CHEN:MPR9:OUT:SSG0304.NUI
8 ==> HD20:CHEN:MPR9:OUT:TEMP3
9 ==> HD20:CHEN:MPR9:OUT:TEMP4
10==> HD20:CHEN:MPR9:OUT:TEMP5
*
* ========= PART 2.  CONTROL FOR THE ADJUSTMENT ===========
#1. NUMBER OF THE ITERATION IN THE FINAL ADJUSTMENTS              ?
*    THE ABOVE HAVEN'T BEEN FULLY TESTED YET, SPECIFY     1
#2. ITERATION CONTROL: USE VALUE '-1' AT THE MOMENT
#3. ORBITAL IMPROVEMENT(Y/N)                                      ?
#4. COMMAND FILE FOR ORBITAL INFORMATION                          ?
#5. CONSIDER DOUBLE DIFF. CORRELATION Y(1) (0 AT THE MOMENT)      ?
#6. COMPUTE RESIDUALS: 1 (YES) ? 2 (DEFAULT RESIDUAL FILE NAME)   ?
#7. STATION COORDINATES SEQ. SOLUTION at EACH m EPOCH             ?
#8. CROSS-CORRELATION VALUE OF COMPARISON                         ?
#9. CUT OFF ELEVATION ANGLE (IN DEGREES)                          ?
#10 DEFAULT MSL METEOROLOGICAL VALUES P(MB), T(C), RH(%)          ?
 11 ESTIMATE THE TROPOSPHERE SCALE AND ITS A PRIORI STD DEVIATION  ⌒
```

II.2

```
#12.VERTICAL TIDAL CORRECTION Y/N(1/0) AND THE FIRST LOVE'S NUMBER     ?
#13.RESTORE PERMANENT TIDE Y/N(1/0)                                    ?
*----------------------------------------------------------------------
1 ==> 1
2 ==> -1
3 ==> Y
4 ==> HD20:CHEN:MPR9:CMD:ORBIN.CMD
5 ==> 0
6 ==> 0
7 ==> 999
8 ==> .999
9 ==> 10.0D0
10==> 1000.00  00.00  50.00
11==> 1    0.80
12==> 1    0.62
13==> 1
*====== PART 3. A-PRIORI STATION COORDINATES AND STD. DEVIATION (M) ====
#1. COORDINATES ?
* FROM THIS FILE(1 OR 2). 1: FOR CART COOR.  2: FOR GEOD. COOR.
* FROM PREVIOUS SOLUTION(3) (NOT IMPLEMENTED YET)
==> 2
#2. IF 3 IS SPECIFIED IN THE ABOVE LINE: PLEASE INSERT FILE NAME AFTER
*   THIS COMMENT (NOT BEGINNING WITH ==> DELETE ALL INPUTS CORRESPONDING TO
*   COMMENT #3 AND COMMENT #4
#3. REFERENCE ELLIPSOID IN ORDER OF: SEMI-MAJOR, INVERSE OF FLAT,
*   X Y Z -SHIFT (FREE FORMAT)
*   ELLIPSOID IS ONE USED IN CONVERSION FROM (OR TO) CARTESIAN COORDINATE
*   X Y Z ARE SHIFT BETWEEN STATION COORDINATE SYSTEM AND EPHEMERIS
*   COORDINATE SYSTEM
    6378135.0     298.2600       0.000       0.000       0.000
*
#4. IF 1 OR 2 IN #1, INPUT THE COORDINATES EXACTLY AS FORMAT
*   DESCRIBED AND THE LINE FOLLOWING EACH STATION COORDINATES ARE
*   CORRESPONDING STD DEVIATION
*   SYMBOL "##": SEQUENCE OF THE STATION; "NN": STATION NAME
*   CORRESPONDING TO THOSE IN THE OBSERVATION FILE
*
## NN       SDD MM SS.SSSSS SDDD MM SS.SSSSS HHHH.HHH
01 PL        40 10 58.05604 -104 43 34.84730 1503.2569
                    1.0D-4          1.0D-4     1.0D-4
02 AL        45 57 21.24086 - 78 04 16.92058  200.7782
                    1.0D-4          1.0D-4     1.0D-4
```

```
03 OW        37 13 57.21511 -118 17 37.65749 1179.9443
                 1.0D-4                1.0D-4      1.0D-4
04 CH        58 45 32.96074 - 94 05 18.08572   -15.0920
                 1.0D+02               1.0D+02     1.0D+02
05 WF        42 36 47.95645 - 71 29 36.02332    88.3462
                 1.0D+02               1.0D+02     1.0D+02
06 BU        35 23 54.58426 -119 23 38.45992    56.6232
                 1.0D+02               1.0D+02     1.0D+02
07 GA        34 30  6.51289 -120 11 55.66095   715.3075
                 1.0D+02               1.0D+02     1.0D+02
08 LA        34 29 39.86912 -119 42 50.01971 1166.6846
                 1.0D+02               1.0D+02     1.0D+02
09 SE        33 57  3.08619 -120  6 20.43013   445.3571
                 1.0D+02               1.0D+02     1.0D+02
10 CF        34 18  2.22346 -119 19 51.44183   309.0608
                 1.0D+02               1.0D+02     1.0D+02
11 BR        33 24 25.24661 -118 24 17.47639   450.4823
                 1.0D+02               1.0D+02     1.0D+02
12 DE        34 01 44.81445 -119 47 03.87717   706.5085
                 1.0D+02               1.0D+02     1.0D+02
13 FT        36 40 11.23     -121 46 23.78       24.59
                 1.0D+03               1.0D+03     1.0D+03
14 SI        34 17 54.01834 -119 20 33.67370    -9.7644
                 1.0D+02               1.0D+02     1.0D+02
15 PA        33 44 37.53928 -118 24 12.78803    71.3572
                 1.0D+02               1.0D+02     1.0D+02
16 VN        34 33 22.54778 -120 36 58.31415    -9.6181
                 1.0D+02               1.0D+02     1.0D+02
17 MJ        35 19 53.59722 -116 53 17.35652   906.4217
                 1.0D+02               1.0D+02     1.0D+02
18 ML        34 30 36.38716 -120 13 46.81878    87.1912
                 1.0D+02               1.0D+02     1.0D+02
-1       ! MUST BEGIN WITH "-1" FOR THIS LINE TO MARK THE END OF COOR. INPUT
## NN     XXXXXXXX.XXX YYYYYYY.YYY ZZZZZZZ.ZZZ    ! GEODETIC FORMAT
==========      PART 4. OBSERVATION FILE INFORMATION    ================
#0.  OBS. FILES, BINARY(0) OR ASCII(1)  ?
*    ONLY 1 CAN BE SPECIFIED AT THE MOMENT.
==> 1
*    ENTER (ANSWER) THE FOLLOWING LINES FOR THE OBSERVATION DATA
*
*    AT THE BEGINNING OF A NEW WINDOW, ENTER FOLLOWING TWO LINES
#1.  A BLANK LINE FOR DELIMITER
```

```
#2.   COMMENT LINE BEGINNING WITH '*'
#3.   THE TIME INTERVAL OF THE OBSERVATION WINDOW:
*     GPS WEEK AND THE TIME AT THE BEGINNING OF THE WINDOW,
*     GPS WEEK AND THE TIME AT THE ENDING OF THE WINDOW.
*     Free FORMAT is used.
*
#4.   Station name & its corresponding meteorological and antenna height
*     file name for the observation window (A64). Station name & its
*     corresponding meteorological and antenna height file name are
*     separated by one space.  Input for other stations are made
*     similarly; one line for each station.  All the stations which appear in
*     the observation files of the window should be input.  A station
*     name should be consistent with the station name in its met. and
*     observation files.
*
#5.   A blank line for separation.
#6.   Obs. & sat. position file name (A64)
#7.   A-priori std. deviation of double difference obs. (mm) (*)
#8.   Clock parameters.(st.2 wrt st.1) and respective std. dev. (sec) (*)
*     This option has not been implemented yet.
#9.   L1:1, L2:2, L1 & L2:3; estimate amb.? Y(1); residual computation
*     for this observation file Y(1).
*
#10.  Repeat steps 4 through 9 for observation files in the same block.
*
*     The following two lines (#11 and #12) mark the beginning of a
*     new block.
#11.  Following the last input of the observation file in the previous
*     block, enter a blank line.
#12.  Enter a line beginning with "(-".
#13.  Similar to the inputs of steps 4 through 12, inputs for a new block
#14.  Repeat step 1 to 13 for new windows
*
*Notice:  don't input "(-" and the end of the last block.
*
*----------------------------------------------------------------------

* window for day 3: start and the stop time
364    5.440E+05 364 5.75000D5
PL HD20:CHEN:dat:SSG:MET:PL03.MET
AL HD20:CHEN:dat:SSG:MET:AL03.MET
OW HD20:CHEN:dat:SSG:MET:OW03.MET
```

```
CH HD20:CHEN:dat:SSG:MET:CH03.MET
WF HD20:CHEN:dat:SSG:MET:WF03.MET
BU HD20:CHEN:dat:SSG:MET:BU03.MET
GA HD20:CHEN:dat:SSG:MET:GA03.MET
LA HD20:CHEN:dat:SSG:MET:LA03.MET
SE HD20:CHEN:dat:SSG:MET:SE03.MET
CF HD20:CHEN:dat:SSG:MET:CF03.MET
BR HD20:CHEN:dat:SSG:MET:BR03.MET
DE HD20:CHEN:dat:SSG:MET:DE03.MET
FT HD20:CHEN:dat:SSG:MET:FT03.MET
SI HD20:CHEN:dat:SSG:MET:SI03.MET
PA HD20:CHEN:dat:SSG:MET:PA03.MET
VN HD20:CHEN:dat:SSG:MET:VN03.MET
MJ HD20:CHEN:dat:SSG:MET:MJ03.MET
ML HD20:CHEN:dat:SSG:MET:ML03.MET


SSG.PREDD.CLK:D3:PLAL3.DATC2
 15
0    1.0D-06    1.0D-06
3  1  0


SSG.PREDD.CLK:D3:PLOW3.DATC2
 15
0    1.0D-06    1.0D-06
3  1  0


SSG.PREDD.CLK:D3:ALCH3.DATC2
 15
0    1.0D-06    1.0D-06
3  1  0


SSG.PREDD.CLK:D3:ALWF3.DATC2
 15
0    1.0D-06    1.0D-06
3  1  0


SSG.PREDD.CLK:D3:OWBU3.DATC2
 15
0    1.0D-06    1.0D-06
3  1  0


SSG.PREDD.CLK:D3:GABU3.DATC2
```

```
 15
0   1.0D-06    1.0D-06
3  1  0


SSG.PREDD.CLK:D3:GALA3.DAT
 15
0   1.0D-06    1.0D-06
3  1  0


(-


SSG.PREDD.CLK:D3:GASE3.DAT
 15
0   1.0D-06    1.0D-06
3  1  0


SSG.PREDD.CLK:D3:GASE3GP2.DAT
 15
0   1.0D-06    1.0D-06
3  1  0
LA    CF                          9
SSG.PREDD.CLK:D3:LACF3.DAT
 15
0   1.0D-06    1.0D-06
3  1  0
CF    BR                         10
SSG.PREDD.CLK:D3:CFBR3.DAT
 15
0   1.0D-06    1.0D-06
3  1  0
BR    PA                    8
SSG.PREDD.CLK:D3:BRPA3.DAT
 15
0   1.0D-06    1.0D-06
3  1  0
GA    VN                         11
SSG.PREDD.CLK:D3:GAVN3.DAT
 15
0   1.0D-06    1.0D-06
3  1  0


SSG.PREDD.CLK:D3:OWFT3.DAT
```

II.7

```
 15
0    1.0D-06    1.0D-06
3  1  0


(-

* window for day 4: start and the stop time
365    2.50D4 365 5.2D4
PL HD20:CHEN:dat:SSG:MET:PL04.MET
AL HD20:CHEN:dat:SSG:MET:AL04.MET
OW HD20:CHEN:dat:SSG:MET:OW04.MET
CH HD20:CHEN:dat:SSG:MET:CH04.MET
WF HD20:CHEN:dat:SSG:MET:WF04.MET
BU HD20:CHEN:dat:SSG:MET:BU04.MET
GA HD20:CHEN:dat:SSG:MET:GA04.MET
LA HD20:CHEN:dat:SSG:MET:LA04.MET
SE HD20:CHEN:dat:SSG:MET:SE04.MET
CF HD20:CHEN:dat:SSG:MET:CF04.MET
BR HD20:CHEN:dat:SSG:MET:BR04.MET
DE HD20:CHEN:dat:SSG:MET:DE04.MET
FT HD20:CHEN:dat:SSG:MET:FT04.MET
SI HD20:CHEN:dat:SSG:MET:SI04.MET
PA HD20:CHEN:dat:SSG:MET:PA04.MET
VN HD20:CHEN:dat:SSG:MET:VN04.MET
MJ HD20:CHEN:dat:SSG:MET:MJ04.MET
ML HD20:CHEN:dat:SSG:MET:ML04.MET

SSG.PREDD.CLK:D4:PLAL4.DATC2
 15
0    1.0D-06    1.0D-06
3  1  0


SSG.PREDD.CLK:D4:PLOW4.DAT
 15
0    1.0D-06    1.0D-06
3  1  0


SSG.PREDD.CLK:D4:ALCH4.DATC2
 15
0    1.0D-06    1.0D-06
3  1  0
```

II.8

```
SSG.PREDD.CLK:D4:ALWF4.DAT
 15
0    1.0D-06    1.0D-06
3  1  0


SSG.PREDD.CLK:D4:ALWF4GP2.DAT
 15
0    1.0D-06    1.0D-06
3  1  0


SSG.PREDD.CLK:D4:OWBU4.DAT
 15
0    1.0D-06    1.0D-06
3  1  0


SSG.PREDD.CLK:D4:OWFT4.DAT
 15
0    1.0D-06    1.0D-06
3  1  0


(-


SSG.PREDD.CLK:D4:GABU4.DAT
 15
0    1.0D-06    1.0D-06
3  1  0


SSG.PREDD.CLK:D4:GALA4.DAT
 15
0    1.0D-06    1.0D-06
3  1  0


SSG.PREDD.CLK:D4:GASE4.DAT
 15
0    1.0D-06    1.0D-06
3  1  0
LA   SI                             9
SSG.PREDD.CLK:D4:LASI4.DAT
 15
0    1.0D-06    1.0D-06
3  1  0
SI   BR                            10
```

```
SSG.PREDD.CLK:D4:BRDE4.DAT
 15
0    1.0D-06    1.0D-06
3  1  0
GA    DE                        8
SSG.PREDD.CLK:D4:GADE4.DAT
 15
0    1.0D-06    1.0D-06
3  1  0
GA    VN                       11
SSG.PREDD.CLK:D4:GAVN4.DAT
 15
0    1.0D-06    1.0D-06
3  1  0


(-

* window for day 5: start and the stop time
365    11.1D4 365 13.8D4
PL HD20:CHEN:dat:SSG:MET:PL05.MET
AL HD20:CHEN:dat:SSG:MET:AL05.MET
OW HD20:CHEN:dat:SSG:MET:OW05.MET
CH HD20:CHEN:dat:SSG:MET:CH05.MET
WF HD20:CHEN:dat:SSG:MET:WF05.MET
BU HD20:CHEN:dat:SSG:MET:BU05.MET
GA HD20:CHEN:dat:SSG:MET:GA05.MET
LA HD20:CHEN:dat:SSG:MET:LA05.MET
SE HD20:CHEN:dat:SSG:MET:SE05.MET
CF HD20:CHEN:dat:SSG:MET:CF05.MET
BR HD20:CHEN:dat:SSG:MET:BR05.MET
DE HD20:CHEN:dat:SSG:MET:DE05.MET
FT HD20:CHEN:dat:SSG:MET:FT05.MET
SI HD20:CHEN:dat:SSG:MET:SI05.MET
PA HD20:CHEN:dat:SSG:MET:PA05.MET
VN HD20:CHEN:dat:SSG:MET:VN05.MET
MJ HD20:CHEN:dat:SSG:MET:MJ05.MET
ML HD20:CHEN:dat:SSG:MET:ML05.MET


SSG.PREDD.CLK:D5:PLAL5.DAT
 15
0    1.0D-06    1.0D-06
3  1  0
```

```
SSG.PREDD.CLK:D5:PLOW5.DATC2
 15
0    1.0D-06    1.0D-06
3  1  0


SSG.PREDD.CLK:D5:ALCH5.DATC2
 15
0    1.0D-06    1.0D-06
3  1  0


SSG.PREDD.CLK:D5:ALWF5.DAT
 15
0    1.0D-06    1.0D-06
3  1  0


SSG.PREDD.CLK:D5:ALWF5GP2.DAT
 15
0    1.0D-06    1.0D-06
3  1  0


SSG.PREDD.CLK:D5:ALCH5GP2.DATC2
 15
0    1.0D-06    1.0D-06
3  1  0


SSG.PREDD.CLK:D5:PLAL5GP2.DAT
 15
0    1.0D-06    1.0D-06
3  1  0


(-


SSG.PREDD.CLK:D5:OWBU5.DAT
 15
0    1.0D-06    1.0D-06
3  1  0


SSG.PREDD.CLK:D5:GABU5.DATC2
 15
0    1.0D-06    1.0D-06
3  1  0
```

```
SSG.PREDD.CLK:D5:GALA5.DAT
 15
0   1.0D-06   1.0D-06
3  1  0


SSG.PREDD.CLK:D5:GASE5.DAT
 15
0   1.0D-06   1.0D-06
3  1  0
LA   SI                          9
SSG.PREDD.CLK:D5:LASI5.DAT
 15
0   1.0D-06   1.0D-06
3  1  0
SI   BR                          10
SSG.PREDD.CLK:D5:BRDE5.DAT
 15
0   1.0D-06   1.0D-06
3  1  0
GA   DE                  8
SSG.PREDD.CLK:D5:GADE5.DAT
 15
0   1.0D-06   1.0D-06
3  1  0
GA   VN                          11
SSG.PREDD.CLK:D5:GAVN5.DAT
 15
0   1.0D-06   1.0D-06
3  1  0


SSG.PREDD.CLK:D5:OWFT5.DAT
 15
0   1.0D-06   1.0D-06
3  1  0


(-


* window for day 6: start and the stop time
365 197000.0D0 365 224039.0D0
PL HD20:CHEN:dat:SSG:MET:PL06.MET
AL HD20:CHEN:dat:SSG:MET:AL06.MET
```

```
OW HD20:CHEN:dat:SSG:MET:OW06.MET
CH HD20:CHEN:dat:SSG:MET:CH06.MET
WF HD20:CHEN:dat:SSG:MET:WF06.MET
BU HD20:CHEN:dat:SSG:MET:BU06.MET
GA HD20:CHEN:dat:SSG:MET:GA06.MET
LA HD20:CHEN:dat:SSG:MET:LA06.MET
SE HD20:CHEN:dat:SSG:MET:SE06.MET
CF HD20:CHEN:dat:SSG:MET:CF06.MET
BR HD20:CHEN:dat:SSG:MET:BR06.MET
DE HD20:CHEN:dat:SSG:MET:DE06.MET
FT HD20:CHEN:dat:SSG:MET:FT06.MET
SI HD20:CHEN:dat:SSG:MET:SI06.MET
PA HD20:CHEN:dat:SSG:MET:PA06.MET
VN HD20:CHEN:dat:SSG:MET:VN06.MET
MJ HD20:CHEN:dat:SSG:MET:MJ06.MET
ML HD20:CHEN:dat:SSG:MET:ML06.MET


SSG.PREDD.CLK:D6:PLAL6.DAT
 15
0   1.0D-06   1.0D-06
3  1  0


SSG.PREDD.CLK:D6:PLAL6GP2.DAT
 15
0   1.0D-06   1.0D-06
3  1  0


SSG.PREDD.CLK:D6:ALCH6.DAT
 15
0   1.0D-06   1.0D-06
3  1  0


SSG.PREDD.CLK:D6:ALCH6GP2.DAT
 15
0   1.0D-06   1.0D-06
3  1  0


SSG.PREDD.CLK:D6:ALCH6GP3.DAT
 15
0   1.0D-06   1.0D-06
3  1  0
```

```
SSG.PREDD.CLK:D6:ALWF6.DAT
 15
0    1.0D-06    1.0D-06
3  1  0


SSG.PREDD.CLK:D6:OWPL6.DAT
 15
0    1.0D-06    1.0D-06
3  1  0


SSG.PREDD.CLK:D6:OWMJ6.DATC2
 15
0    1.0D-06    1.0D-06
3  1  0
OW    BU                    7
SSG.PREDD.CLK:D6:OWBU6.DAT
 15
0    1.0D-06    1.0D-06
3  1  0


SSG.PREDD.CLK:D6:OWFT6.DAT
 15
0    1.0D-06    1.0D-06
3  1  0


(-
BU    PA                    8
SSG.PREDD.CLK:D6:BUPA6.DAT
 15
0    1.0D-06    1.0D-06
3  1  0


SSG.PREDD.CLK:D6:BUPA6GP2.DAT
 15
0    1.0D-06    1.0D-06
3  1  0


SSG.PREDD.CLK:D6:BUVN6.DAT
 15
0    1.0D-06    1.0D-06
3  1  0
```

```
SSG.PREDD.CLK:D6:BUVN6GP2.DAT
 15
0    1.0D-06    1.0D-06
3  1  0


SSG.PREDD.CLK:D6:BULA6.DAT
 15
0    1.0D-06    1.0D-06
3  1  0


SSG.PREDD.CLK:D6:DEBR6.DAT
 15
0    1.0D-06    1.0D-06
3  1  0


SSG.PREDD.CLK:D6:LADE6.DAT
 15
0    1.0D-06    1.0D-06
3  1  0


SSG.PREDD.CLK:D6:LASI6.DAT
 15
0    1.0D-06    1.0D-06
3  1  0


SSG.PREDD.CLK:D6:LASE6.DAT
 15
0    1.0D-06    1.0D-06
3  1  0


SSG.PREDD.CLK:D6:LASE6GP2.DAT
 15
0    1.0D-06    1.0D-06
3  1  0


(-

* ORBITAL SESSION 1: start and the stop time
365 283000.0D0 365 311000.0D0
PL HD20:CHEN:dat:SSG:MET:PL07.MET
AL HD20:CHEN:dat:SSG:MET:AL07.MET
OW HD20:CHEN:dat:SSG:MET:OW07.MET
```

```
CH HD20:CHEN:dat:SSG:MET:CH07.MET
WF HD20:CHEN:dat:SSG:MET:WF07.MET
BU HD20:CHEN:dat:SSG:MET:BU07.MET
GA HD20:CHEN:dat:SSG:MET:GA07.MET
LA HD20:CHEN:dat:SSG:MET:LA07.MET
SE HD20:CHEN:dat:SSG:MET:SE07.MET
CF HD20:CHEN:dat:SSG:MET:CF07.MET
BR HD20:CHEN:dat:SSG:MET:BR07.MET
DE HD20:CHEN:dat:SSG:MET:DE07.MET
FT HD20:CHEN:dat:SSG:MET:FT07.MET
SI HD20:CHEN:dat:SSG:MET:SI07.MET
PA HD20:CHEN:dat:SSG:MET:PA07.MET
VN HD20:CHEN:dat:SSG:MET:VN07.MET
MJ HD20:CHEN:dat:SSG:MET:MJ07.MET
ML HD20:CHEN:dat:SSG:MET:ML07.MET


SSG.PREDD.CLK:D7:PLAL7.DAT
 15
0    1.0D-06    1.0D-06
3  1  0


SSG.PREDD.CLK:D7:PLAL7GP2.DAT
 15
0    1.0D-06    1.0D-06
3  1  0


SSG.PREDD.CLK:D7:PLOW7.DATC2
 15
0    1.0D-06    1.0D-06
3  1  0


SSG.PREDD.CLK:D7:ALCH7.DAT
 15
0    1.0D-06    1.0D-06
3  1  0


SSG.PREDD.CLK:D7:ALCH7GP2.DAT
 15
0    1.0D-06    1.0D-06
3  1  0


SSG.PREDD.CLK:D7:OWMJ7.DAT
```

```
 15
0    1.0D-06    1.0D-06
3   1   0

SSG.PREDD.CLK:D7:OWBU7.DAT
 15
0    1.0D-06    1.0D-06
3   1   0

SSG.PREDD.CLK:D7:OWFT7.DAT
 15
0    1.0D-06    1.0D-06
3   1   0

(-

SSG.PREDD.CLK:D7:BUPA7.DAT
 15
0    1.0D-06    1.0D-06
3   1   0

SSG.PREDD.CLK:D7:BUVN7.DAT
 15
0    1.0D-06    1.0D-06
3   1   0

SSG.PREDD.CLK:D7:BULA7.DAT
 15
0    1.0D-06    1.0D-06
3   1   0

SSG.PREDD.CLK:D7:BUBR7.DAT
 15
0    1.0D-06    1.0D-06
3   1   0

SSG.PREDD.CLK:D7:LADE7.DAT
 15
0    1.0D-06    1.0D-06
3   1   0

SSG.PREDD.CLK:D7:LASI7.DAT
```

```
  15
0   1.0D-06    1.0D-06
3  1  0


SSG.PREDD.CLK:D7:LASE7.DAT
  15
0   1.0D-06    1.0D-06
3  1  0


SSG.PREDD.CLK:D7:LAML7.DAT
  15
0   1.0D-06    1.0D-06
3  1   0
```

II.2 Command File for the Orbit Integration and Improvement

```
**                                                           **
**   ******* ORBIT INTEGRATION AND IMPROVEMENT INFORMATION ******   **
**                                                           **
* Notice: the rules of inputs are similar to the
*         command file for the adjustment
*         for the test just input as shown in the sample
*         command file.
* Orbit improvement with the ephemeris (1: yes; 0: no)      ?         *
==> 1
*
* ========= PART 1. FORCE MODELLING INFORMATION ===========
*
#1. File name for the gravity coef.(free format)                          ?
==> HD20:CHEN:DAT:GRA:GRAVITY.GEML2NOTIDE
#2. degree and order of the gravity field                                 ?
==> 8
#3. Gravity potential coefficients:  normalized yes(1)                    ?
==> 1
#4. Effect of the moon yes(1)                                             ?
==> 1
#5. Effect of the sun yes(1)                                              ?
==> 1
```

```
#6   Interval (in hours) to approximate the positions of the moon and the
*    sun for an observation window                                            ?
==> 0.3D0
#7.  Use TDT time for UT1 to call SR.s of moon and sun (in second)           ?
==> 1
#8.  0.0D0 for this input
*    (for test only) Off-set between time for SRs of the Moon and the Sun
*    and the time of TDT time (in seconds)                                    ?
==> 0.0D0
#9.  In the orbit improvement with observations, how many radiation parameters
*    are estimated -- 1:direct radiation. only; 2: both direct and y-bias;
*    0:none                                                                   ?
==> 2
#10  In the orbit improvement with ephemeris, how many radiation parameters
*    are estimated -- 1:direct radiation. only; 2: both direct and y-bias;
*    0:none                                                                   ?
==> 2
#11  1 for this input.
*    (for test only) include the Y-bias radiation in the force model         ?
==> 1
#12  The solid Earth tidal gravity ? Yes (1)                                  ?
==> 0
#13  The second Love's number for the second and the third order tidal harmonics ?
*    the third order effect has not been implemented.
==> 0.29D0   0.14D0
#14  0 for this input.  (other value is only for test of program)
*    Include the secular variation for the partial (1 or 2, if 1 then
*    include the Earth's oblatness for the partials for the radiation
*    not fully implemented and tested yet.
==> 0
*
* =============== PART 2. SATELLITE INFORMATION  ================
*
#1.  Initial epoch for integration: GPS week and time (IN SECONDS)      ?
*
*    Notice: at the moment, the time must be the same as the start time
*    of the first observation window as it is specified in the adjustment
*    control file
==> 364    5.440E+05
#2   Initial conditions at the initial epoch                                  ?
*    the satellites can be in any order
*PRN       a           e           i           Ω           ω           T0   direct radiat. y-bias
```

```
*
*    Don't beginning with '==>' for this input
 9 0.265623261E+08 0.121493911E-01 0.111643361E+01 -0.157521289E+01  0.117180498E+01 0.553454727E+06 0.9702E-07 0.4018E-09
12 0.265591489E+08 0.881343351E-02 0.110775774E+01 -0.157117860E+01 -0.983411606E+00 0.544006091E+06 0.8835E-07 0.4380E-09
 3 0.265843487E+08 0.117557431E-01 0.110795390E+01  0.535399656E+00 -0.369656238E+01 0.522894181E+06 0.8645E-07 0.5721E-09
 6 0.265612205E+08 0.442294421E-02 0.111981352E+01 -0.157277045E+01  0.207931852E+01 0.554837317E+06 0.9911E-07 0.5696E-09
11 0.265594507E+08 0.114892375E-01 0.109871589E+01  0.545950257E+00 -0.268847361E+01 0.533103710E+06 0.8823E-07 0.2621E-09
13 0.265595419E+08 0.305333824E-02 0.109386909E+01  0.537837448E+00 -0.283902650E+00 0.556496647E+06 0.9092E-07 0.2734E-09
#3. Antenna phase center offset in the i direction                                    ?
==> 0.211
#4. Antenna phase center offset in the k direction (to the center of the Earth)
==> 0.886
#5. Variances of orbit elements (in the orbit improvement using ephemeris)?
==> 500. 4.0D-5 4.0D-5 4.0D-5 1.6D-6 1.0D  2.0D-9    1.0D-9
#6. 0.00 for this input
*    Correlation between T0 and ω (for test only)
==> -0.00
#7. Variances of orbit elements (in the final orbit improvement using phase
*    observations)?
==> 5.00D+1 2.000E-6 2.000E-6 4.000E-6 4.000E-9 1.000E-1  2.0D-8    2.0D-9
*    The above three inputs should be moved to the line after #2  in a
*    later version.
*
* =============== PART 3. TIME & THE EARTH ORIENTATION INFORMATION ==============
*
#1. POLAR MOTION  AND TIME CORRECTIONS (FREE FORMAT) ?
*    DON'T BEGIN INPUT LINES WITH '==>' FOR THIS INPUT
*    THE VALUES CAN BE AT ANY TIME INTERVAL
*    YEAR, MONTH,  DAY, HOUR;    XP,    YP,     UT1-UTC,   GPS-UTC        ?
*                          (in arc-seconds)   (in seconds)
    1986  12    30.0  0.0    0.1572 0.3118    -0.13617    4
    1987  1      4.0  0.0    0.1591 0.3054    -0.14257    4
    1987  1      9.0  0.0    0.1569 0.2991    -0.15103    4
#2. SEPARATE TIDAL VARIATIONS IN UT1 for interpolation              ?
==> 1
#3. specify "0" for this purpose
*    (for test only) INTEGRATE IN BARYCENTRIC TIME SCALE ? YES(1), NO (0)
==> 0
#4. (FOR TEST ONLY) OFFSET FOR THE GPS TIME (IN DAYS)
*    for test only; specify "0.0" for general purpose
==> 0.0D0
*
* =============== PART 4. INTEGRATION INFORMATION ===================
```

II.20

```
*
#1. Number of iterations in the orbital improvement process using
*    ephemeris files                                                    ?
==> 0
#2. input 1.0D-4
*    (for test only) Convergence control in the starter                              ?
*    The maximum allowed sum of the differences between the previous
*    loop and the current one
==> 1.0D-4
#3. Step size of the integration (in seconds)                    ?
==> 120
#4. The lengths of segmentations for orbital representation (in hours) ?
==> 2.0D0
#5. Order of the integrator                                      ?
==> 9
#6. input 1.0D-9
*    (for test only) Convergence control in the starter for partial
*    derivatives
==> 1.0D-9
#7. Step size of the integration for partial derivatives (in seconds)  ?
==> 120
#8. The order of the integrator for partial derivatives          ?
==> 9
#9. Order of the representing polynomials for satellite positions      ?
==> 11
*
* =========== PART 5. ORBIT IMPROVEMENT WITH THE EPHEMERIS DATA =========
* Warning: input from #0 through #6 are for test only, the users should
*     leave it as it is in this sample file.
#0    specify 0 for this input
*    (This option is only for test purpose)
#0.1 Test the consistency of partial derivatives and with initial
*     integration
*
==> 0
#0.2 no input if previous input is '0'.
* (test only)  initial condition to generate simulated orbits.
* 13 0.265595868E+8 0.305437881E-2 0.1093869107E+1 0.5378353864E+0 0.2847464758E+0 0.5564908889E+6 0.8980E-7 -0.689E-9
*
#1. specify "F"
*    (for test only) Computation of clock offset coefficients
==> F
```

```
#2. (for test only) OUTPUT CLOCK FILE NAME                                              ?
==> HD20:CHEN:MPR9:OUT:SVCLK.OUT
#3. (for test only) GM correction Y(1), priori accuracy, and its value ?
==> 0   5.0D7  0.398600440D+15
#4. (for test only) Scale factor Y(1), translation estimation Y(1)                      ?
==> 0 0
#5. (for test only) Prior values and accuracy, (scale, X,Y,Z)                           ?
==> 0.0   0.0   0.0    0.0  1.0D-6 100.0  100.0    100.0
#6. (for test only) Scale factor in the force model? Y(1)                               ?
==> 0
#7. Maximum time interval of the positions of a satellite from
*    the ephemeris file or simulated orbit                              ?
==> 10.0
*8. Enter the following lines
#a. Delimiter (blank)
#b. a comment line
#c. GPS time interval during which positions of satellites are computed
*    GPS week and time at the beginning of the interval; GPS week and time
*    at the end of the interval, and length of sub-intervals
#d. ephemeris filename.
#e. ephemeris type.
*    specify 1 for the broadcast ephemeris.
#f. the format of the ephemeris.
#g. comment line.
#h. (for test only leave as it was in this sample command file)
*    interval for SV clock approximation, its length of segmentation, and
*    the order of the approximating polynomial.
#i. Repeat steps #a through #i for other ephemeris files.  They can be
*    the same ephemeris file, but for different time period.
*
* Caution: you can not enter comment lines arbitrarily after
*    the following line
-------------------------------------------------------------

* orbital session 1: start and the stop time
 364    5.440E+05 364 6.048D5 15000.0D0
HD20:CHEN:dat:SSG:EPH:f018.mac80
1
CC
* Clock coefficient approximation interval (developed for debug only)
5.4400E+05 571000.0 1
```

APPENDIX III

COMMAND FILE FOR "GNKPL"

The following is the command file to generate approximate Keplerian elements from a broadcast ephemeris file.

```
* COMMAND FILE TO GENERATE APPROXIMATE KEPERIAN ELEMENTS
6
CC
31
HD20:CHEN:MPR9:FD:KPL03sum.BR
HD20:CHEN:MPR9:FD:KPL03out.BR
3 6 9 11 12 13
5.4400E+05
 0.1582  0.3018
HD20:CHEN:dat:SSG:EPH:f018.mac80
BR
```

The first line is used for comments and is skipped during reading; the second line is the number of satellites whose Keplerian elements are going to be calculated; in the third line, the format of the ephemeris file is input, and the specification of this ephemeris format is the same as those in PREGE (see Appendix I); the forth line is the debug level. In line 5, the name of summary file is input; the sixth line is the output file name; the seventh line is PRN number of the satellites whose approximate Keplerian elements are required to be calculated; line 8 is the GPS time of the epoch at which the Keplerian elements are to be calculated; line 9 contains the polar wobble values (in arc-seconds) at the epoch; line 10 is input ephemeris file name; in line 11 "BR" indicates that the preceding line is a broadcast ephemeris.

APPENDIX IV

OUTPUT OF THE FIVE DAY ORBITAL SOLUTION

The following is the 5 days solution with orbital improvement. It contains

1. Station coordinates correction(Cartesian)
2. Troposphere correction
3. Ambiguities
4. Radiation parameters
5. Station coordinate summaries
6. Baseline discrepancies.

The covariances of the baselines and the covariance matrices for all the stations are omitted.

RE-EVALUATION OF NUISANCE PARAMETERS

```
AMBIGUITY FIXING LOOP 1
STATION COORD. CORRECTIONS:
  ST: PL      -0.8680E-06      -0.1051E-04      -0.7986E-05
  ST: AL       0.1942E-06       0.3831E-05       0.4147E-05
  ST: OW       0.7873E-06       0.6888E-05       0.3070E-05
  ST: CH      -0.4521E-01       0.3555E-01       -.1954
  ST: WF      -0.1072E-01      -0.6416E-01       0.4234E-01
  ST: BU      -0.7025E-02      -0.2307E-01      -0.1696E-01
  ST: GA       0.5618E-03      -0.4526E-01      -0.5755E-02
  ST: LA      -0.1180E-01       -.1296           0.1458E-01
  ST: SE      -0.8091E-02      -0.6429E-01       0.1144E-01
  ST: CF      -0.2479E-01      -0.7131E-01       0.3928E-01
  ST: BR       0.3415E-02      -0.3665E-01       0.2989E-01
  ST: DE       0.1047E-01      -0.2952E-01      -0.1271E-01
  ST: FT       -.6155           -.7963           .5314
  ST: SI      -0.3619E-01      -0.6843E-01       0.3020E-01
  ST: PA       0.3952E-01      -0.1474E-01      -0.7350E-02
  ST: VN      -0.8086E-02      -0.6039E-01      -0.2257E-01
  ST: MJ       0.1694E-01      -0.2905E-01       0.2223E-02
  ST: ML       0.4951E-02      -0.3905E-01       0.3201E-02
```

Table 1 Troposphere Scale Corrections
& Zenith Delay Corrections (in mm) for Jan. 3

notice: Zenith Delay Computed from Default Met. Data
by using SR. HOPF
Default Met. Data :
Pres. = 1000.00 Temp. = .00 Rel.   Huml. =   50.00

| Stations | Corrections | | | |
	Scale	& rms	Zenith Delay, in (mm)	rms
PL	.0265	.002	61	5
AL	-.0021	.001	-4	3
OW	.0557	.003	128	6
CH	.0250	.002	57	4
WF	-.0088	.002	-20	4
BU	.0412	.003	95	5
GA	.0486	.003	112	6
LA	.0504	.003	116	7
SE	.0444	.003	102	6
CF	.0410	.003	94	7
BR	.0391	.003	90	7
FT	.1067	.003	246	5
PA	.0429	.005	99	12
VN	.0571	.003	132	6

OBSERVATION SSG.PREDD.CLK:D3:PLAL3.DATC2
STATIONS: PL AL

AMBIGUITY WRT REFERENCE SATELLITE :   11
AMBIGUITY   3 :   130555.65   +/- 5.81
AMBIGUITY   6 :   129105.46   +/- 1.99
AMBIGUITY   9 :   -564400.76   +/- 3.15
AMBIGUITY 13 :   -2074177.53   +/- 4.79
AMBIGUITY 12 :   -3514735.69   +/- 5.86

```
OBSERVATION SSG.PREDD.CLK:D3:PLOW3.DATC2
STATIONS:  PL OW

AMBIGUITY WRT REFERENCE SATELLITE :   11
AMBIGUITY   3 :             290720.07   +/-   3.20
AMBIGUITY   6 :             291429.15   +/-   1.38
AMBIGUITY   9 :            -874390.11   +/-   2.17
AMBIGUITY  13 :           -2043429.05   +/-   3.54
AMBIGUITY  12 :           -3906525.35   +/-   4.17

OBSERVATION SSG.PREDD.CLK:D3:ALCH3.DATC2
STATIONS:  AL CH

AMBIGUITY WRT REFERENCE SATELLITE :   11
AMBIGUITY   3 :             737718.47   +/-   3.34
AMBIGUITY   6 :             739161.27   +/-   3.55
AMBIGUITY   9 :            -434960.00   +/-   4.42
AMBIGUITY  13 :            -984122.39   +/-   5.45
AMBIGUITY  12 :           -1149952.09   +/-   6.88

OBSERVATION SSG.PREDD.CLK:D3:ALWF3.DATC2
STATIONS:  AL WF

AMBIGUITY WRT REFERENCE SATELLITE :   11
AMBIGUITY   3 :             284840.57   +/-   1.54
AMBIGUITY   6 :             284197.03   +/-   1.04
AMBIGUITY   9 :            -347164.11   +/-   1.58
AMBIGUITY  39 :            -347149.44   +/-   1.98
AMBIGUITY  41 :                  5.70   +/-   1.04
AMBIGUITY  69 :            -347219.95   +/-   1.57
AMBIGUITY  12 :            -189166.82   +/-   2.39
AMBIGUITY  13 :            -157353.60   +/-   2.28

OBSERVATION SSG.PREDD.CLK:D3:OWBU3.DATC2
STATIONS:  OW BU

AMBIGUITY WRT REFERENCE SATELLITE :    6
AMBIGUITY   3 :                -40.01   +/-    .67
AMBIGUITY  11 :            2555131.01   +/-    .42
AMBIGUITY   9 :            4331394.28   +/-    .39
AMBIGUITY  13 :            7696459.76   +/-    .65
AMBIGUITY  12 :           12252700.92   +/-    .86

OBSERVATION SSG.PREDD.CLK:D3:GABU3.DATC2
STATIONS:  GA BU

AMBIGUITY WRT REFERENCE SATELLITE :    6
AMBIGUITY   3 :                  4.28   +/-    .47
AMBIGUITY  11 :            3238455.07   +/-    .34
AMBIGUITY   9 :            8372644.35   +/-    .33
AMBIGUITY  13 :           14533616.52   +/-    .54
AMBIGUITY  12 :           23292657.55   +/-    .66
```

```
OBSERVATION SSG.PREDD.CLK:D3:GALA3.DAT
STATIONS:  GA LA

AMBIGUITY WRT REFERENCE SATELLITE :     6
AMBIGUITY   3 :                 112.56   +/-    .36
AMBIGUITY  11 :             2910978.32   +/-    .33
AMBIGUITY   9 :             7563141.35   +/-    .30
AMBIGUITY  13 :            12208566.61   +/-    .49
AMBIGUITY  12 :            19669642.28   +/-    .57


OBSERVATION SSG.PREDD.CLK:D3:GASE3.DAT
STATIONS:  GA SE

AMBIGUITY WRT REFERENCE SATELLITE :     6
AMBIGUITY   3 :                   1.99   +/-    .74


OBSERVATION SSG.PREDD.CLK:D3:GASE3GP2.DAT
STATIONS:  GA SE

AMBIGUITY WRT REFERENCE SATELLITE :    13
AMBIGUITY  33 :            -3987611.75   +/-    .74
AMBIGUITY  36 :            -3987612.78   +/-    .55
AMBIGUITY  11 :            -2535186.63   +/-    .46
AMBIGUITY   9 :            -2020445.62   +/-    .43
AMBIGUITY  12 :             3208489.12   +/-    .48


OBSERVATION SSG.PREDD.CLK:D3:LACF3.DAT
STATIONS:  LA CF

AMBIGUITY WRT REFERENCE SATELLITE :     6
AMBIGUITY   3 :                   3.05   +/-    .42
AMBIGUITY  11 :             3195406.20   +/-    .34
AMBIGUITY   9 :             8499116.72   +/-    .34
AMBIGUITY  13 :            14022617.73   +/-    .54
AMBIGUITY  12 :            22971853.57   +/-    .68


OBSERVATION SSG.PREDD.CLK:D3:CFBR3.DAT
STATIONS:  CF BR

AMBIGUITY WRT REFERENCE SATELLITE :     6
AMBIGUITY   3 :                 131.61   +/-    .49
AMBIGUITY  11 :            -5518651.86   +/-    .42
AMBIGUITY   9 :           -14907077.67   +/-    .38
AMBIGUITY  13 :           -24379461.04   +/-    .63
AMBIGUITY  12 :           -39393131.86   +/-    .81


OBSERVATION SSG.PREDD.CLK:D3:BRPA3.DAT
STATIONS:  BR PA

AMBIGUITY WRT REFERENCE SATELLITE :     6
AMBIGUITY   3 :                 -58.94   +/-   1.21
AMBIGUITY  11 :            -4560215.29   +/-   1.42


OBSERVATION SSG.PREDD.CLK:D3:GAVN3.DAT
```

```
STATIONS:   GA VN

AMBIGUITY WRT REFERENCE SATELLITE :     6
AMBIGUITY   3 :                    -35.84   +/-   .38
AMBIGUITY  11 :               1500982.15   +/-   .34
AMBIGUITY   9 :               3823993.65   +/-   .32
AMBIGUITY  13 :               6627801.56   +/-   .50
AMBIGUITY  12 :              10947311.52   +/-   .61


OBSERVATION SSG.PREDD.CLK:D3:OWFT3.DAT
STATIONS:   OW FT

AMBIGUITY WRT REFERENCE SATELLITE :     6
AMBIGUITY   3 :                  -1835.43   +/-   .82
AMBIGUITY  11 :               4210350.07   +/-   .63
AMBIGUITY  36 :                     -2.98   +/-   .56
AMBIGUITY   9 :              10675897.09   +/-   .73
AMBIGUITY  13 :              13441769.13   +/-  1.13
AMBIGUITY  12 :              21719889.09   +/-  1.35
```

Table 1   Troposphere Scale Corrections
& Zenith Delay Corrections (in mm) for Jan. 4

notice: Zenith Delay Computed from Default Met. Data
by using SR. HOPF

Default Met. Data :
Pres. = 1000.00 Temp. =   .00 Rel. Huml. =   50.00

Stations	Scale	& rms	Zenith Delay, in (mm)	rms
PL	.0292	.003	67	6
AL	.0171	.002	39	4
OW	.0615	.003	142	6
CH	.0275	.002	63	5
WF	.0134	.002	31	5
BU	.0665	.003	153	6
GA	.0663	.003	153	7
LA	.0650	.003	150	7
SE	.0668	.003	154	7

		BR		.0607 .003		140	7		
		DE		.0703 .003		162	7		
		FT		.0218 .003		50	7		
		SI		.0723 .003		167	6		
		VN		.0704 .003		162	6		

```
OBSERVATION SSG.PREDD.CLK:D4:PLAL4.DATC2
STATIONS:  PL AL

AMBIGUITY WRT REFERENCE SATELLITE :     6
AMBIGUITY   3 :                    1193.95    +/-   5.34
AMBIGUITY  11 :                 -159667.26    +/-   1.89
AMBIGUITY  41 :                 -159666.06    +/-   1.91
AMBIGUITY   9 :                 -850464.08    +/-   3.25
AMBIGUITY  13 :                -2439079.43    +/-   5.02
AMBIGUITY  36 :                      -5.47    +/-   1.25
AMBIGUITY  43 :                -2439082.50    +/-   4.84

OBSERVATION SSG.PREDD.CLK:D4:PLOW4.DAT
STATIONS:  PL OW

AMBIGUITY WRT REFERENCE SATELLITE :    11
AMBIGUITY   3 :                  221652.07    +/-   3.05
AMBIGUITY   6 :                  222372.68    +/-   1.27
AMBIGUITY   9 :                -1054767.49    +/-   2.15
AMBIGUITY  13 :                -2088677.32    +/-   3.48

OBSERVATION SSG.PREDD.CLK:D4:ALCH4.DATC2
STATIONS:  AL CH

AMBIGUITY WRT REFERENCE SATELLITE :    11
AMBIGUITY   3 :                     176.48    +/-   3.57
AMBIGUITY   6 :                     257.87    +/-   3.50
AMBIGUITY   9 :                     802.59    +/-   4.48
AMBIGUITY  13 :                 -350244.83    +/-   5.52
AMBIGUITY  36 :                     262.54    +/-   3.84
AMBIGUITY  43 :                 -350238.27    +/-   5.51
AMBIGUITY  12 :                 -513578.44    +/-   6.86

OBSERVATION SSG.PREDD.CLK:D4:ALWF4.DAT
STATIONS:  AL WF

AMBIGUITY WRT REFERENCE SATELLITE :     6
AMBIGUITY   3 :                     513.56    +/-   1.41
AMBIGUITY  11 :                 -126207.16    +/-   1.40
AMBIGUITY  41 :                 -126209.72    +/-   1.03
AMBIGUITY   9 :                 -299662.20    +/-   1.16
AMBIGUITY  36 :                      -4.56    +/-   1.31
```

```
OBSERVATION SSG.PREDD.CLK:D4:ALWF4GP2.DAT
STATIONS:  AL WF

AMBIGUITY WRT REFERENCE SATELLITE :    13
AMBIGUITY · 39 :               -370817.15    +/-  1.59
AMBIGUITY  12 :                 -39600.52    +/-  1.84


OBSERVATION SSG.PREDD.CLK:D4:OWBU4.DAT
STATIONS:  OW BU

AMBIGUITY WRT REFERENCE SATELLITE :     6
AMBIGUITY   3 :                    -23.02    +/-   .64
AMBIGUITY  11 :                 745421.45    +/-   .40
AMBIGUITY   9 :                3186975.63    +/-   .38
AMBIGUITY  13 :                6487937.46    +/-   .63
AMBIGUITY  12 :               11294604.33    +/-   .83


OBSERVATION SSG.PREDD.CLK:D4:OWFT4.DAT
STATIONS:  OW FT

AMBIGUITY WRT REFERENCE SATELLITE :     6
AMBIGUITY   3 :                  -1396.03    +/-   .76
AMBIGUITY  11 :                2531033.70    +/-   .62
AMBIGUITY   9 :                5720754.02    +/-   .92


OBSERVATION SSG.PREDD.CLK:D4:GABU4.DAT
STATIONS:  GA BU

AMBIGUITY WRT REFERENCE SATELLITE :     6
AMBIGUITY   3 :                     19.88    +/-   .46
AMBIGUITY  11 :                1546056.72    +/-   .34
AMBIGUITY   9 :                6589449.00    +/-   .33
AMBIGUITY  13 :               12729561.54    +/-   .53
AMBIGUITY  12 :               21940980.82    +/-   .65


OBSERVATION SSG.PREDD.CLK:D4:GALA4.DAT
STATIONS:  GA LA

AMBIGUITY WRT REFERENCE SATELLITE :     6
AMBIGUITY   3 :                     18.56    +/-   .37
AMBIGUITY  11 :                1220491.03    +/-   .33
AMBIGUITY   9 :                5928236.00    +/-   .30
AMBIGUITY  13 :               10561162.70    +/-   .49
AMBIGUITY  12 :               17775780.47    +/-   .56


OBSERVATION SSG.PREDD.CLK:D4:GASE4.DAT
STATIONS:  GA SE

AMBIGUITY WRT REFERENCE SATELLITE :     6
AMBIGUITY   3 :                     77.95    +/-   .40
AMBIGUITY  11 :                 473410.27    +/-   .34
AMBIGUITY   9 :                2249746.27    +/-   .31
AMBIGUITY  13 :                4378373.50    +/-   .50
AMBIGUITY  12 :                7602490.51    +/-   .61
```

```
OBSERVATION SSG.PREDD.CLK:D4:LASI4.DAT
STATIONS:  LA SI

AMBIGUITY WRT REFERENCE SATELLITE :     6
AMBIGUITY   3 :                    -75.40    +/-   .38
AMBIGUITY  11 :                3150154.25    +/-   .58
AMBIGUITY   9 :                8627048.92    +/-   .36
AMBIGUITY  41 :                3150156.73    +/-   .43
AMBIGUITY  13 :               13968247.94    +/-   .58
AMBIGUITY  12 :               22865878.88    +/-   .65

OBSERVATION SSG.PREDD.CLK:D4:BRDE4.DAT
STATIONS:  BR DE

AMBIGUITY WRT REFERENCE SATELLITE :     6
AMBIGUITY   3 :                    -74.21    +/-   .47
AMBIGUITY  11 :                 136153.74    +/-   .42
AMBIGUITY   9 :                 617427.87    +/-   .38
AMBIGUITY  13 :                1197492.69    +/-   .65
AMBIGUITY  12 :                2287102.66    +/-   .79

OBSERVATION SSG.PREDD.CLK:D4:GADE4.DAT
STATIONS:  GA DE

AMBIGUITY WRT REFERENCE SATELLITE :     6
AMBIGUITY   3 :                     95.68    +/-   .39
AMBIGUITY  11 :                 267383.52    +/-   .35
AMBIGUITY   9 :                1304478.14    +/-   .32
AMBIGUITY  13 :                2495594.06    +/-   .52
AMBIGUITY  12 :                4374818.63    +/-   .62

OBSERVATION SSG.PREDD.CLK:D4:GAVN4.DAT
STATIONS:  GA VN

AMBIGUITY WRT REFERENCE SATELLITE :     9
AMBIGUITY   3 :                -395422.46    +/-   .61
AMBIGUITY   6 :                -395480.62    +/-   .35
AMBIGUITY  11 :                -395498.48    +/-   .35
AMBIGUITY  13 :                2911557.23    +/-   .42
AMBIGUITY  12 :                7314042.89    +/-   .49
```

Table 1 Troposphere Scale Corrections
        & Zenith Delay Corrections (in mm)   for Jan. 5

notice: Zenith Delay Computed from Default Met. Data
        by using SR. HOPF
Default Met. Data :
Pres. = 1000.00 Temp. =   .00 Rel. Huml. =   50.00

| | Corrections | | |
Stations	Scale & rms	Zenith Delay, rms in (mm)	
PL	.0331 .002	76	5
AL	.0291 .001	67	3
OW	.0472 .002	109	5
CH	.0300 .002	69	4
WF	.0041 .002	9	4
BU	.0437 .002	101	5
GA	.0427 .003	98	6
LA	.0368 .003	85	6
SE	.0426 .003	98	6
BR	.0418 .003	96	6
DE	.0419 .003	96	6
FT	.0259 .002	59	5
SI	.0378 .003	87	6
VN	.0488 .003	113	5

```
OBSERVATION SSG.PREDD.CLK:D5:PLAL5.DAT
STATIONS:  PL AL

AMBIGUITY WRT REFERENCE SATELLITE :      6
AMBIGUITY   3 :                  3727.76    +/-   5.15
AMBIGUITY  11 :               -226092.37    +/-   1.86
AMBIGUITY   9 :               -934902.48    +/-   3.26
AMBIGUITY  13 :              -2638656.21    +/-   4.84

OBSERVATION SSG.PREDD.CLK:D5:PLOW5.DATC2
STATIONS:  PL OW

AMBIGUITY WRT REFERENCE SATELLITE :      6
AMBIGUITY   3 :                 -1551.69    +/-   2.78
AMBIGUITY  11 :               -892251.91    +/-   1.31
AMBIGUITY   9 :              -1697639.49    +/-   2.00
AMBIGUITY  13 :              -2807649.89    +/-   3.36
AMBIGUITY  12 :              -4758858.28    +/-   4.12
```

```
OBSERVATION SSG.PREDD.CLK:D5:ALCH5.DATC2
STATIONS:  AL CH

AMBIGUITY WRT REFERENCE SATELLITE :     6
AMBIGUITY   3 :                    -3395.08    +/-   3.95
AMBIGUITY  11 :                  -722524.74    +/-   3.92
AMBIGUITY  41 :                  -722524.95    +/-   3.61
AMBIGUITY   9 :                 -1133617.69    +/-   3.12
AMBIGUITY  36 :                        .61    +/-   1.00
AMBIGUITY  13 :                 -1674460.11    +/-   5.39

OBSERVATION SSG.PREDD.CLK:D5:ALWF5.DAT
STATIONS:  AL WF

AMBIGUITY WRT REFERENCE SATELLITE :     9
AMBIGUITY   6 :                    1080.43    +/-   1.17

OBSERVATION SSG.PREDD.CLK:D5:ALWF5GP2.DAT
STATIONS:  AL WF

AMBIGUITY WRT REFERENCE SATELLITE :    13
AMBIGUITY  39 :                  -432573.16    +/-   1.58
AMBIGUITY  12 :                   -43795.31    +/-   1.80

OBSERVATION SSG.PREDD.CLK:D5:ALCH5GP2.DATC2
STATIONS:  AL CH

AMBIGUITY WRT REFERENCE SATELLITE :    43
AMBIGUITY  71 :                   951944.09    +/-   5.48
AMBIGUITY  39 :                   540833.17    +/-   4.62
AMBIGUITY  12 :                  -169826.63    +/-   6.79

OBSERVATION SSG.PREDD.CLK:D5:PLAL5GP2.DAT
STATIONS:  PL AL

AMBIGUITY WRT REFERENCE SATELLITE :    43
AMBIGUITY  39 :                  1703738.58    +/-   4.32
AMBIGUITY  41 :                  2412532.19    +/-   4.74
AMBIGUITY  12 :                 -1564164.96    +/-   7.00

OBSERVATION SSG.PREDD.CLK:D5:OWBU5.DAT
STATIONS:  OW BU

AMBIGUITY WRT REFERENCE SATELLITE :     6
AMBIGUITY   3 :                     132.23    +/-    .62
AMBIGUITY  11 :                  1771820.38    +/-    .41
AMBIGUITY   9 :                  3668429.92    +/-    .38
AMBIGUITY  13 :                  7112986.95    +/-    .65
AMBIGUITY  12 :                 11995623.98    +/-    .87

OBSERVATION SSG.PREDD.CLK:D5:GABU5.DATC2
STATIONS:  GA BU

AMBIGUITY WRT REFERENCE SATELLITE :     9
```

```
AMBIGUITY   3 :                -2998365.29    +/-    .62
AMBIGUITY   6 :                -2998513.25    +/-    .34
AMBIGUITY  11 :                -2854787.12    +/-    .36
AMBIGUITY  13 :                 6082256.38    +/-    .47
AMBIGUITY  12 :                15455100.12    +/-    .56

OBSERVATION SSG.PREDD.CLK:D5:GALA5.DAT
STATIONS:  GA LA

AMBIGUITY WRT REFERENCE SATELLITE :     9
AMBIGUITY   3 :                -2405164.18    +/-    .54
AMBIGUITY   6 :                -2405259.16    +/-    .31
AMBIGUITY  11 :                -2405180.89    +/-    .32
AMBIGUITY  13 :                 4771447.13    +/-    .42
AMBIGUITY  12 :                11904678.97    +/-    .47

OBSERVATION SSG.PREDD.CLK:D5:GASE5.DAT
STATIONS:  GA SE

AMBIGUITY WRT REFERENCE SATELLITE :     9
AMBIGUITY   3 :                -1024373.36    +/-    .58
AMBIGUITY   6 :                -1024434.72    +/-    .34
AMBIGUITY  11 :                 -925865.04    +/-    .36
AMBIGUITY  13 :                 2127435.25    +/-    .43
AMBIGUITY  12 :                 5279730.56    +/-    .49

OBSERVATION SSG.PREDD.CLK:D5:LASI5.DAT
STATIONS:  LA SI

AMBIGUITY WRT REFERENCE SATELLITE :     6
AMBIGUITY   3 :                      19.95    +/-    .38
AMBIGUITY  11 :                 3330492.41    +/-   1.17
AMBIGUITY  41 :                 3330487.81    +/-    .36
AMBIGUITY   9 :                 8814751.81    +/-    .33
AMBIGUITY  13 :                14694591.35    +/-    .53
AMBIGUITY  12 :                23953651.97    +/-    .62

OBSERVATION SSG.PREDD.CLK:D5:BRDE5.DAT
STATIONS:  BR DE

AMBIGUITY WRT REFERENCE SATELLITE :     6
AMBIGUITY   3 :                    -277.77    +/-    .47
AMBIGUITY  11 :                  525804.93    +/-    .44
AMBIGUITY   9 :                 1110132.87    +/-    .41
AMBIGUITY  13 :                 1677187.54    +/-    .68
AMBIGUITY  12 :                 3083999.84    +/-    .82

OBSERVATION SSG.PREDD.CLK:D5:GADE5.DAT
STATIONS:  GA DE

AMBIGUITY WRT REFERENCE SATELLITE :     9
AMBIGUITY   3 :                 -984540.26    +/-    .58
AMBIGUITY   6 :                 -984618.41    +/-    .34
AMBIGUITY  11 :                 -903614.54    +/-    .37
```

```
AMBIGUITY  13 :                    709074.59   +/-    .44
AMBIGUITY  12 :                   2469973.58   +/-    .51

OBSERVATION SSG.PREDD.CLK:D5:GAVN5.DAT
STATIONS:  GA VN

AMBIGUITY WRT REFERENCE SATELLITE :      9
AMBIGUITY   3 :                  -1407186.90   +/-    .57
AMBIGUITY   6 :                  -1407245.40   +/-    .33
AMBIGUITY  11 :                  -1407246.30   +/-    .35
AMBIGUITY  13 :                   2860686.91   +/-    .42
AMBIGUITY  12 :                   7274287.58   +/-    .48

OBSERVATION SSG.PREDD.CLK:D5:OWFT5.DAT
STATIONS:  OW FT

AMBIGUITY WRT REFERENCE SATELLITE :      6
AMBIGUITY   3 :                     -1881.49   +/-    .76
AMBIGUITY  11 :                   2666466.97   +/-    .52
AMBIGUITY   9 :                   7039941.21   +/-    .63
AMBIGUITY  13 :                  13090169.18   +/-   1.08
AMBIGUITY  12 :                  21729816.75   +/-   1.30
```

Table 1   Troposphere Scale Corrections
          & Zenith Delay Corrections (in mm) for Jan. 6

     notice: Zenith Delay Computed from Default Met. Data
             by using SR. HOPF
Default Met. Data :
Pres. = 1000.00 Temp. =   .00 Rel. Huml. =   50.00

Stations	Corrections		
	Scale & rms	Zenith Delay, in (mm)	rms
PL	.0320 .002	74	5
AL	.0353 .001	81	3
OW	.0368 .002	85	5
CH	.0357 .002	82	4
WF	.0185 .002	42	4
BU	.0355 .002	82	5
LA	.0235 .003	54	6
SE	.0318 .003	73	6

IV.12

BR	.0253 .003	58	6
DE	.0280 .003	64	6
FT	.0273 .002	63	5
SI	.0198 .003	45	6
PA	.0299 .003	69	6
VN	.0428 .003	98	6
MJ	.0176 .003	40	6

```
OBSERVATION SSG.PREDD.CLK:D6:PLAL6.DAT
STATIONS:  PL AL

AMBIGUITY WRT REFERENCE SATELLITE :     6
AMBIGUITY   3 :                    1404.02    +/-   4.87
AMBIGUITY  11 :                 -241298.46    +/-   1.79
AMBIGUITY   9 :                 -967635.68    +/-   3.27

OBSERVATION SSG.PREDD.CLK:D6:PLAL6GP2.DAT
STATIONS:  PL AL

AMBIGUITY WRT REFERENCE SATELLITE :    13
AMBIGUITY  36 :                 2873355.18    +/-   4.83
AMBIGUITY  41 :                 2632037.71    +/-   4.45
AMBIGUITY  39 :                 1905719.08    +/-   3.99
AMBIGUITY  12 :                -1171827.05    +/-   6.85
AMBIGUITY  43 :                       .75    +/-   1.37

OBSERVATION SSG.PREDD.CLK:D6:ALCH6.DAT
STATIONS:  AL CH

AMBIGUITY WRT REFERENCE SATELLITE :     6
AMBIGUITY   3 :                   -1503.16    +/-   3.87
AMBIGUITY  11 :                 -686944.93    +/-   3.63
AMBIGUITY  41 :                 -686948.10    +/-   3.56
AMBIGUITY   9 :                -1120647.78    +/-   3.06

OBSERVATION SSG.PREDD.CLK:D6:ALCH6GP2.DAT
STATIONS:  AL CH

AMBIGUITY WRT REFERENCE SATELLITE :    13
AMBIGUITY  36 :                 1813407.90    +/-   5.27
AMBIGUITY  39 :                  692781.57    +/-   4.43
AMBIGUITY  71 :                 1126479.21    +/-   5.41
AMBIGUITY  69 :                  692719.56    +/-   4.47
AMBIGUITY  12 :                 -161744.83    +/-   6.74

OBSERVATION SSG.PREDD.CLK:D6:ALCH6GP3.DAT
```

```
STATIONS:  AL CH

AMBIGUITY WRT REFERENCE SATELLITE :    43
AMBIGUITY 101 :                    1126417.60    +/-  5.45
AMBIGUITY  42 :                    -161745.15    +/-  7.04


OBSERVATION SSG.PREDD.CLK:D6:ALWF6.DAT
STATIONS:  AL WF

AMBIGUITY WRT REFERENCE SATELLITE :     6
AMBIGUITY   3 :                        680.03    +/-  1.36
AMBIGUITY  11 :                    -196748.78    +/-  1.00
AMBIGUITY   9 :                    -396003.77    +/-  1.16


OBSERVATION SSG.PREDD.CLK:D6:OWPL6.DAT
STATIONS:  OW PL

AMBIGUITY WRT REFERENCE SATELLITE :     6
AMBIGUITY   3 :                       1007.00    +/-  2.66
AMBIGUITY  11 :                     550328.82    +/-  1.34
AMBIGUITY   9 :                    1732039.53    +/-  2.11
AMBIGUITY  13 :                    2717044.46    +/-  3.33
AMBIGUITY  41 :                     550330.66    +/-  1.28
AMBIGUITY  39 :                    1732039.36    +/-  2.02
AMBIGUITY  12 :                    4635416.60    +/-  4.16


OBSERVATION SSG.PREDD.CLK:D6:OWMJ6.DATC2
STATIONS:  OW MJ

AMBIGUITY WRT REFERENCE SATELLITE :     6
AMBIGUITY   3 :                        113.25    +/-   .65
AMBIGUITY  11 :                       1060.75    +/-   .58
AMBIGUITY   9 :                      10176.86    +/-   .48
AMBIGUITY  13 :                      21211.83    +/-   .81
AMBIGUITY  12 :                      38907.78    +/-  1.14


OBSERVATION SSG.PREDD.CLK:D6:OWBU6.DAT
STATIONS:  OW BU

AMBIGUITY WRT REFERENCE SATELLITE :     6
AMBIGUITY   3 :                         -3.66    +/-   .66
AMBIGUITY  11 :                    1624111.87    +/-   .51
AMBIGUITY   9 :                    4733875.29    +/-   .53
AMBIGUITY  36 :                          -.10    +/-   .54
AMBIGUITY  13 :                    7425993.59    +/-   .69
AMBIGUITY  12 :                   12378905.74    +/-   .91


OBSERVATION SSG.PREDD.CLK:D6:OWFT6.DAT
STATIONS:  OW FT

AMBIGUITY WRT REFERENCE SATELLITE :     6
AMBIGUITY   3 :                       -1956.50    +/-   .73
AMBIGUITY  11 :                    3072616.58    +/-   .51
AMBIGUITY   9 :                    7189770.91    +/-   .63
```

```
AMBIGUITY  13 :                    13000751.55   +/-   1.07
AMBIGUITY  12 :                    21814127.05   +/-   1.30

OBSERVATION SSG.PREDD.CLK:D6:BUPA6.DAT
STATIONS:  BU PA

AMBIGUITY WRT REFERENCE SATELLITE :     6
AMBIGUITY   3 :                         164.87   +/-    .94
AMBIGUITY  11 :                    -8209559.66   +/-    .87

OBSERVATION SSG.PREDD.CLK:D6:BUPA6GP2.DAT
STATIONS:  BU PA

AMBIGUITY WRT REFERENCE SATELLITE :    13
AMBIGUITY  33 :                    39926215.05   +/-   1.14
AMBIGUITY   9 :                    13991812.04   +/-    .66
AMBIGUITY  41 :                    31869912.33   +/-    .78
AMBIGUITY  36 :                    40060184.68   +/-    .89
AMBIGUITY  12 :                   -27667723.22   +/-    .95

OBSERVATION SSG.PREDD.CLK:D6:BUVN6.DAT
STATIONS:  BU VN

AMBIGUITY WRT REFERENCE SATELLITE :     6
AMBIGUITY   3 :                         -57.14   +/-    .74
AMBIGUITY  11 :                    -1627481.48   +/-   1.08

OBSERVATION SSG.PREDD.CLK:D6:BUVN6GP2.DAT
STATIONS:  BU VN

AMBIGUITY WRT REFERENCE SATELLITE :    13
AMBIGUITY   9 :                         -16.66   +/-    .59
AMBIGUITY  36 :                    10696379.94   +/-   1.65
AMBIGUITY  12 :                    -1842078.08   +/-    .75

OBSERVATION SSG.PREDD.CLK:D6:BULA6.DAT
STATIONS:  BU LA

AMBIGUITY WRT REFERENCE SATELLITE :     6
AMBIGUITY   3 :                          48.97   +/-    .50
AMBIGUITY  11 :                     -576305.08   +/-    .47
AMBIGUITY   9 :                    -1908219.25   +/-    .48
AMBIGUITY  36 :                           -.88   +/-    .53
AMBIGUITY  13 :                    -3149498.60   +/-    .58
AMBIGUITY  12 :                    -5644951.78   +/-    .69

OBSERVATION SSG.PREDD.CLK:D6:DEBR6.DAT
STATIONS:  DE BR

AMBIGUITY WRT REFERENCE SATELLITE :     6
AMBIGUITY   3 :                         148.41   +/-    .47
AMBIGUITY  11 :                      -53529.16   +/-    .47
AMBIGUITY   9 :                     -402868.23   +/-    .41
AMBIGUITY  13 :                     -601701.97   +/-    .70
```

```
AMBIGUITY   41 :                        -53530.03   +/-    .56
AMBIGUITY   12 :                      -1166669.32   +/-    .83

OBSERVATION SSG.PREDD.CLK:D6:LADE6.DAT
STATIONS:  LA DE

AMBIGUITY WRT REFERENCE SATELLITE :      6
AMBIGUITY    3 :                             -.75   +/-    .37
AMBIGUITY   11 :                      -1858432.00   +/-    .32
AMBIGUITY    9 :                      -6247616.34   +/-    .31
AMBIGUITY   13 :                      -8370232.37   +/-    .49
AMBIGUITY   12 :                     -13420555.82   +/-    .59

OBSERVATION SSG.PREDD.CLK:D6:LASI6.DAT
STATIONS:  LA SI

AMBIGUITY WRT REFERENCE SATELLITE :      6
AMBIGUITY    3 :                            -15.51   +/-    .52
AMBIGUITY   11 :                       3071055.44   +/-    .57
AMBIGUITY    9 :                       8493417.53   +/-    .36
AMBIGUITY   33 :                            -17.00   +/-    .51
AMBIGUITY   41 :                       3071055.89   +/-    .43
AMBIGUITY   13 :                      14417251.01   +/-    .57
AMBIGUITY   12 :                      23810491.71   +/-    .65

OBSERVATION SSG.PREDD.CLK:D6:LASE6.DAT
STATIONS:  LA SE

AMBIGUITY WRT REFERENCE SATELLITE :      6
AMBIGUITY    3 :                            -34.12   +/-    .52
AMBIGUITY   11 :                      -1458150.73   +/-    .54

OBSERVATION SSG.PREDD.CLK:D6:LASE6GP2.DAT
STATIONS:  LA SE

AMBIGUITY WRT REFERENCE SATELLITE :     13
AMBIGUITY   33 :                       6363494.95   +/-    .80
AMBIGUITY    9 :                       1866416.99   +/-    .43
AMBIGUITY   41 :                       4905378.86   +/-    .47
AMBIGUITY   36 :                       6363530.03   +/-    .60
AMBIGUITY   12 :                      -3678165.97   +/-    .50
```

Table 1 Troposphere Scale Corrections
        & Zenith Delay Corrections (in mm) for Jan. 7

notice: Zenith Delay Computed from Default Met. Data
        by using SR. HOPF
Default Met. Data :
Pres. = 1000.00 Temp. =   .00 Rel. Huml. =   50.00

| | | Corrections | |

Stations	Scale & rms	Zenith Delay, rms in (mm)
PL	.0434 .002	100 4
AL	.0179 .002	41 3
OW	.0430 .002	99 5
CH	.0235 .002	54 4
BU	.0380 .002	87 4
LA	.0230 .003	53 6
SE	.0257 .003	59 5
BR	.0310 .003	71 5
DE	.0264 .003	61 6
FT	.0162 .002	37 5
SI	.0317 .002	73 5
PA	.0365 .002	84 5
VN	.0297 .002	68 5
MJ	.0445 .003	103 6
ML	.0322 .003	74 6

```
OBSERVATION SSG.PREDD.CLK:D7:PLAL7.DAT
STATIONS:  PL AL

AMBIGUITY WRT REFERENCE SATELLITE :    11
AMBIGUITY    3 :                  249975.34   +/-   4.76
AMBIGUITY    6 :                  249820.61   +/-   1.94
AMBIGUITY   41 :                     233.92   +/-   1.28
AMBIGUITY    9 :                 -701535.32   +/-   2.86
AMBIGUITY   13 :                -2300099.26   +/-   4.47
AMBIGUITY   12 :                -3785195.41   +/-   6.65

OBSERVATION SSG.PREDD.CLK:D7:PLAL7GP2.DAT
STATIONS:  PL AL

AMBIGUITY WRT REFERENCE SATELLITE :    43
AMBIGUITY   42 :                -1484947.11   +/-   7.25

OBSERVATION SSG.PREDD.CLK:D7:PLOW7.DATC2
```

```
STATIONS:  PL OW

AMBIGUITY WRT REFERENCE SATELLITE :     6
AMBIGUITY   3 :                    -316.68    +/-   2.65
AMBIGUITY  11 :                 -520330.49    +/-   1.39
AMBIGUITY   9 :                -1615369.51    +/-   2.05
AMBIGUITY  13 :                -2651736.65    +/-   3.39
AMBIGUITY  12 :                -4639843.50    +/-   4.15

OBSERVATION SSG.PREDD.CLK:D7:ALCH7.DAT
STATIONS:  AL CH

AMBIGUITY WRT REFERENCE SATELLITE :    11
AMBIGUITY   3 :                  712594.54    +/-   3.60
AMBIGUITY   6 :                  713779.22    +/-   3.88
AMBIGUITY  41 :                     -13.88    +/-   1.72
AMBIGUITY   9 :                 -496552.61    +/-   4.83
AMBIGUITY  13 :                -1228647.13    +/-   5.72
AMBIGUITY  12 :                -1536614.44    +/-   8.44

OBSERVATION SSG.PREDD.CLK:D7:ALCH7GP2.DAT
STATIONS:  AL CH

AMBIGUITY WRT REFERENCE SATELLITE :    43
AMBIGUITY  71 :                 1228703.75    +/-   5.48
AMBIGUITY  42 :                 -307964.78    +/-   8.47

OBSERVATION SSG.PREDD.CLK:D7:OWMJ7.DAT
STATIONS:  OW MJ

AMBIGUITY WRT REFERENCE SATELLITE :     6
AMBIGUITY   3 :                     258.78    +/-    .66
AMBIGUITY  11 :                    5496.49    +/-    .60
AMBIGUITY   9 :                   14678.61    +/-    .49
AMBIGUITY  13 :                   26690.45    +/-    .83
AMBIGUITY  12 :                   43365.10    +/-   1.43

OBSERVATION SSG.PREDD.CLK:D7:OWBU7.DAT
STATIONS:  OW BU

AMBIGUITY WRT REFERENCE SATELLITE :     6
AMBIGUITY   3 :                      90.75    +/-    .59
AMBIGUITY  11 :                 1563157.81    +/-    .41
AMBIGUITY   9 :                 4170181.32    +/-    .38
AMBIGUITY  13 :                 7719670.82    +/-    .64
AMBIGUITY  12 :                12497541.17    +/-   1.05

OBSERVATION SSG.PREDD.CLK:D7:OWFT7.DAT
STATIONS:  OW FT

AMBIGUITY WRT REFERENCE SATELLITE :     6
AMBIGUITY   3 :                   -1809.49    +/-    .74
AMBIGUITY  11 :                 2687130.64    +/-    .53
AMBIGUITY   9 :                 7099554.64    +/-    .63
```

```
AMBIGUITY  13 :                    12947894.32    +/-   1.08
AMBIGUITY  12 :                    21950446.11    +/-   1.32

    OBSERVATION SSG.PREDD.CLK:D7:BUPA7.DAT
    STATIONS:  BU PA

AMBIGUITY WRT REFERENCE SATELLITE :       9
AMBIGUITY   3 :                     6129172.90    +/-    .94
AMBIGUITY   6 :                     6129077.05    +/-    .54
AMBIGUITY  11 :                     6129172.15    +/-    .70
AMBIGUITY  13 :                   -18278572.07    +/-    .67
AMBIGUITY  12 :                   -45180016.84    +/-   1.18

    OBSERVATION SSG.PREDD.CLK:D7:BUVN7.DAT
    STATIONS:  BU VN

AMBIGUITY WRT REFERENCE SATELLITE :       6
AMBIGUITY   3 :                          56.57    +/-    .48
AMBIGUITY  11 :                     -1246119.97    +/-    .35
AMBIGUITY   9 :                     -4009700.76    +/-    .37
AMBIGUITY  13 :                     -7560436.26    +/-    .62
AMBIGUITY  12 :                    -12266124.72    +/-    .78

    OBSERVATION SSG.PREDD.CLK:D7:BULA7.DAT
    STATIONS:  BU LA

AMBIGUITY WRT REFERENCE SATELLITE :       6
AMBIGUITY   3 :                         109.91    +/-    .42
AMBIGUITY  11 :                      -271016.48    +/-    .35
AMBIGUITY   9 :                     -1206114.84    +/-    .32
AMBIGUITY  13 :                     -2448375.48    +/-    .52
AMBIGUITY  12 :                     -4549773.07    +/-    .71

    OBSERVATION SSG.PREDD.CLK:D7:BUBR7.DAT
    STATIONS:  BU BR

AMBIGUITY WRT REFERENCE SATELLITE :       6
AMBIGUITY   3 :                         241.80    +/-    .63
AMBIGUITY  11 :                     -2400573.92    +/-    .60
AMBIGUITY   9 :                     -7441652.17    +/-    .53
AMBIGUITY  13 :                    -13198093.50    +/-   1.01

    OBSERVATION SSG.PREDD.CLK:D7:LADE7.DAT
    STATIONS:  LA DE

AMBIGUITY WRT REFERENCE SATELLITE :       6
AMBIGUITY   3 :                         -75.89    +/-    .38
AMBIGUITY  11 :                     -1518816.08    +/-    .33
AMBIGUITY   9 :                     -5343238.92    +/-    .30
AMBIGUITY  13 :                     -8723745.13    +/-    .49
AMBIGUITY  12 :                    -14198501.17    +/-    .61

    OBSERVATION SSG.PREDD.CLK:D7:LASI7.DAT
    STATIONS:  LA SI
```

```
AMBIGUITY WRT REFERENCE SATELLITE :     6
AMBIGUITY   3 :                    -75.39   +/-    .38
AMBIGUITY  11 :                2004450.33   +/-    .33
AMBIGUITY   9 :                7471721.47   +/-    .31
AMBIGUITY  13 :               12656476.27   +/-    .50
AMBIGUITY  12 :               21600194.51   +/-    .60


OBSERVATION SSG.PREDD.CLK:D7:LASE7.DAT
STATIONS:  LA SE

AMBIGUITY WRT REFERENCE SATELLITE :     6
AMBIGUITY   3 :                     60.65   +/-    .40
AMBIGUITY  11 :               -1358644.63   +/-    .33
AMBIGUITY   9 :               -4156693.61   +/-    .32
AMBIGUITY  13 :               -6712845.24   +/-    .51
AMBIGUITY  12 :              -10747023.74   +/-    .65


OBSERVATION SSG.PREDD.CLK:D7:LAML7.DAT
STATIONS:  LA ML

AMBIGUITY WRT REFERENCE SATELLITE :     6
AMBIGUITY   3 :                   -112.32   +/-    .46
AMBIGUITY  11 :               -1903921.28   +/-    .35
AMBIGUITY   9 :               -6763961.83   +/-    .39
AMBIGUITY  13 :              -11098760.50   +/-    .61
AMBIGUITY  12 :              -18171660.64   +/-    .80
```

2.1 RADIATION PARAMETERS

PRN	direct	y-component
9	0.970282425E-07	0.403878874E-09
12	0.882616760E-07	0.438963262E-09
3	0.865436115E-07	0.574607189E-09
6	0.991520364E-07	0.571772222E-09
11	0.883175091E-07	0.261808613E-09
13	0.909335599E-07	0.275311879E-09

```
   REFERENCE ELLIPSOID
   -------------------
AE = 6378135.0F-1 = 298.2600,XE =   .000,YE =   .000,ZE = .000
```

Table 2 Priori & Posteriori Station Coordinates
        (in Geodetic & Cartesian)and their Discrepancies

	Stations	Latitude : degree , minute , second Longitude: degree , minute , second Height : meter Cartesian: meter X , Y , Z		Discrepancy in Coord. Components & Position mm
		PRIORI	Derived RMS (mm)	
		40 10 58.05604	40 10 58.05604 0	0
		-104 43 34.84730	-104 43 34.84730 0	0
		1503.256	1503.256 0	0
	PL			

	-1240708.269	-1240708.269	0	0
	-4720454.201	-4720454.201	0	0
	4094481.781	4094481.781	0	0
				0
AL	45 57 21.24086	45 57 21.24086	0	0
	- 78 4 16.92058	- 78 4 16.92058	0	0
	200.778	200.778	0	0
	918127.499	918127.499	0	0
	-4346061.915	-4346061.915	0	0
	4561984.260	4561984.260	0	0
				0
OW	37 13 57.21511	37 13 57.21511	0	0
	-118 17 37.65749	-118 17 37.65749	0	0
	1179.944	1179.944	0	0
	-2410422.594	-2410422.594	0	0
	-4477802.462	-4477802.462	0	0
	3838686.837	3838686.837	0	0
				0
CH	58 45 32.96074	58 45 32.95836	15	-74
	- 94 5 18.08572	- 94 5 18.08868	17	-48
	-15.092	-15.276	16	-184
	-236417.009	-236417.055	17	-45
	-3307612.055	-3307612.019	19	36
	5430055.889	5430055.694	9	-195
				203
WF	42 36 47.95645	42 36 47.95620	5	-8
	- 71 29 36.02332	- 71 29 36.02466	7	-31
	88.346	88.417	12	71
	1492232.879	1492232.869	7	-11
	-4458091.715	-4458091.779	9	-64
	4296045.975	4296046.017	8	42
				77
BU	35 23 54.58426	35 23 54.58337	2	-27
	-119 23 38.45992	-119 23 38.45971	3	5
	56.623	56.632	5	9
	-2554674.241	-2554674.248	3	-7
	-4534923.635	-4534923.658	4	-23
	3674025.631	3674025.614	3	-17
				29
GA	34 30 6.51289	34 30 6.51202	2	-27
	-120 11 55.66095	-120 11 55.66004	4	23
	715.307	715.336	6	29
	-2647055.562	-2647055.561	5	1
	-4548316.902	-4548316.947	5	-45
	3592861.568	3592861.563	4	-6
				45

	34 29 39.86912	34 29 39.86733	2	−55
	−119 42 50.01971	−119 42 50.01759	4	54
	1166.684	1166.790	7	106
LA				
	−2608883.240	−2608883.252	5	−12
	−4571283.072	−4571283.202	5	−130
	3592440.489	3592440.503	4	15
				131
	33 57 3.08619	33 57 3.08542	3	−24
	−120 6 20.43013	−120 6 20.42915	5	25
	445.357	445.413	8	56
SE				
	−2656791.887	−2656791.895	6	−8
	−4582160.419	−4582160.484	6	−64
	3542173.968	3542173.980	5	11
				65
	34 18 2.22346	34 18 2.22315	3	−9
	−119 19 51.44183	−119 19 51.44131	5	13
	309.060	309.144	10	84
CF				
	−2583875.878	−2583875.903	6	−25
	−4598589.214	−4598589.286	7	−71
	3574215.874	3574215.914	6	39
				84
	33 24 25.24661	33 24 25.24687	3	8
	−118 24 17.47639	−118 24 17.47560	6	20
	450.482	450.524	9	42
BR				
	−2535535.778	−2535535.775	7	3
	−4688425.811	−4688425.847	7	−37
	3491976.567	3491976.597	5	30
				47
	34 1 44.81445	34 1 44.81374	3	−22
	−119 47 3.87717	−119 47 3.87624	5	24
	706.508	706.518	8	10
DE				
	−2628754.256	−2628754.245	6	10
	−4592961.047	−4592961.077	6	−30
	3549517.950	3549517.938	5	−13
				34
	36 40 11.23000	36 40 11.22443	1	−172
	−121 46 23.78000	−121 46 23.78419	2	−104
	24.590	25.710	5	1120
FT				
	−2697026.298	−2697026.914	3	−615
	−4354392.350	−4354393.146	3	−796
	3788077.196	3788077.727	3	531
				1137
	34 17 54.01834	34 17 54.01773	3	−19
	−119 20 33.67370	−119 20 33.67362	5	2
	−9.764	−9.683	8	81

		Priori	Posteriori	std	resid
SI			-2584758.154	6	-36
		-2584758.118	-4597954.754	6	-68
		-4597954.686	3573827.375	5	30
		3573827.345			82
PA		33 44 37.53928	33 44 37.53919	3	-3
		-118 24 12.78803	-118 24 12.78641	6	42
		71.357	71.348	10	-9
		-2525452.960	-2525452.920	7	40
		-4670035.485	-4670035.500	8	-15
		3522886.868	3522886.861	6	-7
					43
VN		34 33 22.54778	34 33 22.54614	2	-50
		-120 36 58.31415	-120 36 58.31322	4	24
		-9.618	-9.585	7	33
		-2678071.775	-2678071.783	5	-8
		-4525451.566	-4525451.627	6	-60
		3597427.507	3597427.484	4	-23
					64
MJ		35 19 53.59722	35 19 53.59694	2	-9
		-116 53 17.35652	-116 53 17.35540	4	28
		906.421	906.437	7	16
		-2356214.800	-2356214.783	5	17
		-4646733.801	-4646733.830	6	-29
		3668460.522	3668460.524	4	2
					33
ML		34 30 36.38716	34 30 36.38667	3	-15
		-120 13 46.81878	-120 13 46.81784	6	24
		87.191	87.219	12	28
		-2648983.135	-2648983.130	7	5
		-4545991.898	-4545991.937	9	-39
		3593264.393	3593264.396	7	3
					39

A POSTERIORI VARIANCE FACTOR :   1.6951

Table 4 Baseline Components Summary

Baseline Name	Baseline Length & its STD		
	azimuth 1'st to 2'nd	azimuth 1'st to 2'nd	
* Priori	Posteriori(Geodetic & Cartesian & rms(mm)		
Latitude	Latitude	X (m)	
Longitude	Longitude	Y (m)	
Height (m)	Height (m)	Z (m)	
PL AL	2240379.4375 m +/-	0	
	- 64 37 52.929 0.000	96 58 1.666 0.000	

```
   5 46 23.18482|   5 46 23.18482      0| -2158835.7679       0
  26 39 17.92672|  26 39 17.92672      0|  -374392.2859       0
  -1302.47800   |  -1302.4780          0|  -467502.4785       0
_____|_____|_____
     PL    OW   |   1221696.5752  m +/-      0
               | 101 11    .448  0.000|  70 18 18.598  0.000
-  2 57    .84093|-  2 57    .84093     0| 1169714.3248       0
- 13 34  2.81019|- 13 34  2.81019      0| -242651.7389       0
  -323.31200    |   -323.3120          0|  255794.9449       0
_____|_____|_____
     AL    CH   |   1779016.3929  m +/-     13
               |  31 17 30.492   .002| 135 54 55.509   .002
 12 48 11.71988| 12 48 11.71750     15| 1154544.5536      17
- 16  1  1.16514|- 16  1  1.16810    17| -1038449.8956     19
  -215.87000    |   -216.0538        16|  -868071.4339      9
_____|_____|_____
     AL    WF   |    642550.2432  m +/-      7
               | -122 56 31.954  .002|  52 27 37.149   .002
-  3 20 33.28441|-  3 20 33.28466     5| -574105.3696       7
  6 34 40.89726|  6 34 40.89592      7|  112029.8642       9
  -112.43200    |   -112.3611        12|  265938.2432       8
_____|_____|_____
     OW    BU   |    226240.3346  m +/-      2
               | 153 46 36.571   .002|  25 34 17.307   .002
-  1 50  2.63085|-  1 50  2.63174     2|  144251.6543       3
-  1  6   .80243|-  1  6   .80222     3|   57121.1957       4
  -1123.32100   |   -1123.3116        5|  164661.2226       3
_____|_____|_____
     GA    BU   |    123698.3848  m +/-      2
               | - 36 14    .437  .003| 143 18 19.839   .003
  0 53 48.07137|  0 53 48.07135      1|  -92381.3130       3
  0 48 17.20103|  0 48 17.20032      2|  -13393.2893       3
  -658.68400    |   -658.7034         4|  -81164.0512       2
_____|_____|_____
     GA    LA   |     44550.5479  m +/-      2
               | - 90 55  7.912   .003|  88 48 23.390   .003
-  0  0 26.64377|-  0  0 26.64469     1|  -38172.3090       2
  0 29  5.64124|  0 29  5.64244      2|   22966.2546       3
   451.37700    |    451.4541         4|     421.0593       2
_____|_____|_____
     GA    SE   |     61720.4361  m +/-      1
               | -171 58 56.115   .008|   7 57 55.322   .008
-  0 33  3.42670|-  0 33  3.42661     1|    9736.3337       3
  0  5 35.23082|  0  5 35.23089      2|   33843.5367       3
  -269.95000    |   -269.9229         5|   50687.5829       3
_____|_____|_____
     LA    CF   |     41268.9403  m +/-      2
               | -121 17 45.430   .011|  58 29 15.709   .011
-  0 11 37.64566|-  0 11 37.64418     1|  -25007.3495       4
  0 22 58.57788|  0 22 58.57628      3|   27306.0840       5
  -857.62400    |   -857.6463         7|   18224.5900       4
_____|_____|_____
     CF    BR   |    131036.9451  m +/-      2
               | -138 53 32.592   .005|  40 35 30.062   .005
-  0 53 36.97685|-  0 53 36.97628     1|  -48340.1277       4
  0 55 33.96544|  0 55 33.96571      3|   89836.5617       6
   141.42200    |    141.3805         8|   82239.3168       4
_____|_____|_____
```

```
||    BR      PA    |      37353.8921   m +/-       2                  ||
||                  | -  0 11   6.539    .030|  179 48 50.868    .030||
||    0 20 12.29267 |    0 20 12.29231     2|     -10082.8548     6  ||
||    0  0  4.68836 |    0  0  4.68919     5|     -18390.3473     8  ||
||   -379.12500     |     -379.1759       10|     -30910.2640     6  ||
||_____ |_____|_____||
||    GA      VN    |      38803.0479   m +/-       2                  ||
||                  |   80 55 25.389    .005|   98 50 22.886    .005||
||    0  3 16.03489 |    0  3 16.03412     1|      31016.2217     3  ||
|| -  0 25  2.65320 | -  0 25  2.65318     2|     -22865.3203     3  ||
||   -724.92500     |     -724.9204        5|      -4565.9218     3  ||
||_____ |_____|_____||
||    OW      FT    |     316122.0926   m +/-       2                  ||
||                  |  100 20 39.791   0.000|   77 33 48.726   0.000||
|| -  0 33 45.98511 | -  0 33 45.99068     1|     286604.3200     3  ||
|| -  3 28 46.12251 | -  3 28 46.12670     2|    -123409.3159     3  ||
||  -1155.35400     |    -1154.2337        5|      50609.1091     3  ||
||_____ |_____|_____||
||    LA      SI    |      40494.9454   m +/-       2                  ||
||                  | -122 24    .626    .008|   57 23 24.372    .007||
|| -  0 11 45.85078 | -  0 11 45.84960     1|     -24125.0978     3  ||
||    0 22 16.34601 |    0 22 16.34397     2|      26671.5527     3  ||
||  -1176.44800     |    -1176.4729        5|      18613.1281     3  ||
||_____ |_____|_____||
||    BR      DE    |     145307.3004   m +/-       2                  ||
||                  |   61 15 57.023    .002|  117 58  5.946    .002||
||    0 37 19.56784 |    0 37 19.56686     1|      93218.4703     3  ||
|| -  1 22 46.40078 | -  1 22 46.40065     2|     -95464.7706     4  ||
||    256.02600     |      255.9938        5|     -57541.3411     3  ||
||_____ |_____|_____||
||    GA      DE    |      64859.1266   m +/-       1                  ||
||                  | -143 50  6.117    .007|   35 55 53.957    .007||
|| -  0 28 21.69844 | -  0 28 21.69828     1|     -18301.3159     3  ||
||    0 24 51.78378 |    0 24 51.78379     2|      44644.1297     4  ||
||     -8.79900     |       -8.8179        5|      43343.6250     3  ||
||_____ |_____|_____||
||    OW      MJ    |     245872.5098   m +/-       2                  ||
||                  | -148 40 26.734    .003|   30 29 38.251    .003||
|| -  1 54  3.61789 | -  1 54  3.61817     2|     -54207.8108     5  ||
||    1 24 20.30097 |    1 24 20.30209     4|     168931.3675     6  ||
||   -273.52300     |     -273.5068        7|     170226.3123     4  ||
||_____ |_____|_____||
||    BU      PA    |     204821.9194   m +/-       3                  ||
||                  | -153 22 35.465    .005|   26  3 41.025    .005||
|| -  1 39 17.04498 | -  1 39 17.04418     2|     -29221.3280     6  ||
||    0 59 25.67189 |    0 59 25.67331     5|     135111.8422     6  ||
||     14.73400     |       14.7157        8|     151138.7533     5  ||
||_____ |_____|_____||
||    BU      VN    |     145547.0521   m +/-       2                  ||
||                  |  129 35  9.010    .002|   49 42 48.624    .002||
|| -  0 50 32.03648 | -  0 50 32.03722     1|     123397.5347     3  ||
|| -  1 13 19.85423 | -  1 13 19.85350     3|      -9472.0310     4  ||
||    -66.24100     |      -66.2170        6|      76598.1294     3  ||
||_____ |_____|_____||
||    BU      LA    |     104483.3135   m +/-       1                  ||
||                  |  163 39 57.031    .004|   16  9  3.366    .004||
|| -  0 54 14.71514 | -  0 54 14.71604     1|      54209.0040     3  ||
|| -  0 19 11.55979 | -  0 19 11.55788     2|      36359.5439     3  ||
```

```
||    1110.06100    |      1110.1575      5|      81585.1105     3 ||
||_____ |_____ |_____ ||
||   LA     DE    |      52030.1190    m +/-      1            ||
||                |    172 48 29.696    .008|    7  9  7.378   .008||
|| - 0 27 55.05467|-  0 27 55.05360      1|      19870.9931     3 ||
|| - 0  4 13.85746|-  0  4 13.85865      2|      21677.8751     4 ||
||   -460.17600   |      -460.2721       5|      42922.5657     3 ||
||_____ |_____ |_____ ||
||   LA     SE    |      70287.1020    m +/-      2            ||
||                |    148 58 45.892    .006|   30 48    .820   .006||
|| - 0 32 36.78293|-  0 32 36.78192      1|      47908.6427     3 ||
|| - 0 23 30.41042|-  0 23 30.41155      2|      10877.2821     4 ||
||   -721.32700   |      -721.3770       5|      50266.5236     3 ||
||_____ |_____ |_____ ||
||   BU     BR    |     238895.4751    m +/-      2            ||
||                |   -157 20 31.766    .003|   22  5 55.937    .003||
|| - 1 59 29.33765|-  1 59 29.33650      2|     -19138.4732     5 ||
||   0 59 20.98353|   0 59 20.98411      4|     153502.1896     6 ||
||    393.85900   |       393.8916       7|     182049.0173     4 ||
||_____ |_____ |_____ ||
||   LA     ML    |      47416.5275    m +/-      4            ||
||                |     87 44 53.696    .006|   91 57 34.542    .006||
||   0  0 56.51804|   0  0 56.51934      1|      40099.8781     6 ||
|| - 0 30 56.79907|-  0 30 56.80025      4|     -25291.2645     7 ||
||  -1079.49300   |     -1079.5713      10|       -823.8928     6 ||
||_____ |_____ |_____ ||
```

Table 3   Baseline Discrepancies in lat., lon., and length in mm

Baseline	Length (in m)	Discrepancies (in mm)			
		North	East	Height	Length
PL AL	2240379.438	0	0	0	0
PL OW	1221696.575	0	0	0	0
AL CH	1779016.393	74	48	184	45
AL WF	642550.243	8	31	-71	16
OW BU	226240.335	27	-5	-9	-23
GA BU	123698.385	1	18	19	11
GA LA	44550.548	28	-31	-77	-33
GA SE	61720.436	-3	-2	-27	2
LA CF	41268.940	-46	41	22	57
CF BR	131036.945	-18	-7	42	7
BR PA	37353.892	11	-21	51	10
GA VN	38803.048	24	-1	-5	4

OW	FT	316122.093	172	104	-1120	-162
LA	SI	40494.945	-36	52	25	62
BR	DE	145307.300	30	-3	32	17
GA	DE	64859.127	-5	0	19	3
OW	MJ	245872.510	9	-28	-16	-22
BU	PA	204821.919	-25	-36	18	6
BU	VN	145547.052	23	-19	-24	-1
BU	LA	104483.313	28	-49	-96	-15
LA	DE	52030.119	-33	31	96	28
LA	SE	70287.102	-31	29	50	10
BU	BR	238895.475	-36	-15	-33	26
LA	ML	47416.528	-40	30	78	-34

VITA

Candidate's full name   :   Ding-Sheng Chen

Date and place of birth :   10 July 1963, Guan-Chen, Chi-Xi, Zhe-Jiang, P.R. China

Permanent address   :   Department of Geodesy, Wuhan Technical University of
                              Surveying and Mapping, Wuhan, P.R. China

School attended   :   1970-1977, Guan-Chen Fourth Elementary School, Chi-Xi ,
                              Zhe-Jiang, P.R. China.

School attended   :   1977-1979, Guan-Chen Junior High School, Chi-Xi, Zhe-
                              Jiang, P.R. China.

Universities attended   :   1979-1983, B.Sc.E., Department of Geodesy, Wuhan
                              Technical University of Surveying and Mapping, Wuhan,
                              P.R. China

                              1984-1986 (graduate study, incomplete), Department of
                              Geodesy, Wuhan Technical University of Surveying and
                              Mapping, Wuhan, P.R. China

Publications   :   Chen, D.S., D.C. Cao, G.L. Yuan and J.S. Ning (1984)
                              "Application of the Fast Fourier Transformation in the
                              Gravitational Field Computation". Wu Ce Zi Liao (Technical
                              Archives), 1984, No. 1, Wuhan Technical University of
                              Surveying and Mapping (in Chinese).

                              Chen D.S. and R.B. Langley (1989). "A Long Arc Approach
                              to GPS Satellite Orbit Improvement." Presented at Canadian
                              Geophysical Union 16th Annual General Meeting, McGill
                              University, Montreal, May, 1989.

                              Chen, D.S. and R.B. Langley (1990). "Experiments in
                              Processing a Standard Data Set with a New Version of the
                              DIPOP GPS Data Analysis Software." Poster Session at
                              Canadian Geophysical Union 17th Annual General Meeting,
                              Ottawa, May, 1990.

                              Chen, D.S. and R.B. Langley (1990). "DIPOP-E: An
                              Enhanced Version of the UNB GPS Differential Positioning
                              Program Package." *Proceedings of Second International
                              Symposium on Precise Positioning with the Global Positioning
                              System - GPS'90,* Ottawa, Canada, Sept. 3-7, pp. 269-284.

Chen, D.S. and R.B. Langley (1990). "A Geometrical Analysis of the Effect of Satellite Orbit Error on GPS Relative Positioning." *Proceedings of Second International Symposium on Precise Positioning with the Global Positioning System - GPS'90*, Ottawa, Canada, Sept. 3-7, pp. 757-771.